NASA TECHNICAL NOTE

NASA TN D-2625

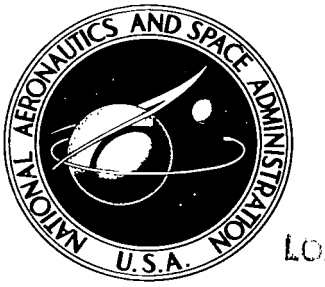

NASA TN D-2625

ANALYSIS OF NOTCH NETWORKS CONTAINING SYNCHRONOUSLY COMMUTATED CAPACITORS OR RC COMBINATIONS

by Bernard A. Asner, Jr.

George C. Marshall Space Flight Center
Huntsville, Ala.

NATIONAL AERONAUTICS AND SPACE ADMINISTRATION • WASHINGTON, D. C. • FEBRUARY 1965

ANALYSIS OF NOTCH NETWORKS CONTAINING SYNCHRONOUSLY COMMUTATED CAPACITORS OR RC COMBINATIONS

By Bernard A. Asner, Jr.

George C. Marshall Space Flight Center
Huntsville, Ala.

NATIONAL AERONAUTICS AND SPACE ADMINISTRATION

For sale by the Office of Technical Services, Department of Commerce,
Washington, D.C. 20230 -- Price $3.00

TABLE OF CONTENTS

TABLE OF CONTENTS (Concluded)

LIST OF ILLUSTRATIONS

LIST OF ILLUSTRATIONS (Cont'd)

LIST OF ILLUSTRATIONS (Concluded)

DEFINITION OF SYMBOLS

Symbol	Definition
A	Amplitude of sine input
A_1	$1/4\,\tau$
C	Capacitor
$e_i(t)$	Input to RC commutated network or system
$e_o(t)$	Output of RC commutated network or system
e_c	Voltage drop across capacitor
E(p)	Laplace transform of e(t)
f	Frequency of square wave
f_c	Frequency of input function
i	Integer
i	Current
i_c	Current flow in capacitor
j	Integer or imaginary number
k	Integer
K	Potentiometer setting
K'	Feedback setting times RC commutated network gain
K_P, K_Q	Potentiometer setting
L	Laplace transform
m	Integer
p	Laplace operator
n	Integer

DEFINITION OF SYMBOLS (Concluded)

Symbol	Definition
P	Square wave
Q	Square wave minus 90°, out of phase with P
R	Resistor
s	Dummy variable
T	Period of square wave
T_c	Period of input function
t	Time
t_1	Dummy variable
x	$\frac{2K'}{\omega\tau}$ or $\frac{1}{\omega\tau}$
Y(p)	Laplace transform of y(t)
α_m	Fourier coefficient
β_m	Fourier coefficient
$\gamma_1(n)$	Initial value of u function for n^{th} cycle
$\gamma_2(n)$	Initial value of v function for n^{th} cycle
λ	K'/τ or $1/\tau$
τ	Time constant
φ	Phase of input function
ω	Circular frequency of square wave
ω_c	Circular frequency of input function

ANALYSIS OF NOTCH NETWORKS CONTAINING SYNCHRONOUSLY COMMUTATED CAPACITORS OR RC COMBINATIONS

By

Bernard A. Asner, Jr.

SUMMARY

An extensive study is made of systems of differential equations that describe an adaptive tracking notch filter. The two basic networks considered are the coupled RC commutated network and the uncoupled RC commutated network. The coupled network leads to differential equations with time varying coefficients of a square wave nature; the other leads to a set of linear differential equations with periodic forcing functions. For the latter case, a frequency response function in closed form is obtained using complex convolution. In both cases, explicit solutions are obtained by introducing jump functions.

Time responses of actual networks are included to show the agreement with the theoretical analysis.

SECTION I. INTRODUCTION

The analysis of linear networks containing synchronously commutated capacitors or RC combinations, classified as linear time varying networks, can be handled in several different ways (Refs. 1 and 2). For mathematical convenience, it is often assumed that the commutating functions are of a known periodic form. One important and practical commutator is a relay type of element that generates a periodic square wave. This report analyzes networks using square wave commutating functions.

The motivation for the analysis was the recent development of an adaptive tracking notch (ATN) filter (Refs. 3 and 4) that utilizes synchronously commutated capacitors or RC combinations. The networks analyzed are used in the ATN filter that will help stabilize large space vehicles, such as the Saturn V, by suppressing structural bending mode signals in the control loop.

Section II presents the detailed derivations of the dynamic equations for a synchronously commutated capacitor network. This network was the initial configuration used to develop the ATN filter. Three additional networks are shown and their dynamic

equations stated. The conversions of the dynamic equations of the four networks from integral to differential form are presented in Section III. The solutions of the resulting differential equations are handled in Section IV. Analytical and experimental time and frequency responses are obtained and compared. Excellent correspondence is found for all cases examined. Section V treats the very practical cases where the square-wave commutating functions are neither symmetrical nor in quadrature with each other.

SECTION II. DERIVATION OF EQUATIONS

A. COMMUTATED CAPACITOR NETWORK

The basic circuit analyzed in this report is the commutated capacitor network shown in Figure 1. The objective of this network is to produce a signal with a fundamental component equal in magnitude but opposite in phase to the bending mode signal to be suppressed, which is present in the input signal $e_i(t)$.

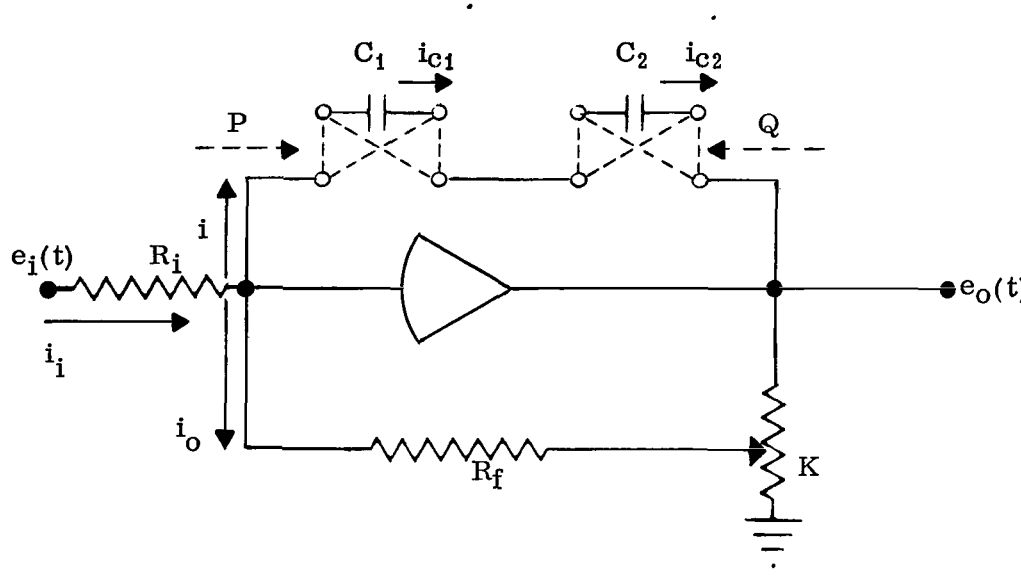

FIGURE 1. RC COMMUTATED NETWORK

The network of Figure 1 consists of a dc operation amplifier with two mechanically commutated capacitors connected in a negative feedback loop. A second negative feedback loop has a fixed and a variable resistor as shown. The capacitors are commutated by double-pole double-throw relays driven by functions P and Q at the frequency of the particular bending mode signal to be suppressed. The forms of the P and Q functions are shown in Figure 2 and are either plus or minus one.

$$P \cdot P = 1 \quad \text{and} \quad Q \cdot Q = 1.$$

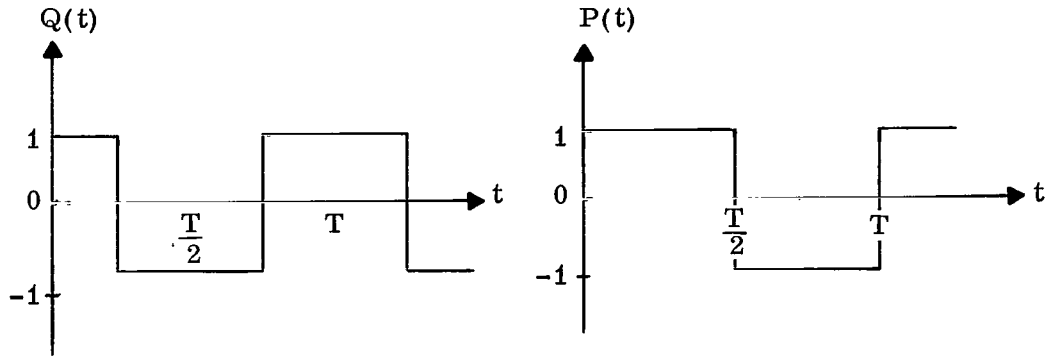

FIGURE 2. COMMUTATING FUNCTIONS

The P and Q functions are obtained from other circuits in the ATN filter.

The output of the network of Figure 1 is obtained as follows:

$$i_i = i + i_o \tag{1}$$

$$i = i_i - i_o = \frac{e_i}{R_i} - \frac{Ke_o}{R_f}. \tag{2}$$

Assuming the grid voltage of the amplifier is zero, the voltages across the capacitors are expressed as

$$e_o = \pm e_{c1} \pm e_{c2} = Pe_{c1} + Qe_{c2} \tag{3}$$

$$e_{c1} = \frac{1}{C_1} \int i_{c1}\, dt \tag{4}$$

$$e_{c2} = \frac{1}{C_2} \int i_{c2}\, dt \tag{5}$$

$$Pi_{c1} = i \qquad Qi_{c2} = i \tag{6}$$

$$i_{c1} = P \cdot i \qquad i_{c2} = Q \cdot i. \tag{7}$$

Now, substituting Equations (4) and (5) into Equation (3),

$$e_o = P\frac{1}{C_1}\int i_{c1}\,dt + Q\frac{1}{C_2}\int i_{c2}\,dt. \qquad (8)$$

Replacing i_{c1} and i_{c2} with $P \cdot i$ and $Q \cdot i$, respectively, from Equation (7), and then substituting the value for i from Equation (2), Equation (8) becomes

$$e_o = \frac{P}{\tau}\int P(e_i - K'e_o)\,dt + \frac{Q}{\tau}\int Q(e_i - K'e_o)\,dt \qquad (9)$$

where

$$C_1 = C_2 = C$$

$$\tau = R_i C$$

$$K' = K\frac{R_i}{R_f}.$$

The solution of this integral equation in e_o is the output of the commutated capacitor network.

The actual cancellation of the bending mode signal is accomplished by summing the output of the commutated capacitor network with the input signal as shown in Figure 3.

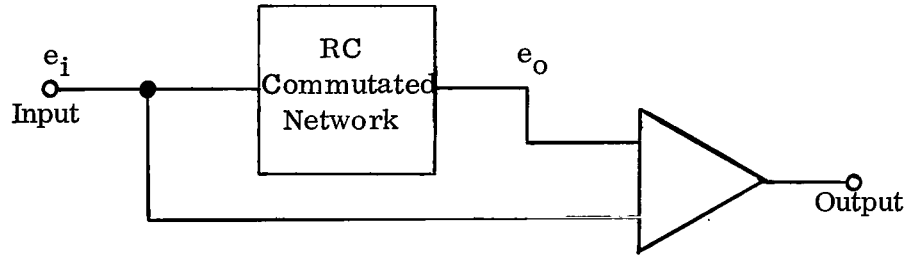

FIGURE 3. NOTCH NETWORK

The amplitude frequency response of the network of Figure 3 exhibits the characteristic "notch."

B. ADDITIONAL CIRCUITS

In addition to the commutated capacitor network of Figure 1, which is the coupled case of the current mode, the following circuits will also be considered:

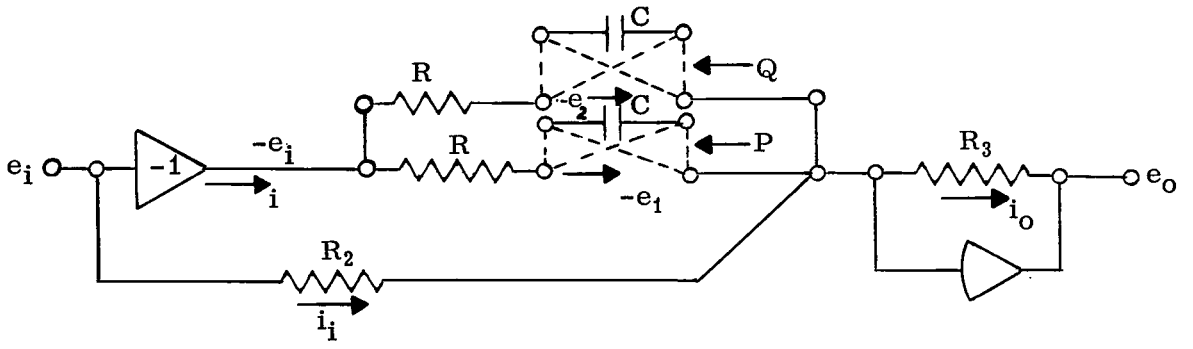

$$e_o = \frac{R_3}{R}\left\{\frac{P}{\tau}\int P\,(e_i - e_1)\,dt + \frac{Q}{\tau}\int Q\,(e_i - e_2)\,dt + e_i\,(K-2)\right\} \qquad (10)$$

where $\tau = RC$ and $K = \frac{R}{R_2}$

FIGURE 4. UNCOUPLED RC COMMUTATED NETWORK, VOLTAGE MODE

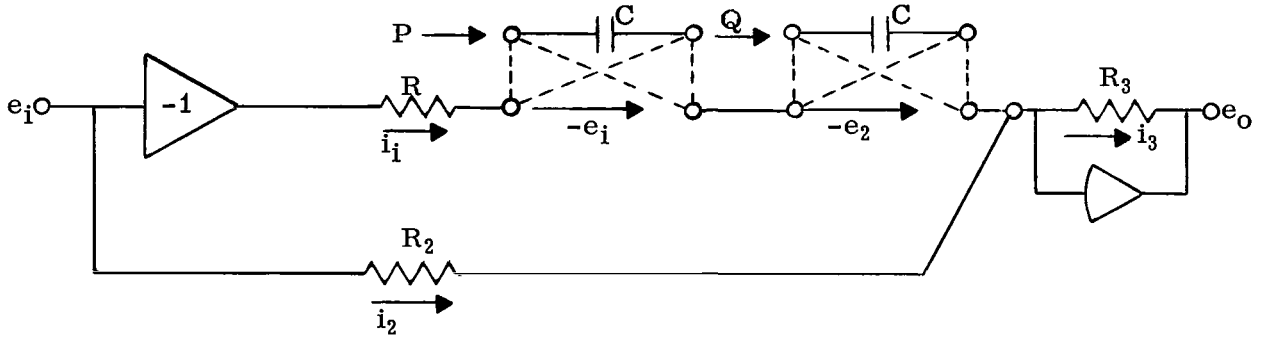

$$e_o = \frac{R_3}{R}\left\{\frac{P}{\tau}\int P\,(Ke_i - \frac{R}{R_3}e_o)\,dt + \frac{Q}{\tau}\int Q\,(Ke_i - \frac{R}{R_3}e_o)\,dt + e_i\,(K-1)\right\} \qquad (11)$$

where $\tau = RC$ and $K = \frac{R}{R_2}$

FIGURE 5. COUPLED RC COMMUTATED NETWORK, VOLTAGE MODE

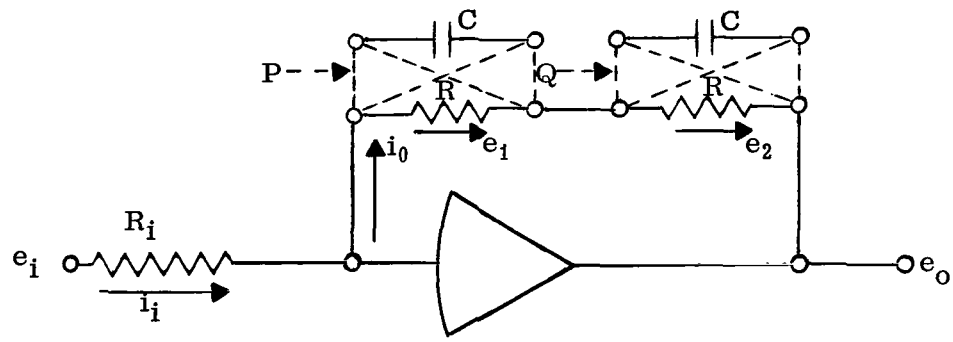

$$e_o = \frac{P}{\tau} \int P \left\{ \frac{R_i}{R_1} e_i - e_1 \right\} dt + \frac{Q}{\tau} \int Q \left\{ \frac{R}{R_1} e_i - e_2 \right\} dt \qquad (12)$$

where $\tau = RC$

FIGURE 6. UNCOUPLED RC COMMUTATED NETWORK, CURRENT MODE

The derivation of the equations for these circuits is given in Reference 3. The terms voltage and current mode refer to the location of the commutated network with respect to the associated operational amplifier. With the proper selection of resistors, the two coupled circuits of Figures 1 and 5 are equivalent, and the circuits of Figures 4 and 6 are equivalent for the uncoupled circuits. Thus, the analysis of the four circuits reduces to Equation (9) of Figure 1 and Equation (10) of Figure 4.

Also note that the circuits of Figures 4 and 5 inherently contain the feedforward path of Figure 3. In contrast, the circuits of Figures 1 and 6 do not have the feedforward path. In Equation (10), the factor K controls the output characteristics of the network shown in Figure 4. For example, if $R_2 = R_3 = R/2$, the network exhibits a bandpass characteristic comparable to the network of Figure 1. To obtain a notch with this network, it is only necessary to adjust the value of K. The value of K that results in the optimum depth of the notch is derived later.

SECTION III. CONVERSION OF THE INTEGRAL EQUATIONS TO A SYSTEM OF DIFFERENTIAL EQUATIONS

One possible approach to the solution of the derived Volterra integral equations is the conversion of the integral equations to a system of first order differential equations with time varying coefficients. The existence of solutions for such systems is treated

extensively in the literature. However, the techniques to obtain an explicit solution are sparse. The time varying coefficients are discontinuous periodic functions, and it is possible to solve the differential equations by introducing a jump function as an auxiliary variable. This jump function enters because time is divided into a succession of equal intervals and the boundary values at the successive points of division can be interpolated by a jump function.

In the following, P(t) and Q(t) have a period of $T = \frac{2\pi}{\omega} = \frac{1}{f}$ as shown in Figure 2. Equations (9) and (10) will be considered; each is treated separately.

A. COUPLED COMMUTATED NETWORKS

If $e_o(0) = 0$, Equation (9) can be reduced to a system of two differential equations using the substitutions:

$$y_1 = \int_0^t P\,[e_i - K'e_o]\,ds \longrightarrow \dot{y}_1 = P\,[e_i - K'e_o]$$

$$y_2 = \int_0^t Q\,[e_i - K'e_o]\,ds \longrightarrow \dot{y}_2 = Q\,[e_i - K'e_o] \qquad (13)$$

Thus

$$\tau e_o(t) = P(t) \int_0^t \frac{dy_1}{ds}\,ds + Q(t) \int_0^t \frac{dy_2}{ds}\,ds = P\,[y_1(t) - y_1(0)] + Q\,[y_2(t) - y_2(0)]$$

or

$$\tau e_o(t) = Py_1(t) + Qy_2(t). \qquad (14)$$

Using the relation $P \cdot P = Q \cdot Q = 1$ and substituting $e_o(t)$ from Equation (14) into Equation (13) yield:

$$\dot{y}_1 + \lambda(y_1 + PQy_2) = Pe_i$$

$$\dot{y}_2 + \lambda(PQy_1 + y_2) = Qe_i \qquad (15)$$

where $\lambda = \frac{K'}{\tau}$.

For convenience, let

$$u = y_1 + y_2, \qquad v = y_1 - y_2. \tag{16}$$

Equation (15) now reads

$$\dot{u} + \lambda(1 + PQ)\,u = (P + Q)\,e_i \qquad u(0) = 0 \tag{17a}$$

$$\dot{v} + \lambda(1 - PQ)\,v = (P - Q)\,e_i \qquad v(0) = 0 \tag{17b}$$

which is a system of two linear independent differential equations with periodically changing coefficients.

The functions $(1 + PQ)$, $(P + Q)$, $(1 - PQ)$, and $(P - Q)$ that appear in Equation (17) are shown in Figure 7.

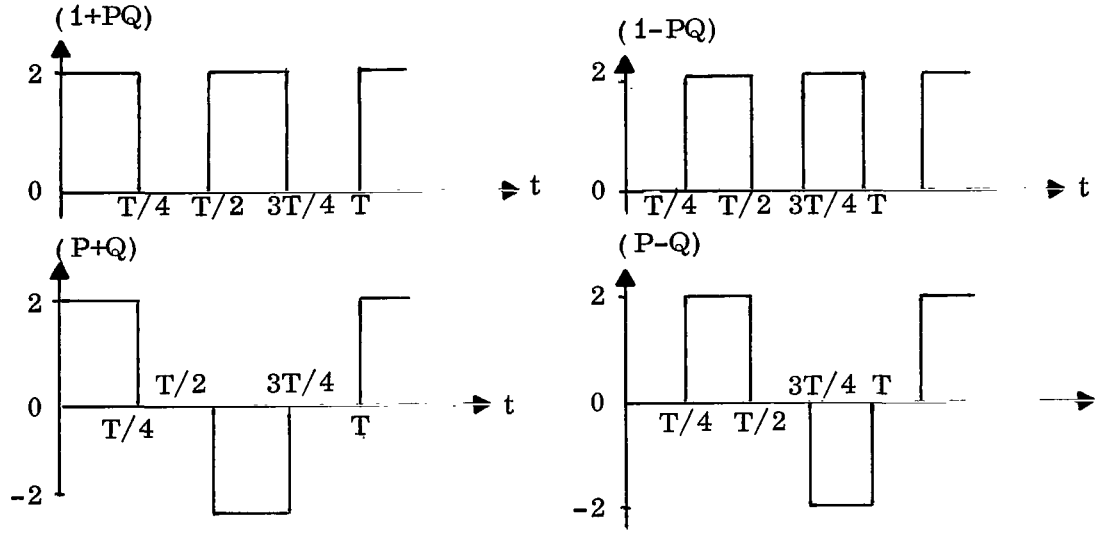

FIGURE 7. FUNCTIONS OF P AND Q

The output in terms of u and v, using Equations (14) and (16), is

$$\tau e_o(t) = \frac{P}{2}(u + v) + \frac{Q}{2}(u - v) = \frac{P + Q}{2}u + \frac{P - Q}{2}v. \tag{18}$$

Reference to Figure 7 shows that $(P + Q)$ and $(P - Q)$ can be expressed as

$$(P+Q) = \begin{cases} 2 & 0 \le t \le T/4 \\ 0 & T/4 \le t \le T/2 \\ -2 & T/2 \le t \le 3T/4 \\ 0 & 3T/4 \le t \le T \\ \cdots & \cdots \end{cases} \qquad (P-Q) = \begin{cases} 0 & 0 \le t \le T/4 \\ 2 & T/4 \le t \le T/2 \\ 0 & T/2 \le t \le 3T/4 \\ -2 & 3T/4 \le t \le T \\ \cdots & \cdots \end{cases}$$

Equation (18) is then

$$\tau e_o(t) = \begin{cases} u & 0 \le t \le T/4 \\ v & T/4 \le t \le T/2 \\ -u & T/2 \le t \le 3T/4 \\ -v & 3T/4 \le t \le T \\ u & T \le t \le 5T/4 \\ v & 5T/4 \le t \le 3T/2 \\ \cdots & \cdots \end{cases} \qquad (19)$$

Hence, the solutions for u (or v) need only be obtained for every odd (or even) quarter-period. The solution of these equations will be postponed until the differential equations for the additional cases are derived.

B. UNCOUPLED COMMUTATED NETWORK

In Equation (10) let $R = R_3$; then

$$e_o = \frac{P}{\tau} \int_0^t P(e_i - e_1)\, ds + \frac{Q}{\tau} \int_0^t Q(e_i - e_2)\, ds + e_i(K - 2). \qquad (20)$$

Now let

$$y_1(t) = \frac{1}{\tau} \int_0^t P(e_i - e_1)\, ds \tag{21}$$

then

$$\dot{y}_1(t) = \frac{P}{\tau} (e_i - e_1). \tag{22}$$

Similarly,

$$y_2(t) = \frac{1}{\tau} \int_0^t Q(e_i - e_2)\, ds \tag{23}$$

$$\dot{y}_2(t) = \frac{Q}{\tau} (e_i - e_2). \tag{24}$$

For this uncoupled case $e_1 = Py_1(t)$ and $e_2 = Qy_2(t)$, so Equations (22) and (24) become

$$\tau\dot{y}_1 + y_1 = Pe_i \tag{25}$$

$$\tau\dot{y}_2 + y_2 = Qe_i \tag{26}$$

and Equation (20) becomes

$$e_o = Py_1 + Qy_2 + (K - 2)e_i. \tag{27}$$

SECTION IV. SOLUTION OF THE DIFFERENTIAL EQUATIONS

A. COUPLED RC COMMUTATED NETWORK

The first set of differential equations to be considered corresponds to the coupled RC commutated network of Figure 1 and the related Equations (17a and 17b). The solutions will be restricted for functions of the input $e_i(t)$ which are believed to be of prime importance.

1. Input Equals A sin $(\omega_c t + \varphi)$, $\omega_c = k\omega$. Let $e_i(t) = A \sin(\omega_c t + \varphi)$ where $\omega_c = k\omega$; k is a positive integer and φ is by definition the phase relationship with respect to the fundamental sine component of P square wave. The previously defined period of P(t) and Q(t) is $T = \frac{2\pi}{\omega}$ or $\omega = \frac{2\pi}{T}$. Consider first Equation (17a) and refer

$$\dot{u} + \lambda(1 + PQ)\, u_i = (P + Q)\, e_i \qquad (28)$$

to Figure 7 for the functions $(1 + PQ)$ and $(P + Q)$. The equation for u becomes a repetition of four separate equations where the boundary conditions between solutions must be matched to obtain a continuous solution (Ref. 5).

For simplicity, t will be measured from the beginning of the nth cycle. The four separate differential equations are

$$\dot{u}_1 + 2\lambda u_1 = 2A \sin(k\omega t + \varphi) \qquad 0 \le t \le T/4 \qquad (29a)$$

$$\dot{u}_2 = 0 \qquad T/4 \le t \le T/2 \qquad (29b)$$

$$\dot{u}_3 + 2\lambda u_3 = -2A \sin(k\omega t + \varphi) \qquad T/2 \le t \le 3T/4 \qquad (29c)$$

$$\dot{u}_4 = 0 \qquad 3T/4 \le t \le T \qquad (29d)$$

where $u = u_j$ $(j = 1, 2, 3, 4)$ in the quarter-period of interest. The value of $u_1(T/4)$ is the initial value of $u_2(t)$. Since $u_2(t)$ is equal to a constant, the initial value of $u_3(t)$ equals the final value of $u_1(t)$.

$$u_3(T/2) = u_1(T/4).$$

Let $\gamma_1(n)$ be the initial value for the nth cycle. The solutions of Equation (29) are:

$$u_1(t) = \frac{2A}{k^2\omega^2+4\lambda^2}\left[2\lambda \sin(k\omega t + \varphi) - k\omega \cos(k\omega t + \varphi) - (2\lambda \sin\varphi - k\omega \cos\varphi)\, e^{-2\lambda t}\right]$$

$$+ \gamma_1(n)\, e^{-2\lambda t} \qquad 0 \le t \le T/4 \qquad (30a)$$

$$u_2(t) = u_1(T/4) \qquad T/4 \le t \le T/2 \qquad (30b)$$

$$u_3(t) = \left[u_1(T/4) + (-1)^k \frac{2A}{k^2\omega^2+4\lambda^2}(2\lambda \sin\varphi - k\omega \cos\varphi)\right] e^{-2\lambda t+\lambda T}$$

$$- \frac{2A}{k^2\omega^2+4\lambda^2}\left[2\lambda \sin(k\omega t + \varphi) - k\omega \cos(k\omega t + \varphi)\right] \quad T/2 \le t \le 3T/4 \qquad (30c)$$

$$u_4(t) = u_3(3T/4) \qquad 3T/4 \le t \le T. \qquad (30d)$$

Since $\sin(k\omega t + \varphi)$ has period $\frac{T}{k}$, the final value of u_4 for the nth cycle is the initial value, $\gamma_1(n+1)$, for the $(n+1)^{st}$ cycle. Thus,

$$\gamma_1(n+1) = u_4(T) = u_3\left(\frac{3T}{4}\right)$$

$$= \left[u_1(T/4) + (-1)^k \frac{2A}{k\omega^2 + 4\lambda^2}(2\lambda \sin\varphi - k\omega\cos\varphi)\right]e^{-\lambda T/2} \qquad (31)$$

$$- \frac{2A}{k^2\omega^2 + 4\lambda^2}\left[2\lambda \sin\left(k\frac{3\pi}{2} + \varphi\right) - k\omega\cos\left(k\frac{3\pi}{2} + \varphi\right)\right].$$

Substituting the value of $u_1(T/4)$ from Equation (30a) into this expression yields:

$$\gamma_1(n+1) - a_1\gamma_1(n) = b_1 \qquad (32)$$

where

$$a_1 = e^{-\lambda T}$$

$$b_1 = \frac{2A}{k^2\omega^2 + 4\lambda^2}\left\{\begin{array}{l} 2\lambda\left[(-1)^k e^{-\lambda T/2}\sin\varphi + e^{-\lambda T/2}\sin\left(k\frac{\pi}{2} + \varphi\right) - e^{-\lambda T}\sin\varphi - \sin\left(k\frac{3\pi}{2} + \varphi\right)\right] \\ -k\omega\left[(-1)^k e^{-\lambda T/2}\cos\varphi + e^{-\lambda T/2}\cos\left(k\frac{\pi}{2} + \varphi\right) - e^{-\lambda T}\cos\varphi - \cos\left(k\frac{3\pi}{2} + \varphi\right)\right] \end{array}\right\}$$

$\gamma_1(n)$ is now extended to include non-integral values of n by introducing the jump function $[\gamma_1(n)]$, where the symbol [x] reads the greatest integer in x, if x is a number. Equation (32) becomes

$$[\gamma_1(n+1)] - a_1[\gamma_1(n)] = b_1. \qquad (33)$$

The solution of this linear difference equation (Ref. 5) is

$$[\gamma_1(n)] = b_1\left[\frac{a_1^n - 1}{a_1 - 1}\right] \qquad 0 \le n, \ [\gamma_1(0) = 0]. \qquad (34)$$

Recovering the initial points of Equation (34) and introducing them in $u_1(t)$ and $u_3(t)$ of Equation (30) result in the solution for $u_1(t)$ and $u_3(t)$.

The analysis for v of Equation (17b) follows exactly as in the solution for u and is summarized below. Corresponding to Equation (29),

$$\begin{aligned}
\dot{v}_1 &= 0 && 0 \le t \le T/4 \\
\dot{v}_2 + 2\lambda v_2 &= 2A \sin(k\omega t + \varphi) && T/4 \le t \le T/2 \\
\dot{v}_3 &= 0 && T/2 \le t \le 3T/4 \\
\dot{v}_4 + 2\lambda v_4 &= -2A \sin(k\omega t + \varphi) && 3T/4 \le t \le T
\end{aligned} \tag{35}$$

Let $\gamma_2(n)$ be the initial value for the nth cycle of the v_1 equation. An analogous difference equation containing a_2 and b_2 similar to Equation (33) is obtained.

From Equation (19), the final solution is

$$e_o(t,n,k) = \frac{1}{\tau}\begin{cases} u_1(t,n,k) & 0 \le t \le T/4 \\ v_2(t,n,k) & T/4 \le t \le T/2 \quad (n=0,1,2,\ldots) \\ -u_3(t,n,k) & T/2 \le t \le 3T/4 \quad (k=1,2,3,\ldots) \\ -v_4(t,n,k) & 3T/4 \le t \le T \end{cases} \tag{36}$$

where

$$u_1(t,n,k) = \frac{2A}{k^2\omega^2+4\lambda^2}\left[2\lambda \sin(k\omega t + \varphi) - k\omega \cos(k\omega t + \varphi) - c_2 e^{-2\lambda t}\right] + b_1 \frac{a_1^n - 1}{a_1 - 1} e^{-2\lambda t} \qquad (0 \le t \le T/4)$$

$$v_2(t,n,k) = \frac{2A}{k^2\omega^2+4\lambda^2}\left[2\lambda \sin(k\omega t + \varphi) - k\omega \cos(k\omega t + \varphi) - c_1 e^{-2\lambda t + \frac{\lambda T}{2}}\right] + b_2 \frac{a_1^n - 1}{a_1 - 1} e^{-2\lambda t}\frac{\lambda T}{2} \qquad \left(\frac{T}{4} \le t \le \frac{T}{2}\right)$$

$$-u_3(t,n,k) = \frac{2A}{k^2\omega^2+4\lambda^2}\left\{\begin{array}{l} 2\lambda \sin(k\omega t+\varphi) - k\omega \cos(k\omega t+\varphi) - \left[c_1+(-1)^k c_2\right] e^{-2\lambda t+\lambda T} \\ \\ + c_2\, e^{-2\lambda t+\frac{\lambda T}{2}} \end{array}\right\}$$

$$- b_1 \frac{a_1^n - 1}{a_1 - 1}\, e^{-2\lambda t+\lambda T/2} \qquad \left(\frac{T}{2} \le t \le \frac{3T}{4}\right)$$

$$-v_4(t,n,k) = \frac{2A}{k^2\omega^2+4\lambda^2}\left\{\begin{array}{l} 2\lambda \sin(k\omega t+\varphi) - k\omega \cos(k\omega t+\varphi) + c_1\, e^{-2\lambda t+\lambda T} \\ \\ -\left[(-1)^k c_2 + c_3\right] e^{-2\lambda t+\frac{3\lambda T}{2}} \end{array}\right.$$

$$- b_2 \frac{a_1^n - 1}{a_1 - 1}\, e^{-2\lambda t+\lambda T} \qquad \left(\frac{3T}{4} \le t \le T\right)$$

and

$$a_1 = a_2 = e^{-\lambda T}$$

$$b_1 = \frac{2A}{k^2\omega^2+4\lambda^2}\left[\left(c_1 + (-1)^k c_2\right) e^{-\lambda T/2} - c_2 e^{-\lambda T} - c_3\right]$$

$$b_2 = \frac{2A}{k^2\omega^2+4\lambda^2}\left[\left(c_3 + (-1)^k c_2\right) e^{-\lambda T/2} - c_1 e^{-\lambda T} - c_2\right]$$

$$c_1 = \left[2\lambda \sin\left(k\frac{\pi}{2}+\varphi\right) - k\omega \cos\left(k\frac{\pi}{2}+\varphi\right)\right]$$

$$c_2 = \left[2\lambda \sin\varphi - k\omega \cos\varphi\right]$$

$$c_3 = \left[2\lambda \sin\left(k\frac{3\pi}{2}+\varphi\right) - k\omega \cos\left(k\frac{3\pi}{2}+\varphi\right)\right]$$

$$\lambda = K'/\tau.$$

Since n is a second independent variable (assuming k fixed), this expression for $e_o(t)$ is valid for cycles during the transient buildup as well as for cycles during the steady state.

Figures 8 through 15 show various cases for the parameters considered. Figure 8 is an enlargement of a typical output wave shape for the input signal frequency equal to the switching frequency of the P and Q commutating functions with $\varphi = 0°$ and depicts the transient buildup. The advantage of the second independent variable n is vividly shown for n = 0 and n = 1. The four solution curves for each cycle can also be noted. Figure 9 is a comparison of wave shapes of the steady state outputs for various frequencies. The amplitudes of the "square waves" are relatively invariant for the values considered; however, this is not true in general. Figure 10 shows the output for k = 3 and k = 5. Figure 11 is a comparison of the output $e_o(t)$ with φ as a parameter. Comparing the case for $\varphi = 22.5°$ with Figure 12 (an equipment run) shows the two wave shapes to be comparable. This can also be noticed by comparing Figure 13 for $\varphi = 80°$ with Figure 14. Figure 15 is also an equipment run and is inserted here for comparison.

2. Notch Frequency Analysis. In the previous section, a very general expression [Equation (36)] for the output $e_o(t)$ was obtained. If the network is to function properly as a filter, the amplitude of the output must be kept to a minimum (by proper choice of parameters) when the circuit is being forced at the resonant or notch frequency ($\omega = \omega_c$). The investigation in this section is concerned with the notch frequency and is separated into three subsections. First the waveshape of the output is treated with φ as a parameter to compare analytical results with actual equipment time recordings. The special case for $\varphi = 0°$ is then considered in detail. Finally, an analysis of the output wave for its first harmonic components is performed for $\varphi = 0°$. The analysis for a variable φ is postponed until special commutating functions are considered.

Case a. $\omega = \omega_c$

In Equation (36) let k = 1. Since $e^{-\lambda T} < 1$

$$\lim_{n \to \infty} a_1^n = \lim_{n \to \infty} a_2^n = \lim_{n \to \infty} e^{-\lambda T n} = 0.$$

Only steady state values are of interest. Therefore, we have assumed the limiting values.

There is no loss of generality if A = 1; hence, by substituting for a_1, b_1, and b_2, Equation (36) becomes

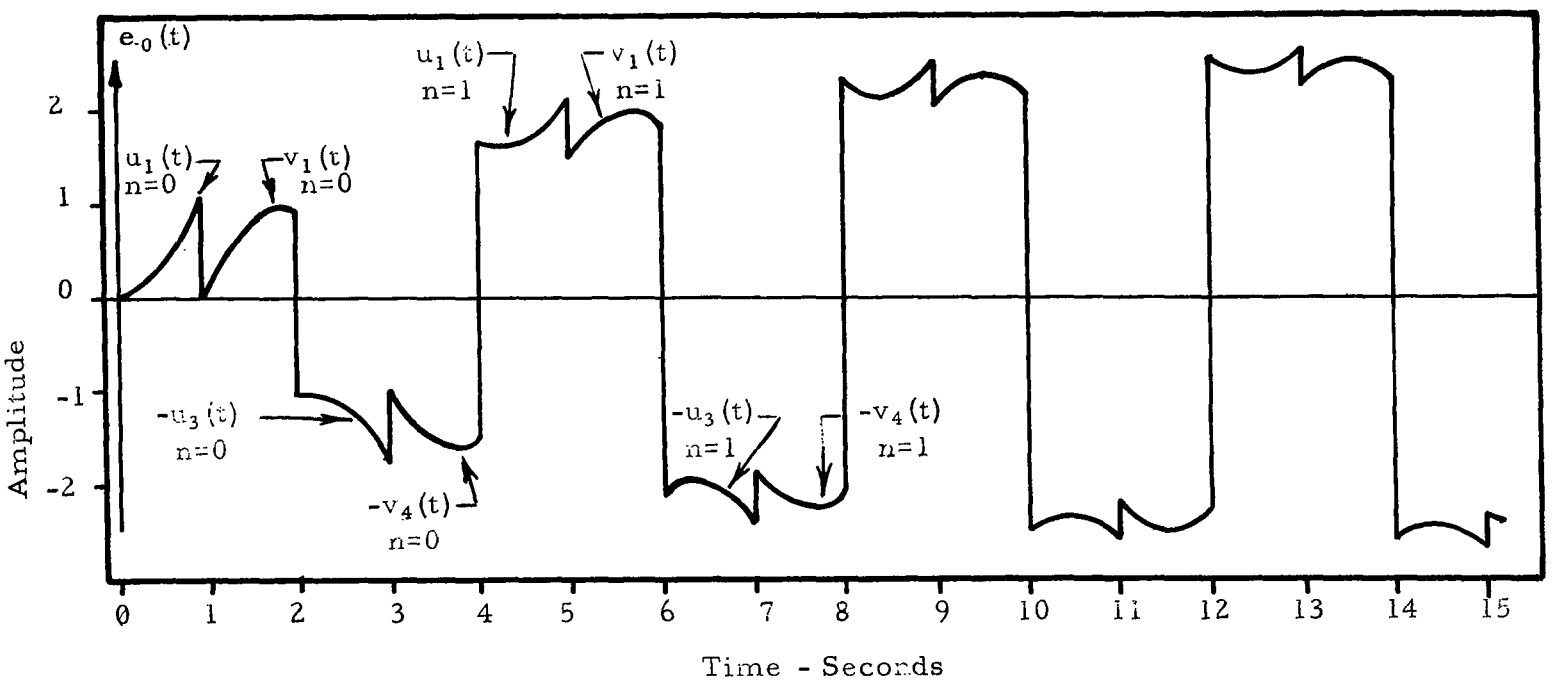

$f = 0.25$ Hz $\quad f_c = 0.25$ Hz $\quad \varphi = 0°$

$k = 1.0$ $\quad K' = 0.25$ $\quad A = 1.0$

$\tau = 1.0$ s

FIGURE 8. RC COMMUTATED NETWORK OUTPUT VS TIME (COUPLED)

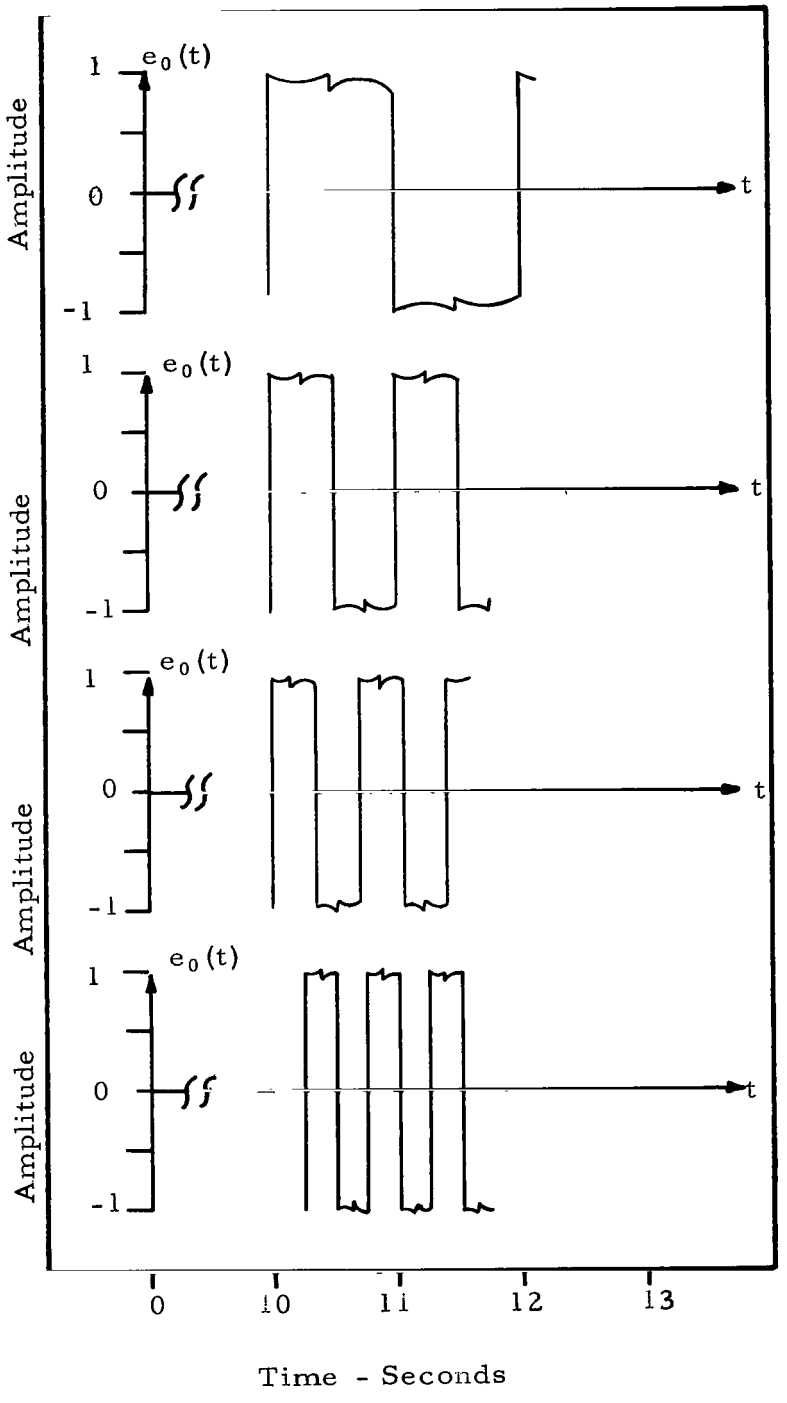

f=0.5 Hz f_c = 0.5 Hz
k = 1.0 K' = 0.675
τ = 1.0 s A= 1.0
φ = 0°

f = 1.0 Hz f_c = 1.0 Hz
k = 1.0 K'= 0.675
τ = 1.0 s A = 1.0
φ = 0°

f = 1.4 Hz f_c = 1.4 Hz
k = 1.0 K' = 0.675
τ = 1.0 s. A = 1.0
φ = 0°

f = 2.0 Hz f_c = 2.0 Hz
k = 1.0 K' = 0.674
τ = 1.0 s A = 1.0
φ = 0°

FIGURE 9. RC COMMUTATED NETWORK OUTPUT VS TIME (COUPLED)

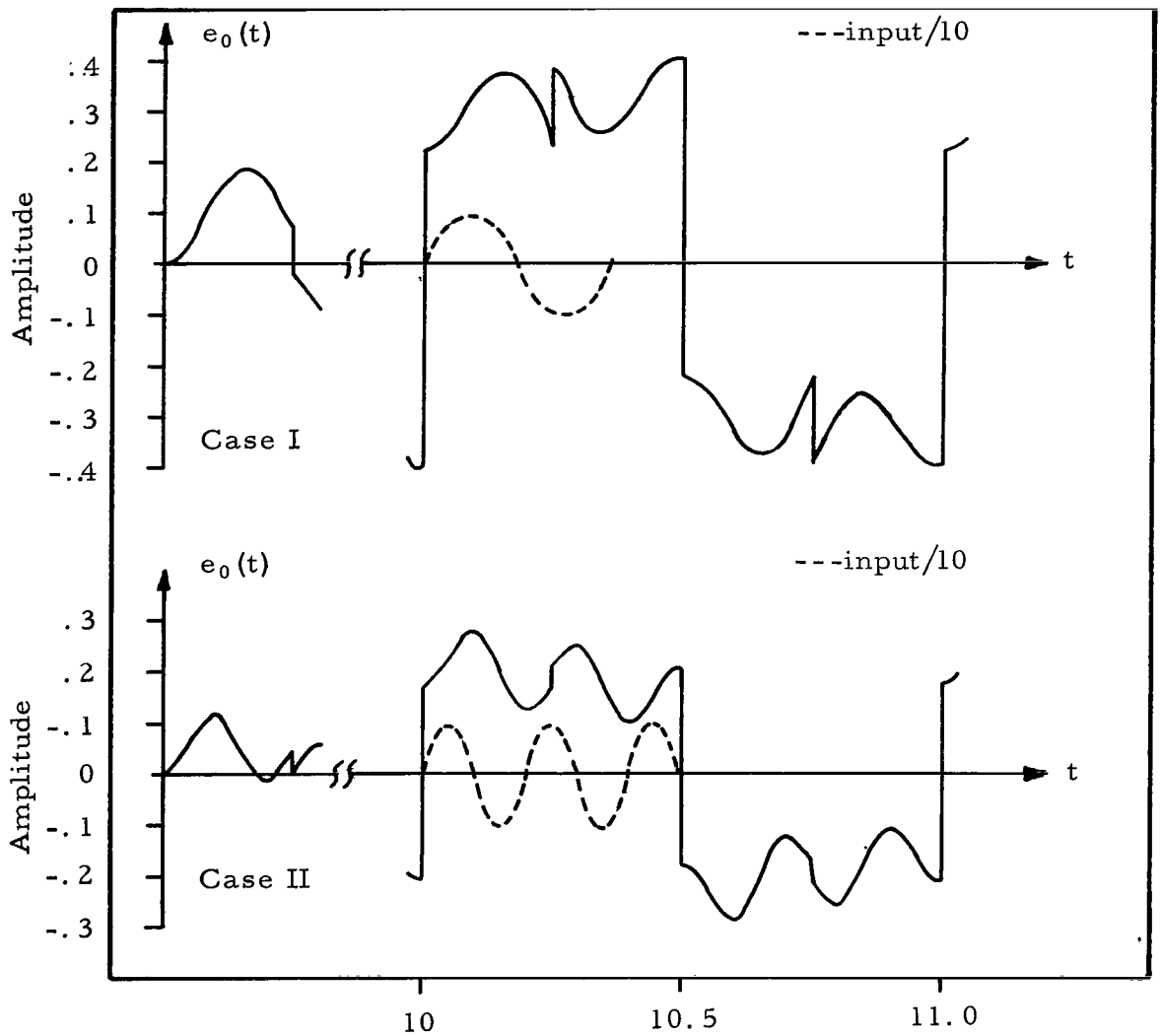

Case I: f = 1.0 Hz f_c = 3.0 Hz k = 3.0 A = 1.0
K' = 0.675 τ = 1.0 s $\varphi = 0°$

Case II: f = 1.0 Hz f_c = 5.0 Hz k = 5.0 A = 1.0
K' = 0.675 τ = 1.0 s $\varphi = 0°$

FIGURE 10. RC COMMUTATED NETWORK OUTPUT VS TIME (COUPLED)

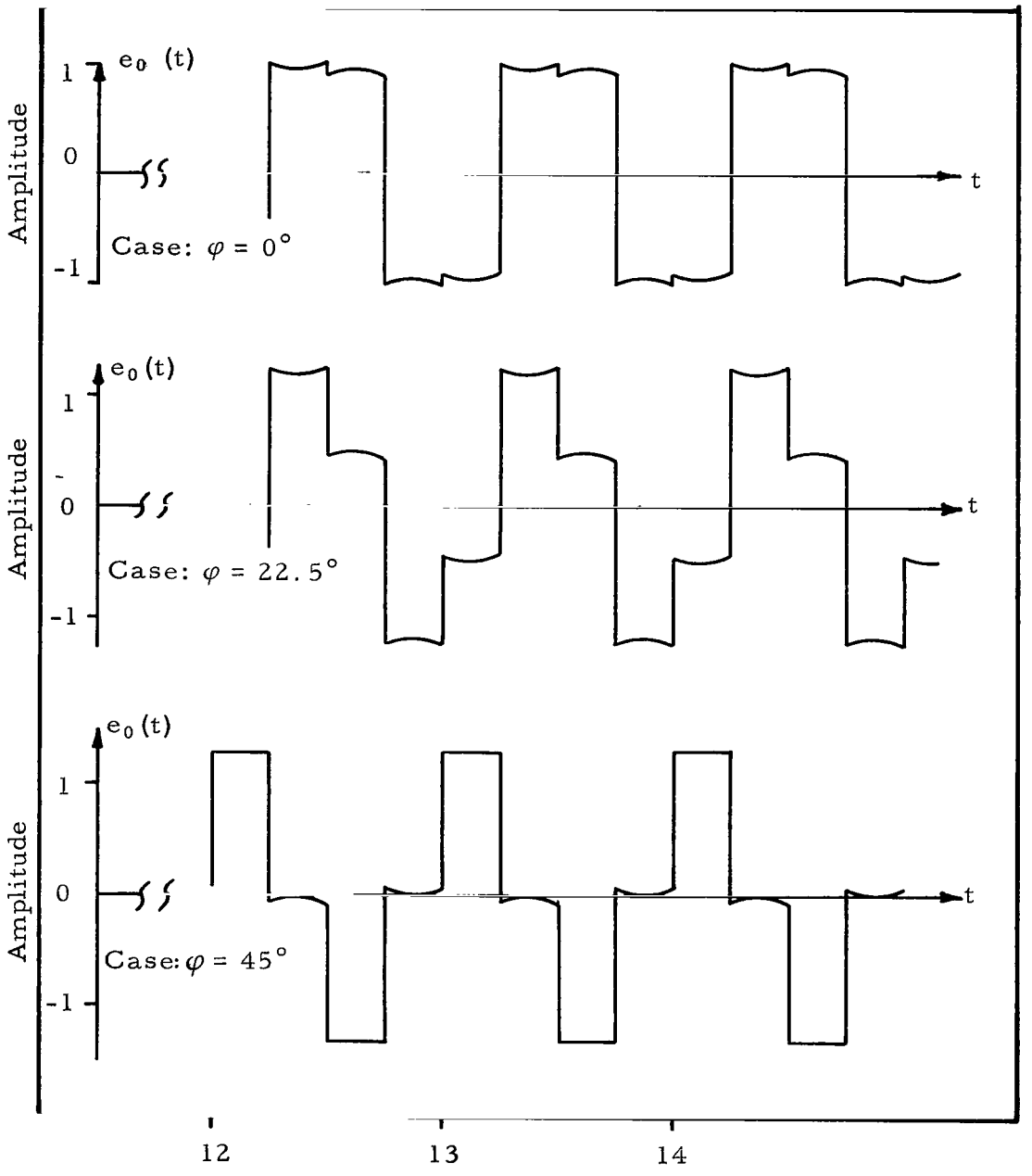

All Cases: f = 1.0 Hz f_c = 1.0 Hz k = 1.0 A = 1.0

K' = 0.675 τ = 1.0 s

FIGURE 11. RC COMMUTATED NETWORK OUTPUT VS TIME (COUPLED)

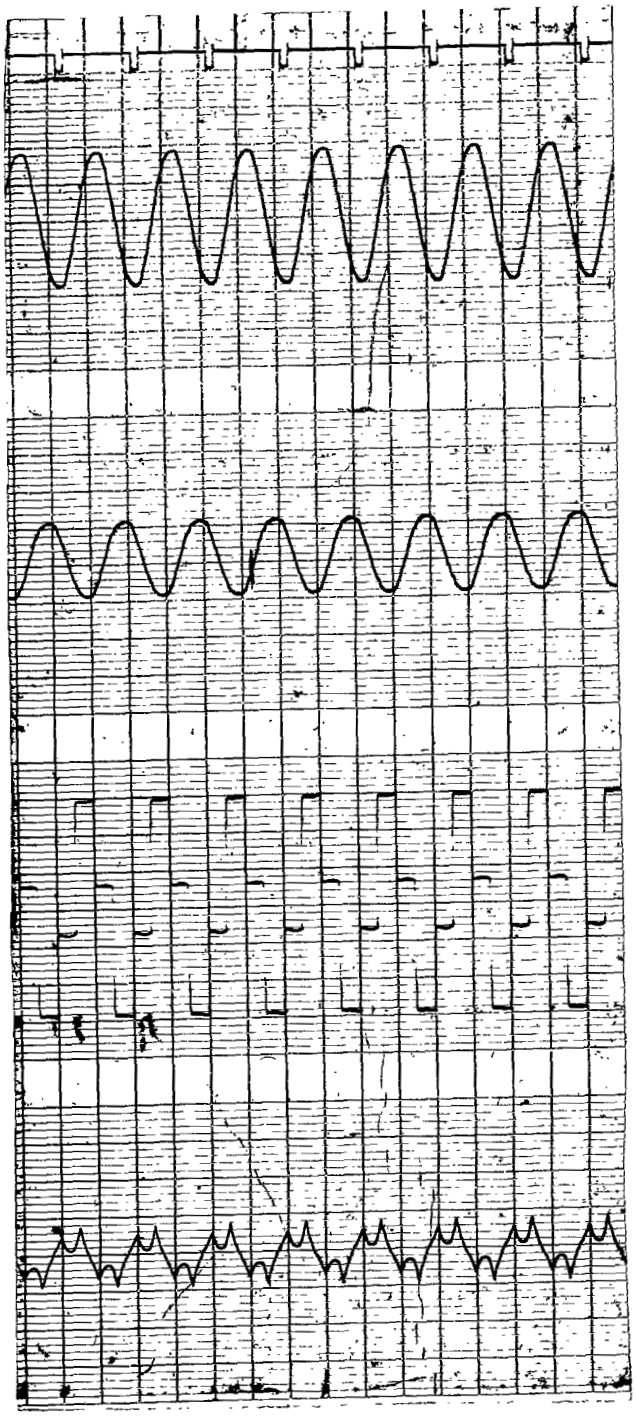

ATN Filter Input

RC Commutated Network Input

RC Commutated Network Output

ATN Filter Output

ATN Input: Freq. = 1.0 Hz
Lock-On Oscillator Freq. = 1.0 Hz
Switching Capacitors = 1.0 μF (τ = 1.0)
Feedback Pot Setting (K') = 0.675

FIGURE 12. TIME TRACES

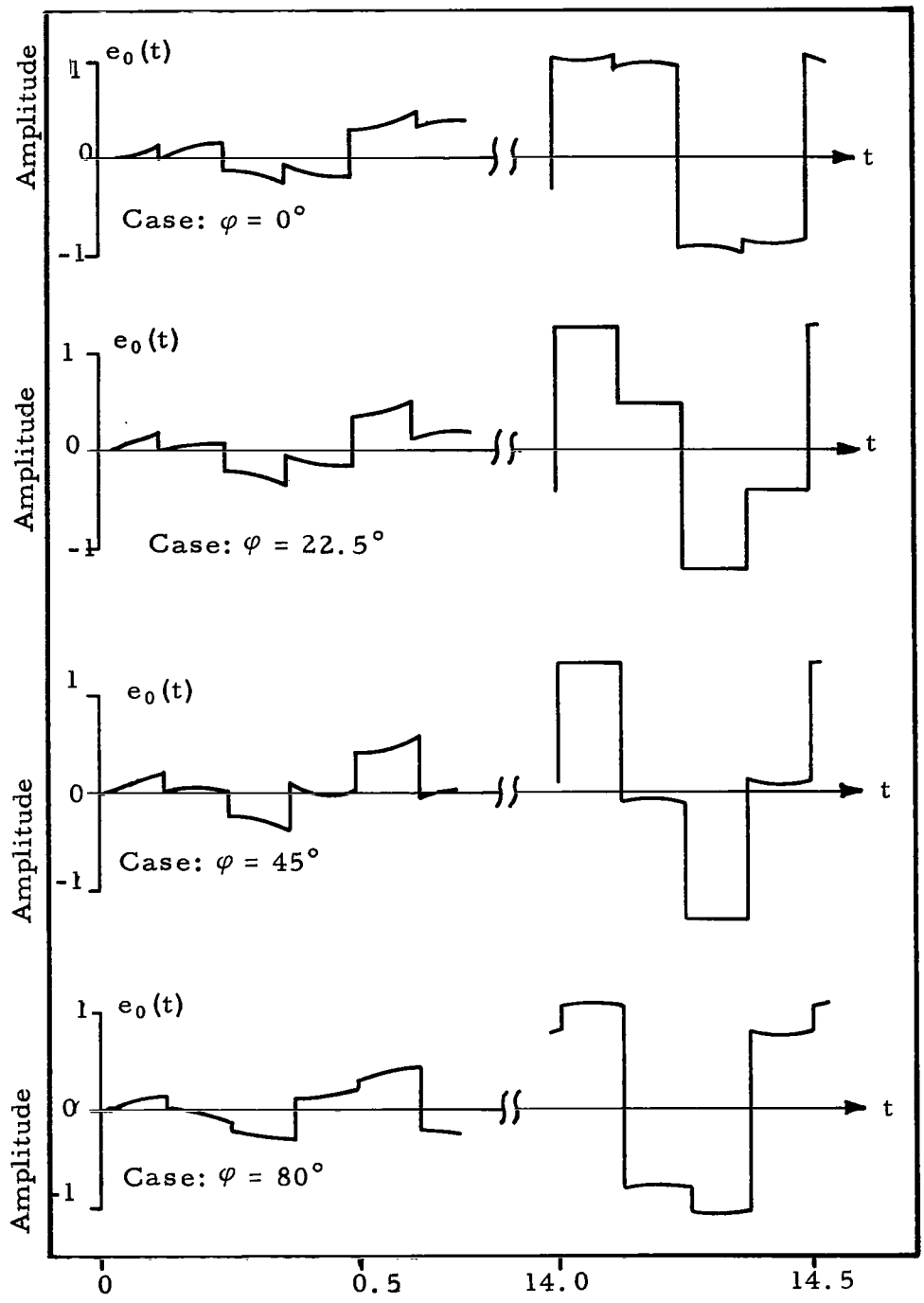

All Cases: f = 2.0 Hz f_c = 2.0 Hz k = 1.0 A = 1.0
K' = 0.675 τ = 1.0 s

FIGURE 13. RC COMMUTATED NETWORK OUTPUT VS TIME (COUPLED)

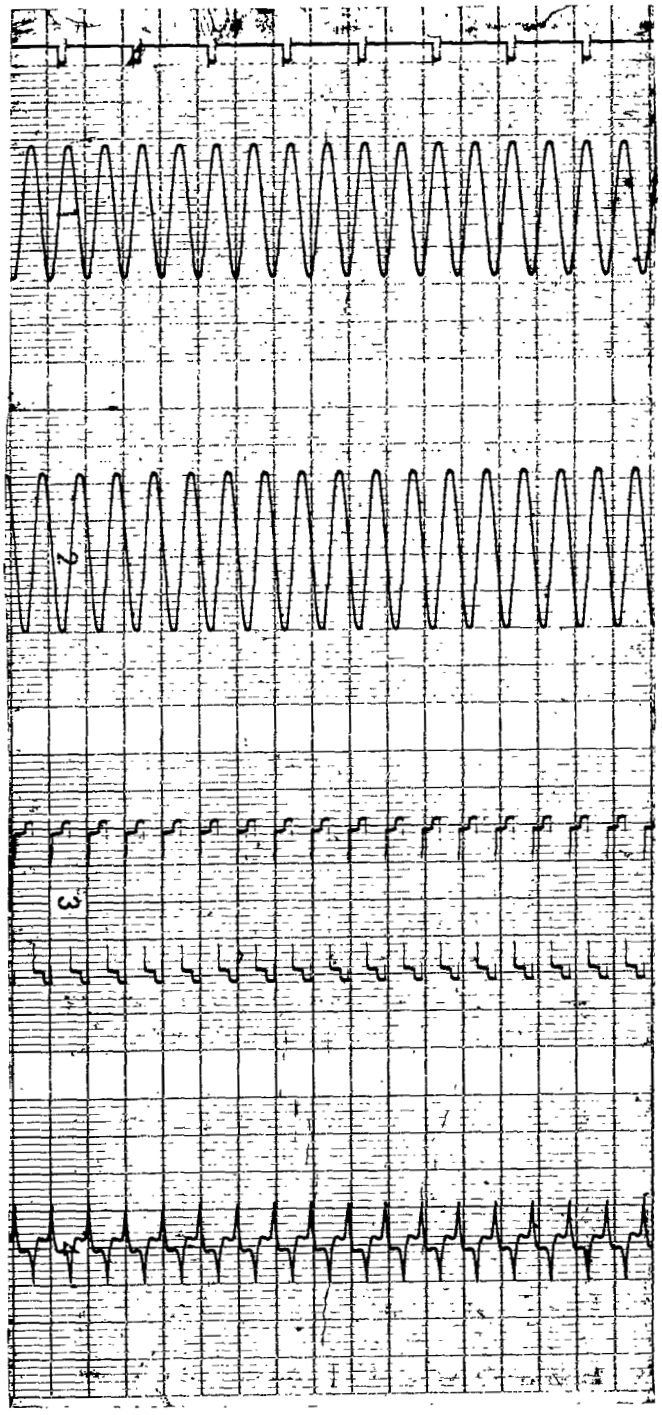

ATN Filter Input

RC Commutated Network Input

RC Commutated Network Output

ATN Filter Output

ATN Input: Freq. = 2.0 Hz
Lock-On Oscillator Freq. = 2.0 Hz
Switching Capacitors = 1.0 μF (τ = 1.0)
Feedback Pot Setting (K') = 0.675

FIGURE 14. TIME TRACES

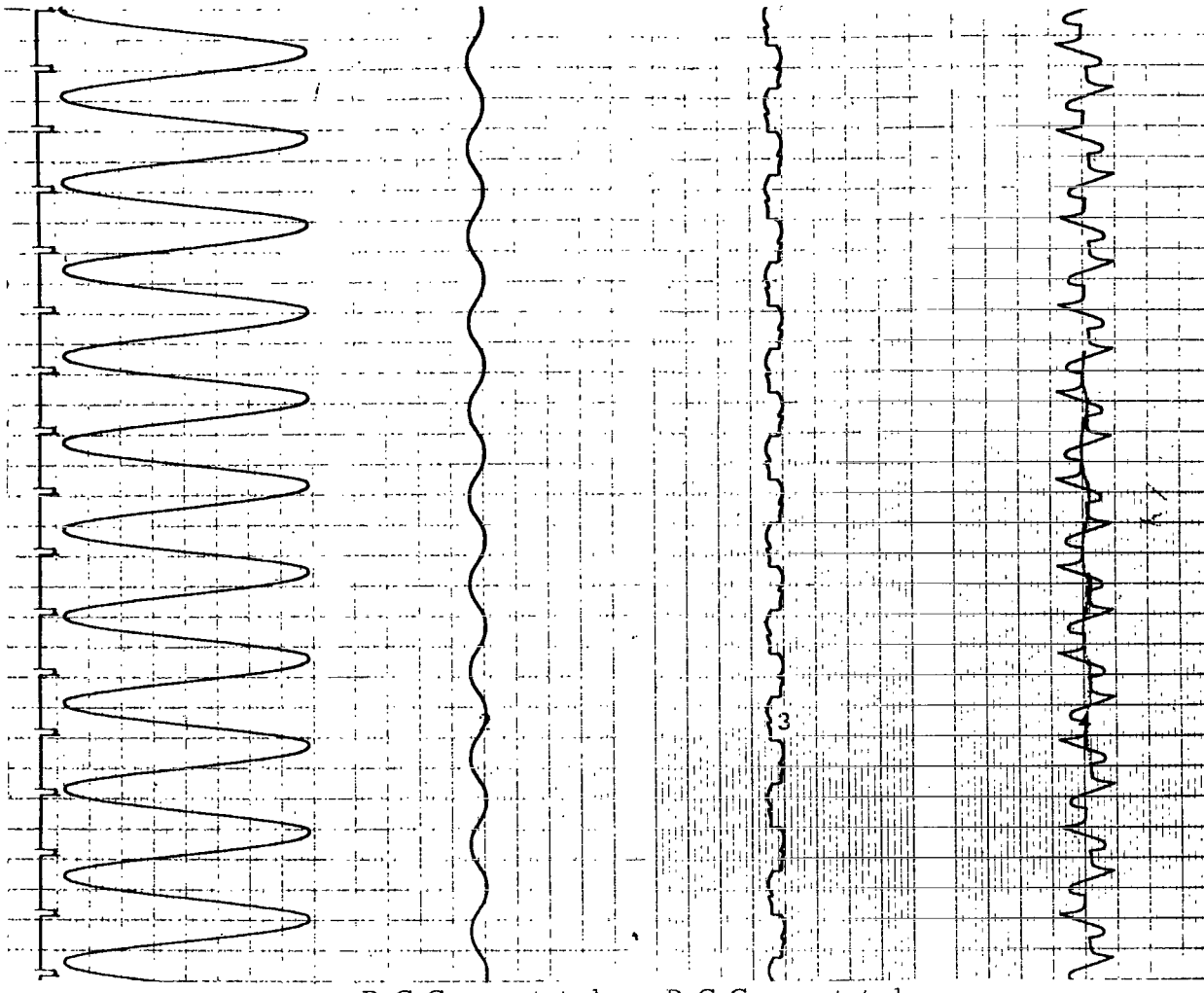

ATN Filter Input
0.2 Volts/line

R C Commutated
Network
Input
0.2 Volts/line

R C Commutated
Network
Output
0.2 Volts/line

ATN Filter
Output
0.2 Volts/line

ATN Input: Freq. = 0.7 Hz
Lock-On Oscillator Free Running Freq. = 1.0 Hz

Switching Capacitors = 0.1 μF
Feedback Pot Setting = 0.852

FIGURE 15. TIME TRACES

$$u_1(t) = \frac{2}{\omega^2+4\lambda^2}\left[2\lambda \sin(\omega t+\varphi) - \omega\cos(\omega t+\varphi) + \frac{(\omega+2\lambda)\cos\varphi + (\omega-2\lambda)\sin\varphi}{1-e^{-\lambda T/2}} e^{-2\lambda t}\right]$$

$$(0 \le t \le T/4)$$

$$v_2(t) = \frac{2}{\omega^2+4\lambda^2}\left[2\lambda \sin(\omega t+\varphi) - \omega\cos(\omega t+\varphi) + \frac{(\omega-2\lambda)\cos\varphi - (\omega+2\lambda)\sin\varphi}{1-e^{-\lambda T/2}} e^{-2\lambda(t-T/4)}\right]$$

$$(T/4 \le t \le T/2)$$

$$-u_3(t) = \frac{2}{\omega^2+4\lambda^2}\left[2\lambda \sin(\omega t+\varphi) - \omega\cos(\omega t+\varphi) - \frac{(\omega+2\lambda)\cos\varphi + (\omega-2\lambda)\sin\varphi}{1-e^{-\lambda T/2}} e^{-2\lambda(t-T/2)}\right] \quad (37)$$

$$(T/2 \le t \le 3T/4)$$

$$-v_4(t) = \frac{2}{\omega^2+4\lambda^2}\left[2\lambda \sin(\omega t+\varphi) - \omega\cos(\omega t+\varphi) - \frac{(\omega-2\lambda)\cos\varphi - (\omega+2\lambda)\sin\varphi}{1-e^{-\lambda T/2}} e^{-2\lambda(t-3T/4)}\right]$$

$$(3T/4 \le t \le T)$$

and

$$e_o(t) = \frac{1}{\tau} \begin{cases} u_1(t) & 0 \le t \le T/4 \\ v_2(t) & T/4 \le t \le T/2 \\ -u_3(t) & T/2 \le t \le 3T/4 \\ -v_4(t) & 3T/4 \le t \le T \end{cases} \qquad (t >> 0)$$

These cases are shown in Figures 9, 11, 12, 13, 14, and 15. Note the similarity of the second graph in Figure 11 to the third time recording of Figure 12. Also note the similarity of Figure 13 for $\varphi = 80°$ to the time recording of Figure 14.

Case b. $\omega = \omega_c$, $\varphi = 0°$

Let $\varphi = 0°$ in Equation (37). Then,

$$u_1(t) = \frac{2}{\omega^2+4\lambda^2}\left[2\lambda \sin \omega t - \omega \cos \omega t + \frac{\omega + 2\lambda}{1 - e^{-\lambda T/2}} e^{-2\lambda t}\right] \qquad (0 \le t \le T/4)$$

$$v_2(t) = \frac{2}{\omega^2+4\lambda^2}\left[2\lambda \sin \omega t - \omega \cos \omega t + \frac{\omega - 2\lambda}{1 - e^{-\lambda T/2}} e^{-2\lambda(t-T/4)}\right] \qquad (T/4 \le t \le T/2) \qquad (38)$$

$$-u_3(t) = \frac{2}{\omega^2+4\lambda^2}\left[2\lambda \sin \omega t - \omega \cos \omega t - \frac{\omega + 2\lambda}{1 - e^{-\lambda T/2}} e^{-2\lambda(t-T/2)}\right] \qquad (T/2 \le t \le 3T/4)$$

$$-v_4(t) = \frac{2}{\omega^2+4\lambda^2}\left[2\lambda \sin \omega t - \omega \cos \omega t - \frac{\omega - 2\lambda}{1 - e^{-\lambda T/2}} e^{-2\lambda(t-3T/4)}\right] \qquad (3T/4 \le t \le T)$$

Typical cases are shown in Figure 9.

Case c. Fourier Analysis

If

$$e_o(t) \sim \frac{\alpha_0}{2} + \sum_{m=1}^{\infty} (\alpha_m \cos m\omega t + \beta_m \sin m\omega t)$$

and Equation (38) is used for $e_o(t)$, the amplitudes for the fundamental frequency are calculated to be

$$\alpha_0 = 0$$

$$\alpha_1 = \frac{2}{\tau T} \cdot \frac{2}{\omega^2+4\lambda^2} \left\{ -\pi + \frac{2}{(\omega^2+4\lambda^2)\left(1 - e^{-\lambda T/2}\right)} \left[(4\lambda^2 + 4\lambda\omega - \omega^2) - e^{-\lambda T/2} (4\lambda^2 - 4\lambda\omega - \omega^2) \right] \right\} \tag{39}$$

$$\beta_1 = \frac{2}{\tau T} \frac{2}{\omega^2+4\lambda^2} \left\{ \lambda T + \frac{2}{(\omega^2+4\lambda^2)\left(1 - e^{-\lambda T/2}\right)} \left[(\omega^2 + 4\lambda\omega - 4\lambda^2) + e^{-\lambda T/2} (\omega^2 - 4\lambda\omega - 4\lambda^2) \right] \right\}.$$

These equations can be put into a very convenient form by letting

$$x = \frac{2\lambda}{\omega} = \frac{2K'}{\lambda\tau}.$$

Thus

$$\alpha_1 = \frac{1}{K'} \cdot \frac{x}{\pi(1+x^2)} \left[-\pi + 2 \frac{(x^2 + 2x - 1) - e^{-\frac{\pi}{2}x} (x^2 - 2x - 1)}{(1 + x^2)\left(1 - e^{-\frac{\pi}{2}x}\right)} \right]$$

$$\beta_1 = \frac{1}{K'} \frac{x}{\pi(1+x^2)} \left[\pi x - 2 \frac{(x^2 - 2x - 1) + e^{-\frac{\pi}{2}x} (x^2 + 2x - 1)}{(1 + x^2)\left(1 - e^{-\frac{\pi}{2}x}\right)} \right]. \tag{40}$$

The functions $\alpha_1 K'$ and $\beta_1 K'$ are shown in Figure 16. In the operating region, the quadrature component α_1 is nearly zero, while $\beta_1 \approx \frac{8}{\pi^2 K'}$. The following extremes are noted:

$$\lim_{x \to 0} \alpha_1 = 0 \qquad \lim_{x \to \infty} \alpha_1 = 0$$

$$\lim_{x \to 0} \beta_1 = \frac{8}{\pi^2 K'} \qquad \lim_{x \to \infty} \beta_1 = \frac{1}{K'}$$

As previously noted, the output of the RC commutated network $e_o(t)$ does not contain the feedforward element, hence the total output (neglecting higher harmonics) of the notch network of Figure 3 is

$$x_o = \alpha_1 \cos \omega t + \beta_1 \sin \omega t - \sin \omega t$$

or

$$x_o \approx 0$$

if

$$K' \approx \frac{8}{\pi^2}.$$

It can also be shown that the notch depth is independent of φ. That is, if

$$e_i = \sin (\omega t + \varphi)$$

then

$$x_o = (\alpha_1 - \sin \varphi) \cos \omega t + (\beta_1 - \cos \varphi) \sin \omega t$$

does not depend on φ. The cumbersome but easy proof consists of substituting for α_1 and β_1 of this last expression, Equation (40), and computing the absolute value of x_o.

3. Discussion of Differential Equation for Input Equal to A sin $(\omega_c t + \varphi)$ with $\omega_c \neq k\omega$. If the condition $\omega_c = k\omega$ is replaced by

$$\omega_c = \frac{\omega}{m} \qquad (m = 1, 2, 3 \ldots) \qquad (41)$$

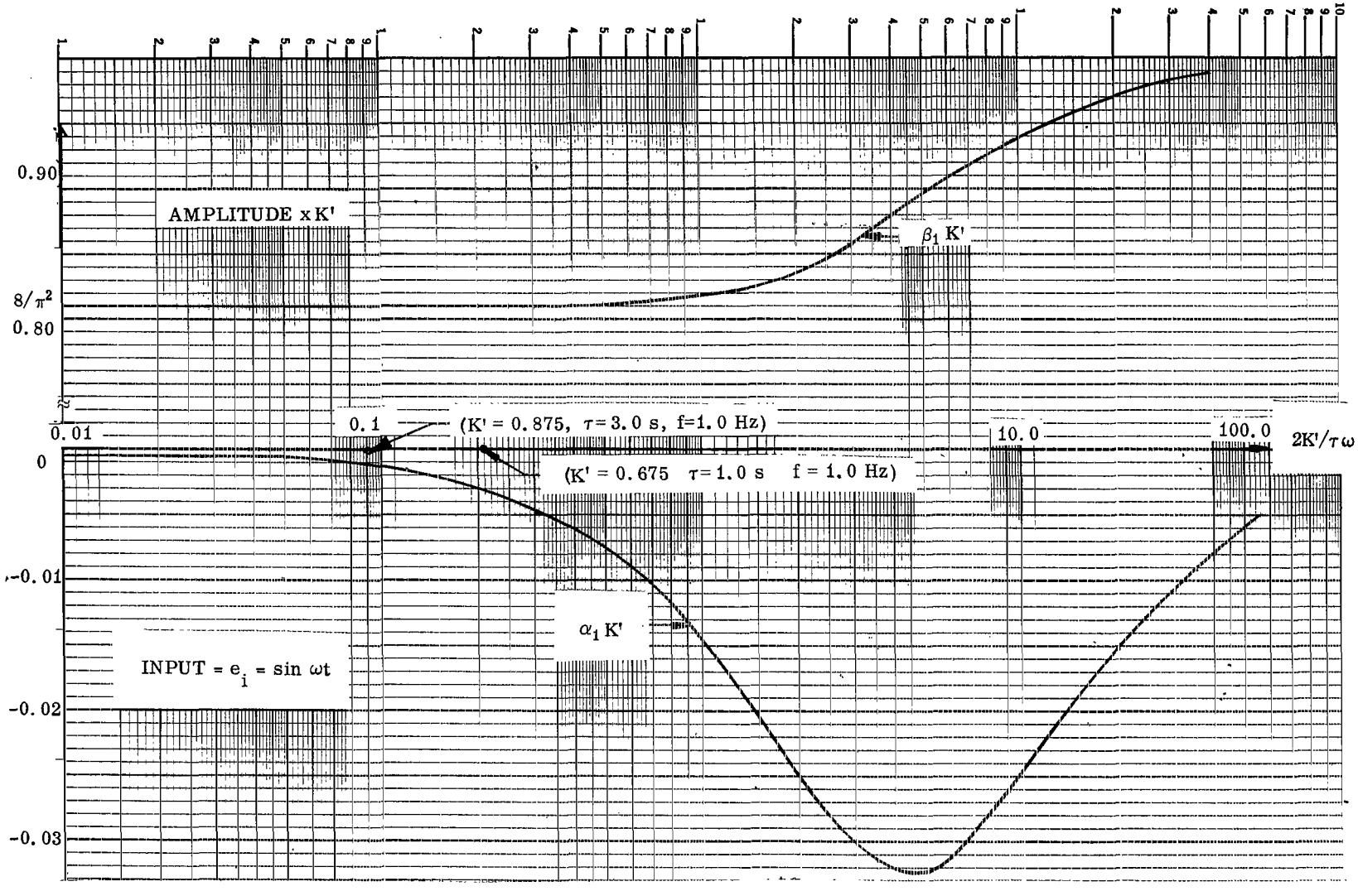

FIGURE 16. QUADRATURE COMPONENTS AMPLITUDES VS $2K'/\tau\omega$ (COUPLED)

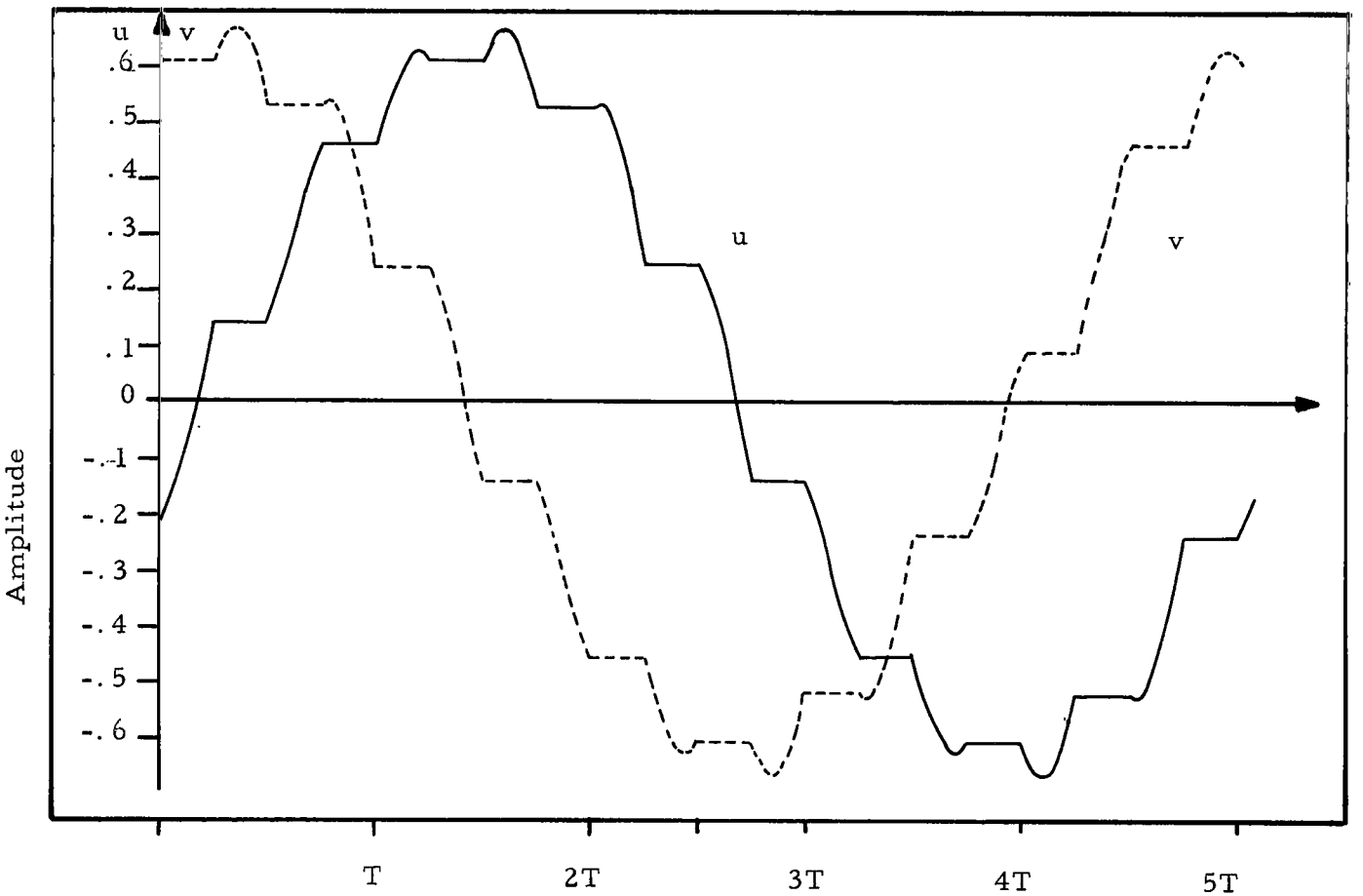

f = 1.0 Hz f_c = 1.2 Hz
k = 6.0 K' = 0.675
τ = 1.0 s A = 1.0
φ = 0° m = 5.0

FIGURE 17. VARIABLES u_i, v_i VS TIME

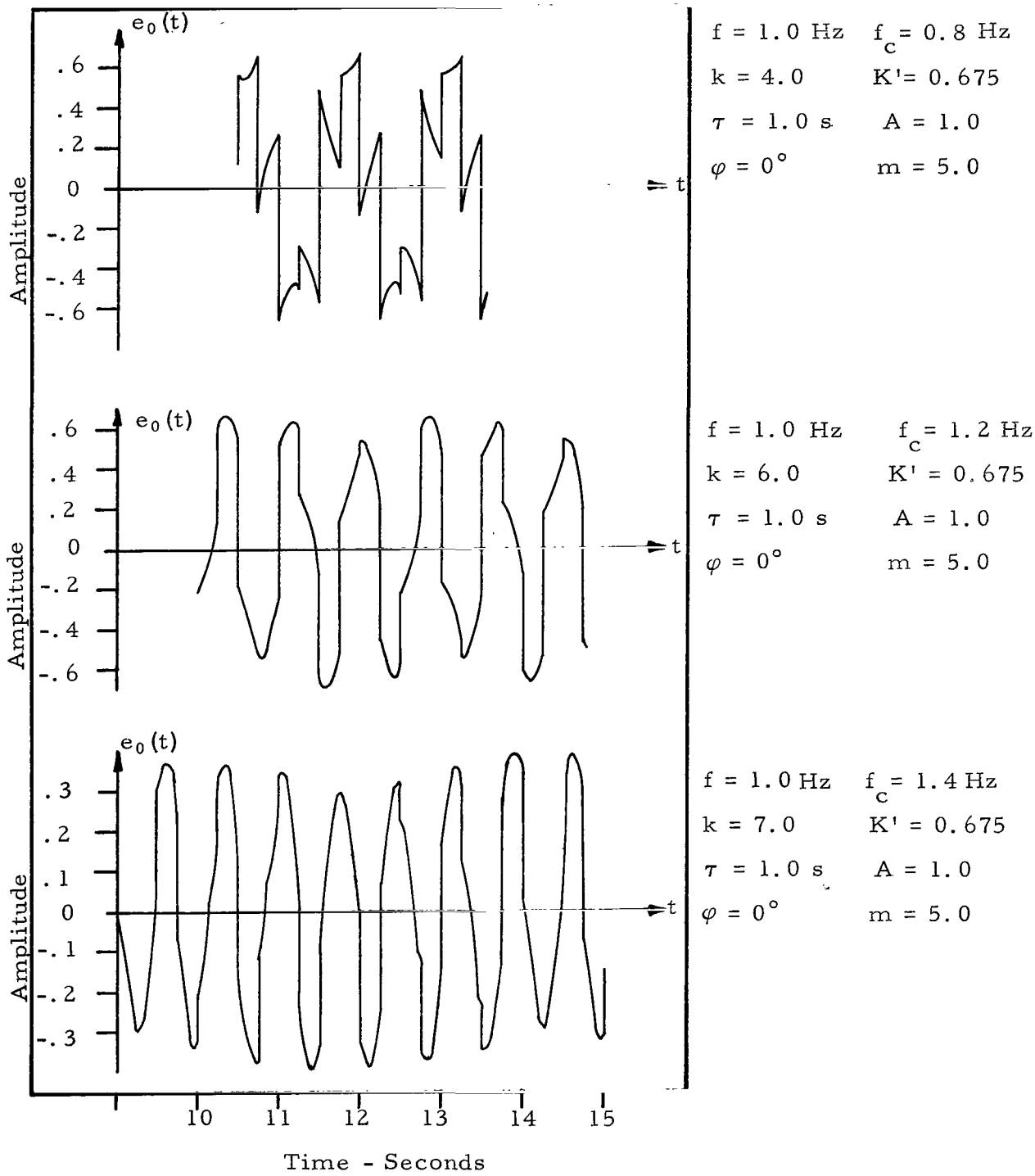

FIGURE 18. RC COMMUTATED NETWORK OUTPUT VS TIME (COUPLED)

then the input function will not repeat until $t = T_c = mT$. This implies that the condition for $\gamma_1(n+1)$ and $\gamma_2(n+1)$ cannot be obtained until $t = mT$. Therefore, the equations for u_j and $v_j (j = 1, 2, \ldots)$ are continued until $j = 4m$. As an example, if $f_c = .1$, then $T_c = 10T$, $\gamma_1(n+1) = u_{40}(10T)$, $\gamma_2(n+1) = v_{40}(10T)$.

As a final case, replace Equation (41) by

$$\omega_c = \frac{k\omega}{m} \tag{42}$$

where k and m are relatively prime integers. The external force has the period $T_c = \frac{m}{k} T$; therefore, u_1 and v_1 will repeat at $j = 4m$ and possess an ultra-subharmonic oscillation (Ref. 6). Although u_{4m} and v_{4m} must be calculated, this does not imply that the period for $e_o(t)$ will be mT. This is best visualized by comparing Figure 17 with the second graph of Figure 18. The period for u and v is 5T, while the resultant curve $e_o(t)$ has a period of 2.5T.

B. UNCOUPLED RC COMMUTATED NETWORK

1. General Solution. In contrast to Equation (17) for the commutated capacitor network, Equations (25 and 26) for the circuit of Figure 4 are adaptable to a more sophisticated analysis, because the time-varying coefficients do not appear in the homogeneous part of the equations for y_1 and y_2. Using Laplace transform theory, it is then possible to obtain a closed form solution. However, to investigate the notch, it is necessary to return to the jump function technique previously considered. In addition, a frequency response function is found by using the real multiplication theorem of Laplace transform theory.

First, consider Equation (25)

$$\tau \dot{y}_1 + y_1 = Pe_i .$$

Since $y_1(0) = 0$, the Laplace transform of each side gives

$$\tau p Y_1(p) + Y_1(p) = L\{Pe_i\} \tag{43}$$

where p is the Laplace operator, $Y_1(p)$ the Laplace transform of $y_1(t)$, and $L\{Pe_i\}$ is the notation for taking the Laplace transform of the quantity in parenthesis.

Solving Equation (43) for $Y_1(p)$,

$$Y_1(p) = \frac{L\{Pe_i\}}{(p + 1/\tau)} = \frac{1}{\tau} L\left\{ [P(t)\ e_i(t)] * e^{-t/\tau} \right\}$$

where the * sign indicates convolution of $P(t)\ e_i(t)$ and $e^{-t/\tau}$. Therefore, by the convolution, or Faltung, theorem,

$$y_1(t) = \frac{1}{\tau} \int_0^t P(t_1)\, e_i(t_1)\, e^{-1/\tau\ (t - t_1)}\ dt_1$$

or

$$y_1(t) = \frac{e^{-t/\tau}}{\tau} \int_0^t P(t_1)\, e_i(t_1)\, e^{t_1/\tau}\ dt_1 \qquad (44)$$

where t_1 is a dummy variable. A similar treatment of Equation (26)

$$\tau \dot{y}_2 + y_2 = Q e_i$$

yields

$$y_2(t) = \frac{e^{-t/\tau}}{\tau} \int_0^t Q(t_1)\, e_i(t_1)\, e^{t_1/\tau}\ dt_1 . \qquad (45)$$

Substituting Equation (44) and (45) into Equation (27) gives the final solution for the output e_o (t)

$$e_o(t) = \frac{P}{\tau} e^{-t/\tau} \int_0^t P(t_1)\, e^{t_1/\tau}\ e_i(t_1)\, dt_1 + \frac{Q}{\tau} e^{-t/\tau} \int_0^t Q(t_1)\, e^{t_1/\tau}\ e_i(t_1)\ dt_1 + (K - 2)\, e_i . \qquad (46)$$

This equation has been programed using Runge Kutta on the IBM 7090 computer for various functions of $e_i(t)$. Representative curves are shown in Figures 19 to 26. Note that the output waveform has been slightly attenuated. This offers no problem since the amplitudes of the output wave can be adjusted by resistors R and R_3 [Equation (10)] to make the output voltage equal to the input voltage at direct current. The attenuation at the notch frequency ($\omega = \omega_c$) is large (Fig. 20), and the slight adjustment of R and R_3 has little effect on the output voltage.

2. Notch Frequency Analysis. Equation (46) is ideal for digital programing; however, its value for determining the optimum selection of K is limited. For that purpose, it is best to let $e_i = A \sin \omega_c t$ and let P and Q have the same switching frequency

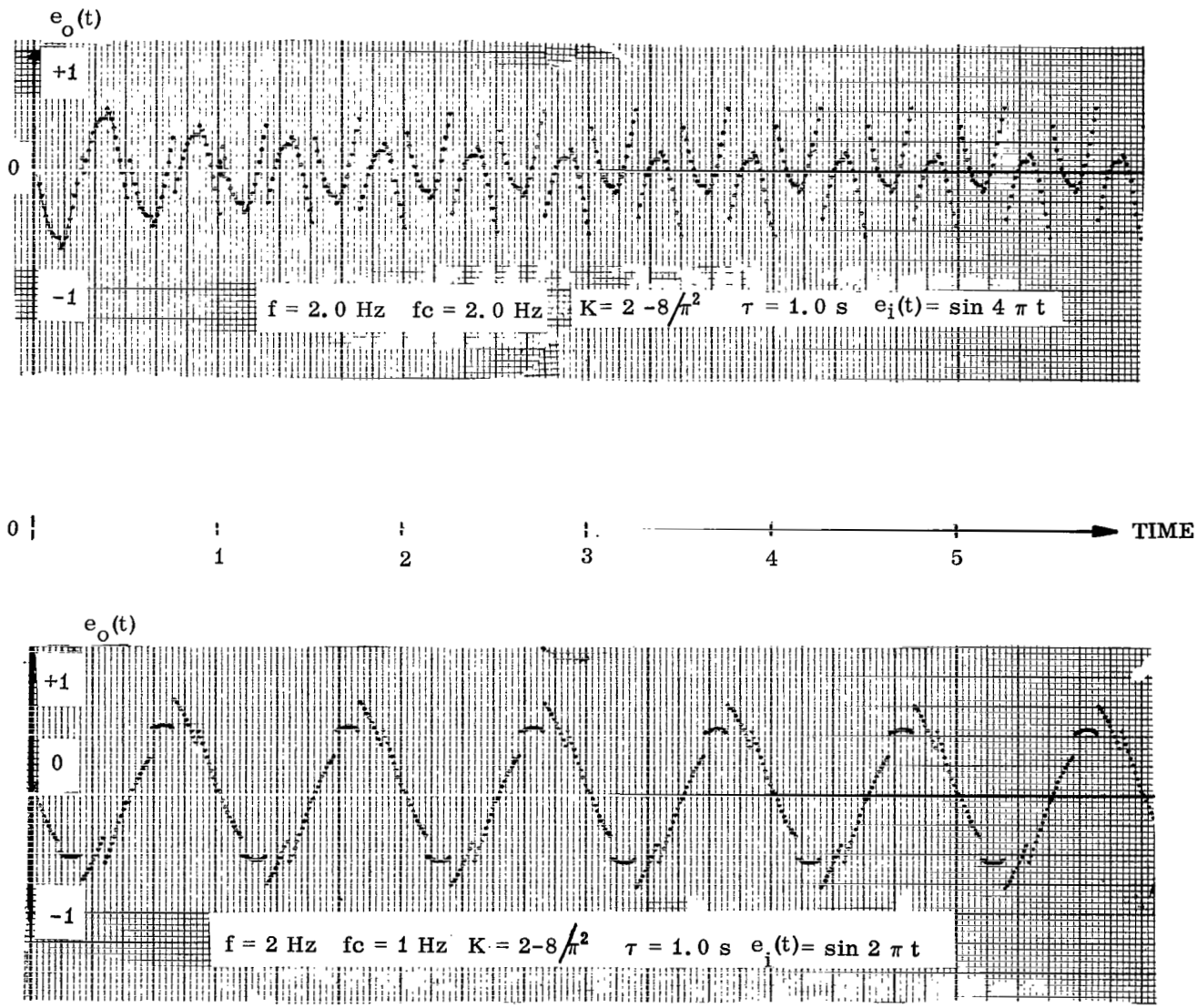

FIGURE 19. UNCOUPLED RC COMMUTATED NETWORK VS TIME

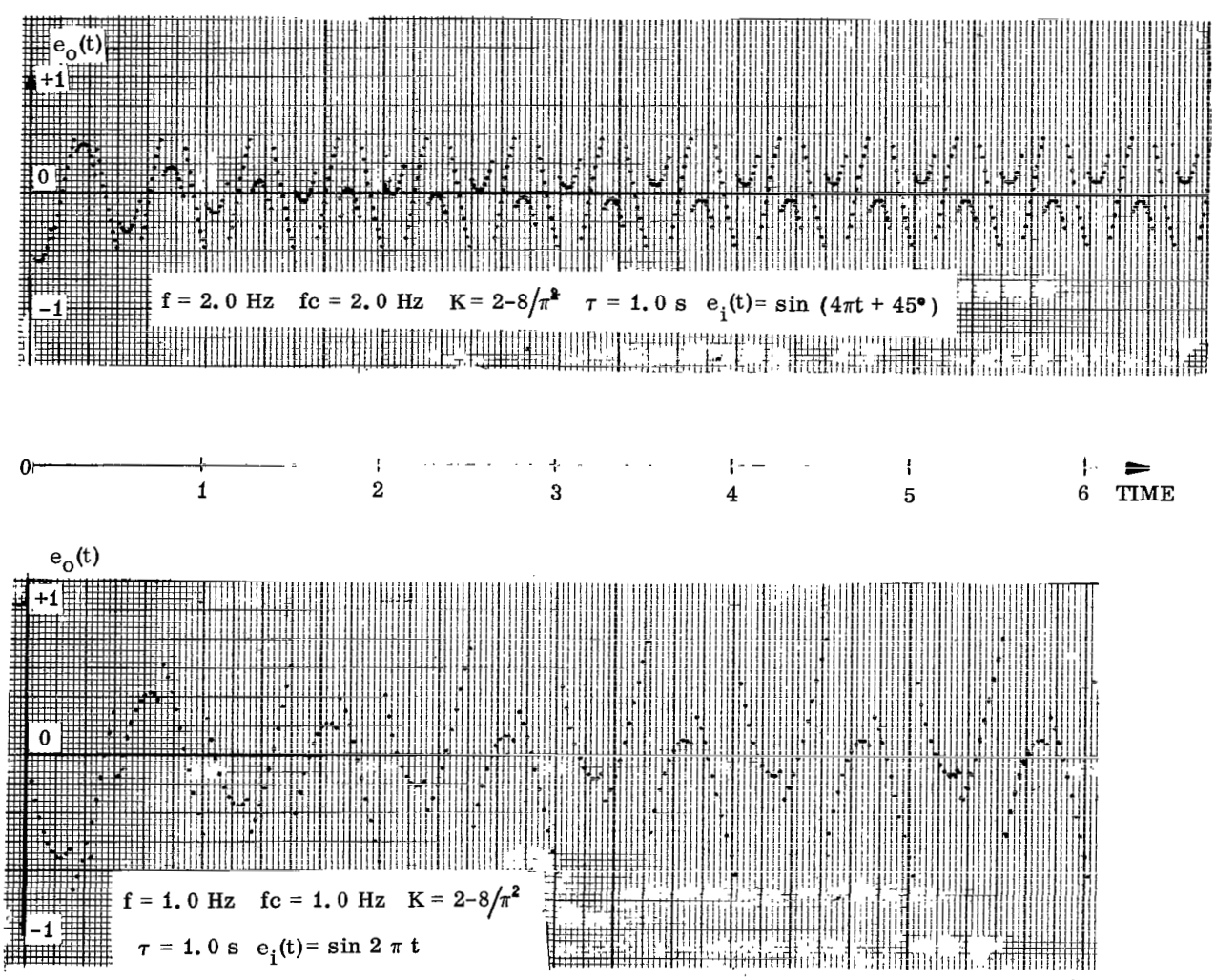

FIGURE 20. UNCOUPLED RC COMMUTATED NETWORK VS TIME

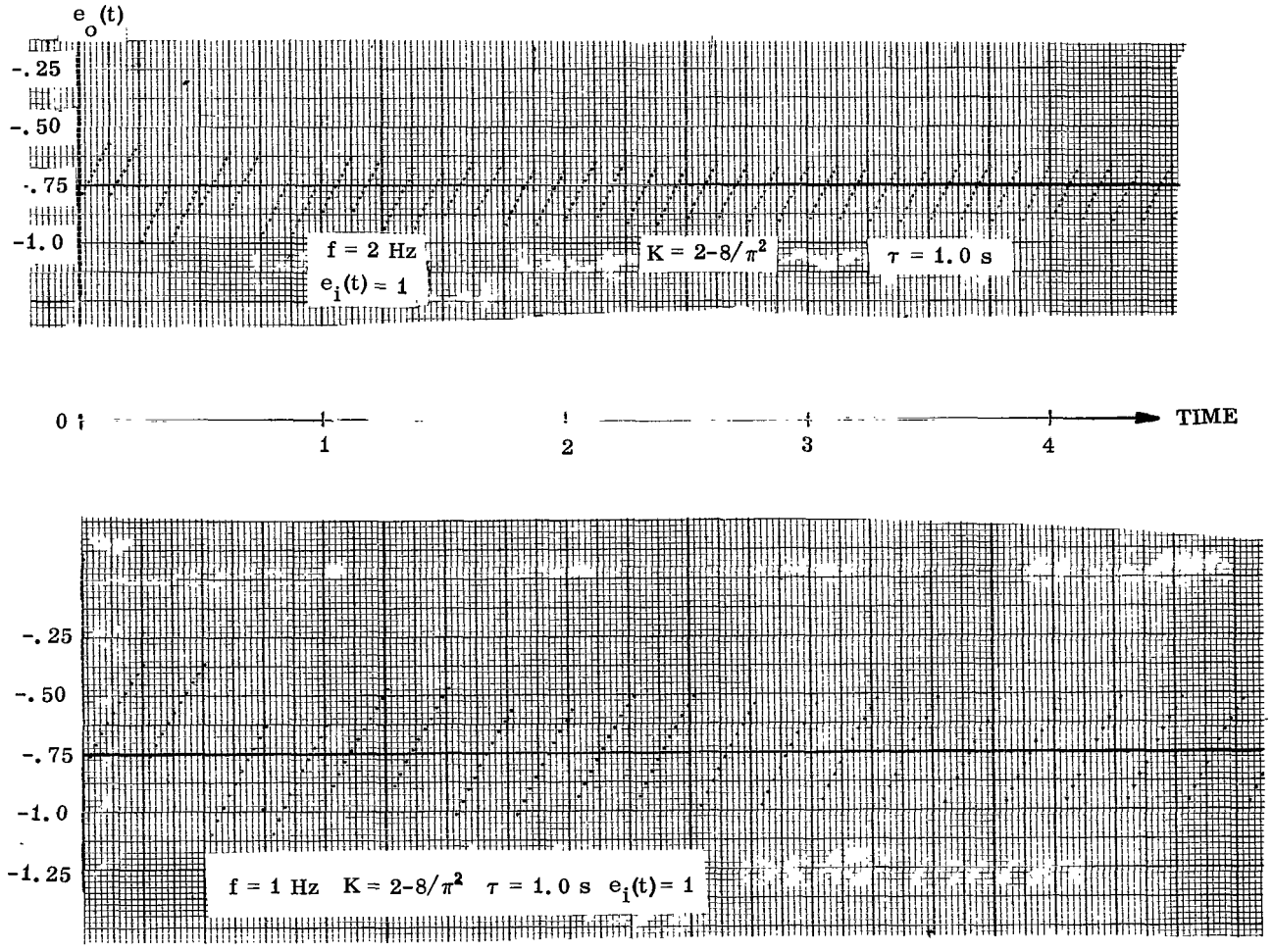

FIGURE 21. UNCOUPLED RC COMMUTATED NETWORK VS TIME

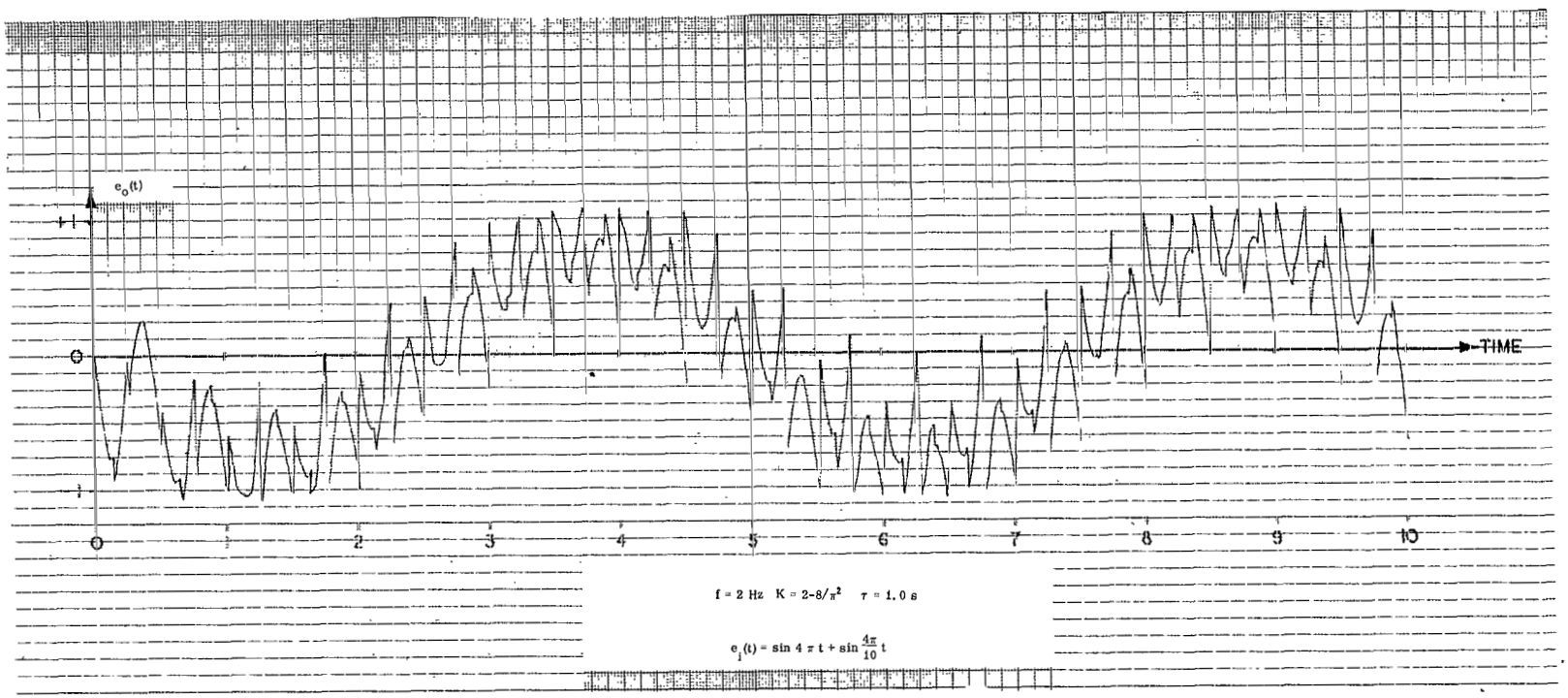

FIGURE 22. UNCOUPLED RC COMMUTATED NETWORK VS TIME

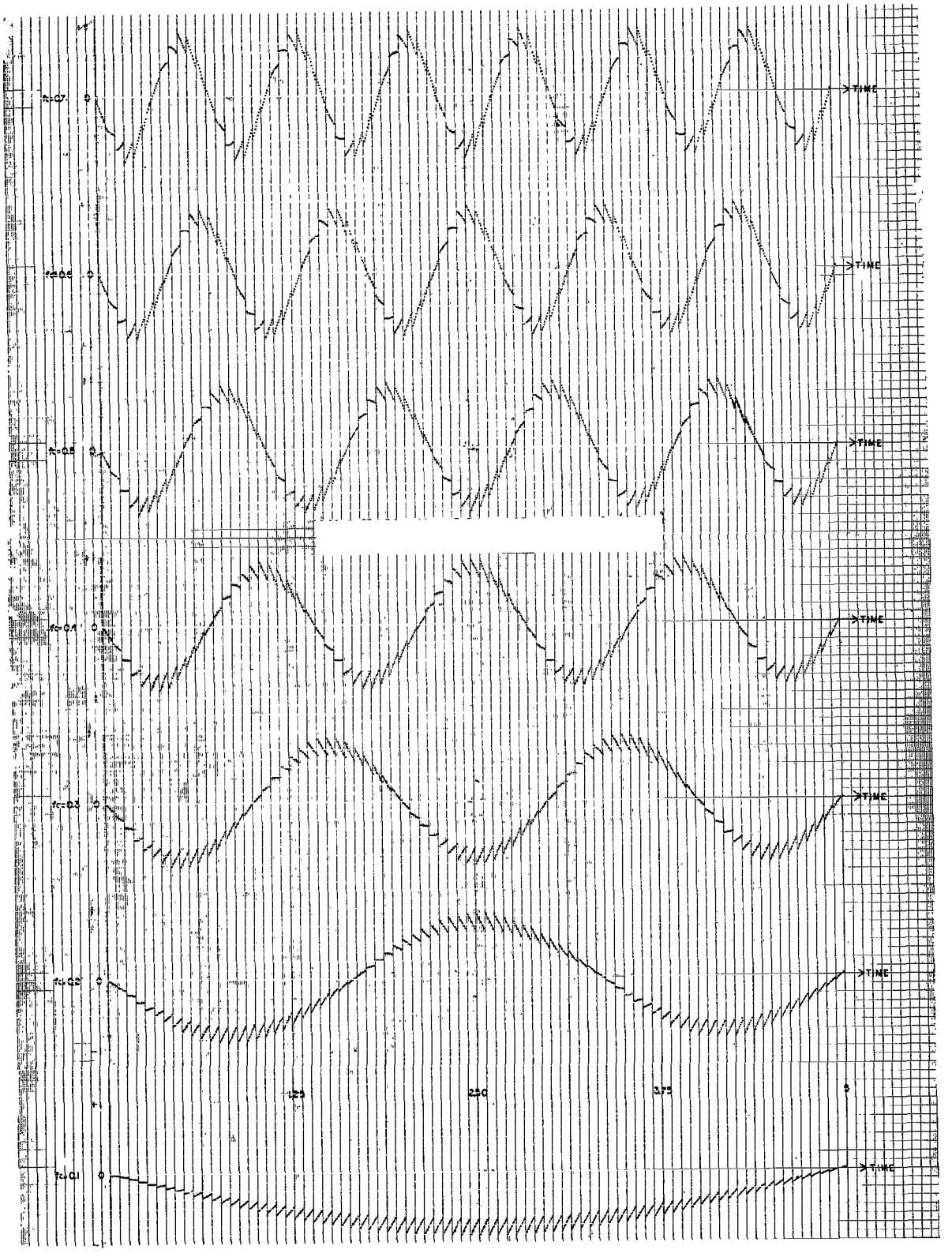

FIGURE 23. UNCOUPLED RC COMMUTATED NETWORK VS TIME

$f = 2$ $K = 2 - 8/\pi^2$ $\tau = 1.0$ s $e_i(t) = \sin 2\pi f_c t$ f_c = parameter

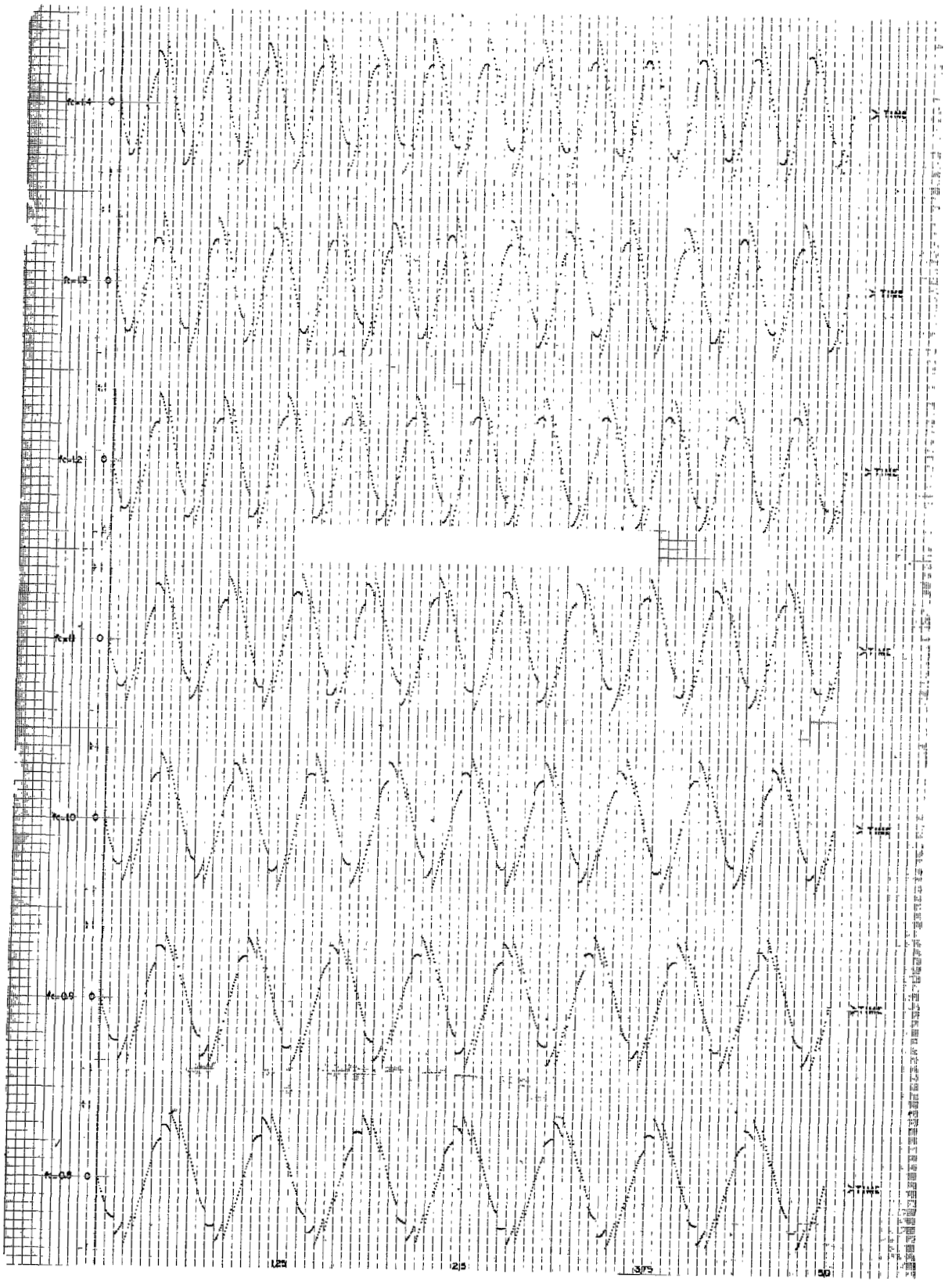

FIGURE 24. UNCOUPLED RC COMMUTATED NETWORK VS TIME

$f = 2 \quad K = 2 - 8/\pi^2 \quad \tau = 1.0\ s \quad e_i(t) = \sin 2\pi f_c t \quad f_c$ = parameter

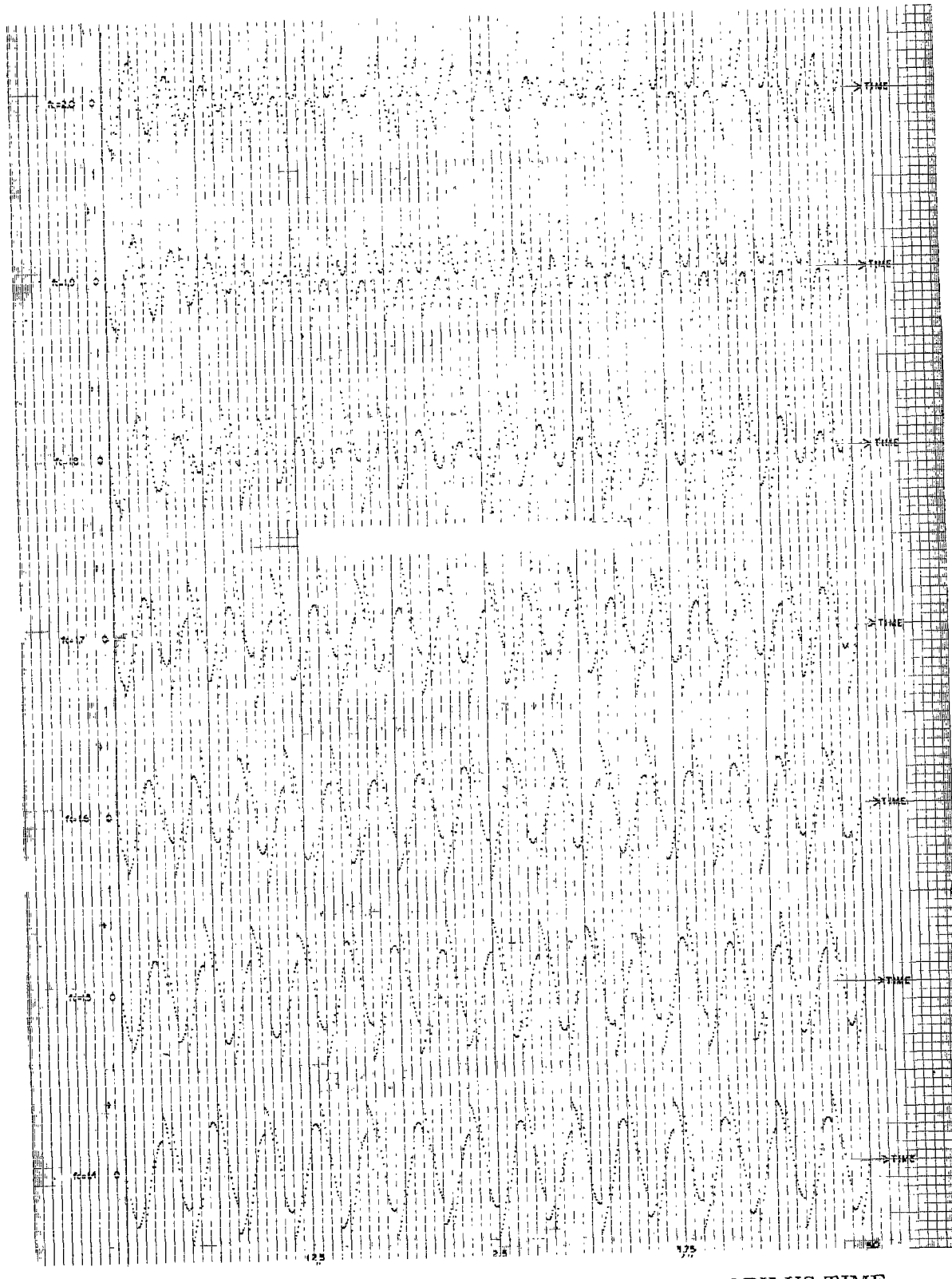

FIGURE 25. UNCOUPLED RC COMMUTATED NETWORK VS TIME

$f = 2$ $K = 2 - 8/\pi^2$ $\tau = 1.0$ s $e_i(t) = \sin 2\pi f_c t$ f_c = parameter

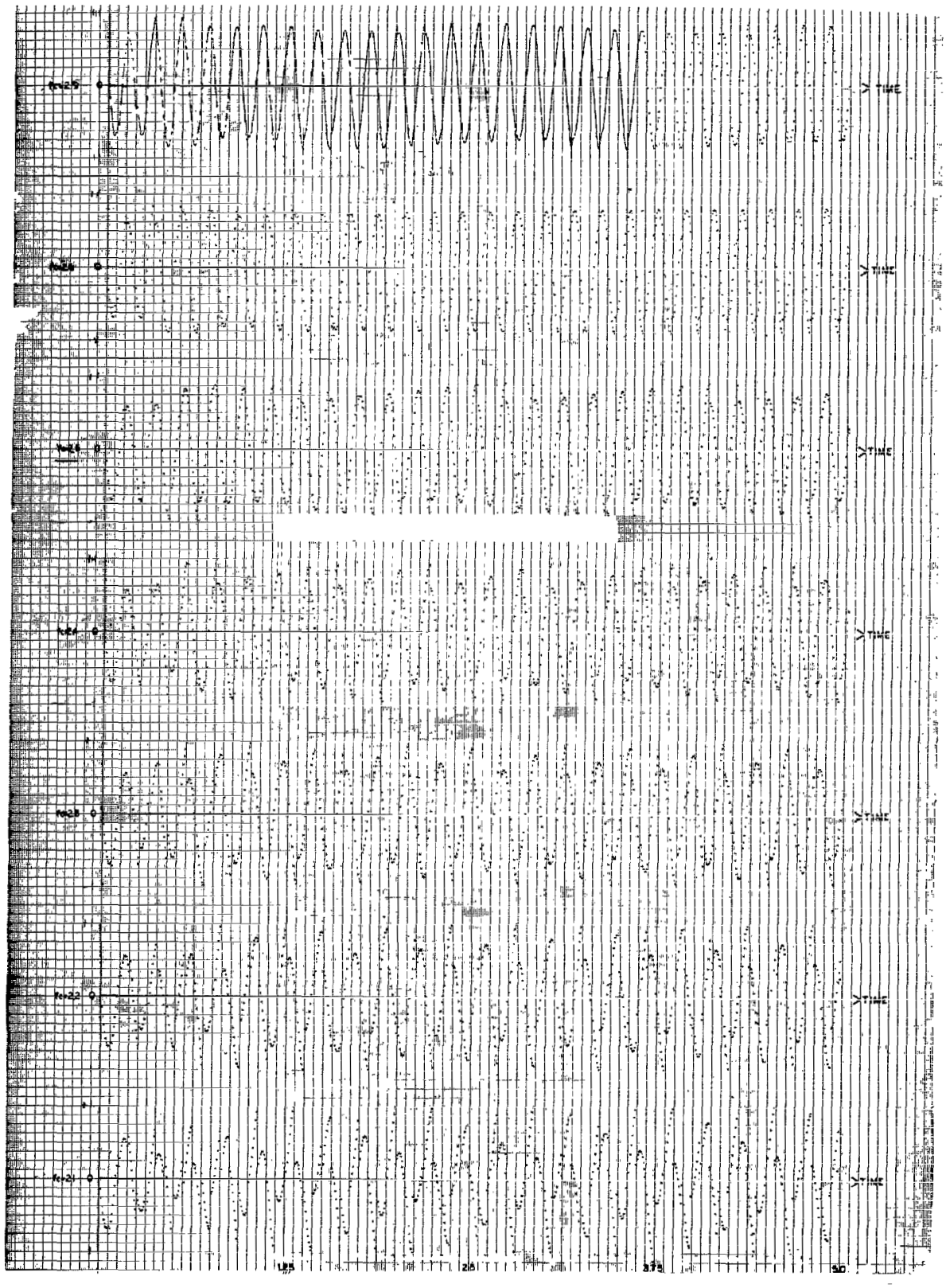

FIGURE 26. UNCOUPLED RC COMMUTATED NETWORK VS TIME

$f = 2$ $K = 2 - 8/\pi^2$ $\tau = 1.0$ s $e_i(t) = \sin 2\pi f_c t$ f_c = parameter

as the input ($\omega = \omega_c$). No generality is lost if the amplitude of the input equals one (A = 1). Equation (25) then becomes a repetition of two separate equations where the boundary conditions between solutions must be utilized to obtain a continuous solution. Thus the difference in the analysis of this section and Section IV-A-1 is that only two equations are to be considered here. These are:

$$\begin{aligned} \tau\dot{y}_{11} + y_{11} &= \sin \omega t \qquad && 0 \le t \le \frac{T}{2} \\ \tau\dot{y}_{12} + y_{12} &= -\sin \omega t \qquad && \frac{T}{2} \le t \le T \end{aligned} \tag{47}$$

where the second subscript refers to the half-period of interest.

Omitting the algebra, the solutions are

$$y_{11}(t) = \frac{\lambda}{\lambda^2+\omega^2}\left[\lambda \sin \omega t - \omega \cos \omega t + \omega\left(\frac{e^{\lambda T/4} - e^{-n\lambda T}\cosh \lambda\, T/4}{\sinh \lambda\, T/4}\right)e^{-\lambda t}\right] \tag{48a}$$

$$(0 \le t \le T/2)$$

$$y_{12}(t) = -\frac{\lambda}{\lambda^2+\omega^2}\left[\lambda \sin \omega t - \omega \cos \omega t - \omega\left(\frac{e^{3\lambda T/4} - e^{-n\lambda T}\cosh \lambda\, T/4}{\sinh \lambda\, T/4}\right)e^{-\lambda t}\right] \tag{48b}$$

$$(T/2 \le t \le T)$$

$$\lambda = 1/\tau$$

Equation (25) could have been solved directly by using the Laplace transform. In fact, this same equation is solved in Reference 7. The approach as presented here by jump functions is twofold. First, it allows the separation of the steady state solution by letting $n \to \infty$. Second, the analysis of the coupled network previously considered led to differential equations with time varying coefficients, where the Laplace transform becomes ineffective.

Returning to Equation (26), there is a repetition of three separate equations:

$$\tau\dot{y}_{21} + y_{21} = \sin \omega t \qquad (0 \le t \le T/4) \tag{49a}$$

$$\tau\dot{y}_{22} + y_{22} = -\sin \omega t \qquad (T/4 \le t \le 3T/4) \tag{49b}$$

$$\tau\dot{y}_{23} + y_{23} = \sin \omega t \qquad (3T/4 \le t \le T) \tag{49c}$$

whose solutions are

$$y_{21} = \frac{\lambda}{\lambda^2+\omega^2}\left(\lambda \sin \omega t - \omega \cos \omega t + \frac{\lambda}{\sinh \frac{\lambda T}{4}} e^{-\lambda t}\right)$$

$$- \left(-\omega + \frac{\lambda}{\sinh \frac{\lambda T}{4}}\right) e^{-\lambda(nT+t)} \qquad \left(0 \le t \le \frac{T}{4}\right) \tag{50a}$$

$$y_{|2\,2} = -\frac{\lambda}{\lambda^2+\omega^2}\left(\lambda \sin \omega t - \omega \cos \omega t - \frac{\lambda}{\sinh \frac{\lambda T}{4}} e^{-\lambda(t-T/2)}\right)$$

$$- \left(-\omega + \frac{\lambda}{\sinh \frac{\lambda T}{4}}\right) e^{-\lambda(nT+t)} \qquad \left(\frac{T}{4} \le t \le \frac{3T}{4}\right) \tag{50b}$$

$$y_{23} = \frac{\lambda}{\lambda^2+\omega^2}\left(\lambda \sin \omega t - \omega \cos \omega t + \frac{\lambda}{\sinh \frac{\lambda T}{4}} e^{-\lambda(t-T)}\right)$$

$$-\left(-\omega + \frac{\lambda}{\sinh \frac{\lambda T}{4}}\right) e^{-\lambda(nT+t)} \qquad \left(\frac{3T}{4} \le t \le T\right). \tag{50c}$$

Equation (27), which describes the output, is

$$e_o = Py_1 + Qy_2 + (K-2)\, e_i$$

and can be rewritten using Equations (48) and (50) as

$$e_o(t) = \begin{cases} y_{11} + y_{21} & + (K-2)\ \sin \omega t & 0 \le t \le T/4 \\ y_{11} - y_{22} & + (K-2)\ \sin \omega t & T/4 \le t \le T/2 \\ y_{12} - y_{22} & + (K-2)\ \sin \omega t & T/2 \le t \le 3T/4 \\ y_{12} + y_{23} & + (K-2)\ \sin \omega t & 3T/4 \le t \le T \end{cases} \qquad (51)$$

Again n is a second independent variable, and this expression is valid for cycles during the transient buildup as well as for cycles during the steady state. Graphs for the notch frequency appear in Figures 19 and 20.

3. Fourier Analysis. If

$$e_o(t) \sim \frac{\alpha_0}{2} + \sum_{m=1}^{\infty} (\alpha_m \cos m\omega t + \beta_m \sin m\omega t)$$

and Equation (51) is used for the steady state values of $e_o(t)$, i.e., $n \to \infty$, the amplitudes for the fundamental are calculated to be:

$$\alpha_0 = 0 \qquad (52a)$$

$$\alpha_1 = \frac{\omega^2}{\pi(\lambda^2+\omega^2)} \left[\frac{8\lambda^2}{\lambda^2+\omega^2} \coth \frac{\pi\lambda}{2\omega} - 2\pi \frac{\lambda}{\omega} \right] \qquad (52b)$$

$$\beta_1 = K-2 + \frac{2\lambda^2}{\lambda^2+\omega^2} + \frac{8\lambda(\omega^2-\lambda^2)}{(\lambda^2+\omega^2)\,T} \coth \frac{\lambda T}{4} . \qquad (52c)$$

If the amplitude of the fundamental (β_1) is forced to zero, then a value of K is obtained as a function of $\lambda = 1/\tau$ and ω. At the same time, the amplitude of the fundamental cosine component (α_1) cannot be allowed to be too large. Since α_1 does not contain the parameter K, its value will not be affected by an optimum choice of K. Therefore let $\beta_1 = 0$ and introduce the substitution $x = 1/\omega\tau$ in Equation (52), which yields

$$\alpha_1 = \frac{1}{\pi} \frac{x}{1+x^2} \left(\frac{8x}{1+x^2} \coth \frac{\pi x}{2} - 2\pi \right) \qquad (53a)$$

$$K = 2 \left[\frac{1-x^2}{1+x^2} + \frac{2}{\pi} \frac{x(x^2-1)}{(1+x^2)^2} \coth \frac{\pi x}{2} \right] . \qquad (53b)$$

These functions are shown in Figure 27. For values of $.27 \le \frac{1}{\omega\tau} \le 11$, $\alpha_1 \ge 0.1$. If $1/\omega\tau$ is restricted from this range, then the notch depth is greater than 10/1 if the proper value of K is selected.

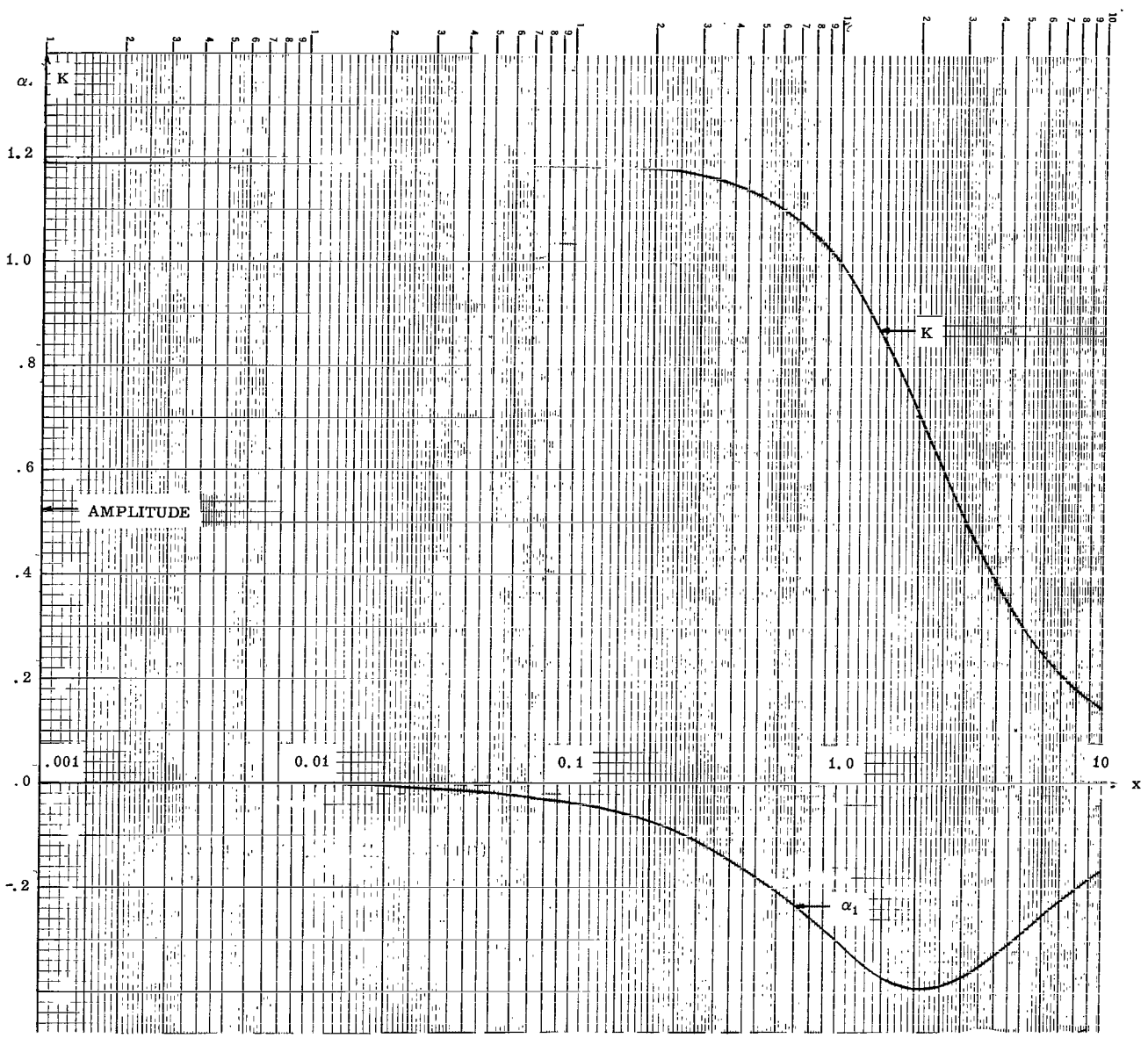

FIGURE 27. α_1 AND K VS x = $1/\omega\tau$ (UNCOUPLED)

4. A Frequency Response Function. Let

$$e_i = Ae^{j\omega_c t}$$

where A is the amplitude and ω_c is the forcing circular frequency. As can be seen from Equation (46), there is again no loss of generality if A = 1. The frequency response function (FRF) to be considered is defined as

$$FRF = \frac{E_o(p)}{E_i(p)} \Bigg| \; p = j\omega_c \tag{54}$$

where $E_o(p)$ and $E_i(p)$ are the Laplace transforms of $e_o(t)$ and $e_i(t)$, respectively. Equations (25), (26), and (27) will be investigated. Inspection of Equation (27) shows the necessity of taking the Laplace transform of $P(t)y_1(t)$ and $Q(t)y_2(t)$, where $y_1(t)$ and $y_2(t)$ are the solutions of Equations (25) and (26) for the given input $e_i = e^{j\omega_c t}$. To obtain these transforms, the following formulae (see Appendix for proofs) are needed:

$$L\left[e^{j\omega_c t}\right] = \frac{1}{p - j\omega_c} \tag{55}$$

$$L\left[P\right] = \frac{1}{p} \tanh \frac{pT}{4} \tag{56}$$

$$L\left[Q\right] = \frac{1}{p}\left[1 - \operatorname{sech} \frac{pT}{4}\right] \tag{57}$$

$$L\left[Pe^{j\omega_c t}\right] = \frac{\tanh (p - j\omega_c)\frac{T}{4}}{(p - j\omega_c)} \tag{58}$$

$$L\left[Qe^{j\omega_c t}\right] = \frac{\left[1 - \operatorname{sech} (p - j\omega_c)\frac{T}{4}\right]}{(p - j\omega_c)}. \tag{59}$$

The Laplace transform of Equation (25) yields

$$Y_1(p) = \frac{1}{\tau p + 1} \; \frac{\tanh (p - j\omega_c)\frac{T}{4}}{p - j\omega c} \tag{60}$$

where Equation (58) and the condition $y_1(0) = 0$ have been used. To obtain the Laplace transform of $P(t)y_1(t)$, i.e., the product of time functions, it suffices to use the "real multiplication" or "complex convolution" theorem (Ref. 5). That is,

$$L[f_1(t)f_2(t)] = \frac{1}{2\pi j}\int_{c_2-j\infty}^{c_2+j\infty} F_1(p-s)\,F_2(s)\,ds. \tag{61}$$

Let $f_1(t) = \dot{P}(t)$, $f_2(t) = y_1(t)$ and use Equations (56), (60), and (61) to give

$$L[Py_1] = \frac{1}{2\pi j}\int_{c_2-j\infty}^{c_2+j\infty} \frac{1}{p-s}\tanh(p-s)\frac{T}{4}\cdot\frac{1}{\tau s+1}\,\frac{\tanh(s-j\omega_c)\frac{T}{4}}{s-j\omega_c}\,ds. \tag{62}$$

Now $F_1(p-s)$ has poles in the s-plane at

$$s = p \pm j(2n+1)\omega \qquad (n = 0,1,2,\ldots).$$

A removable singularity exists at $s = p$, and $F_2(s)$ has poles in the s-plane at

$$s = j[\omega_c \pm (2n+1)\omega] \qquad (n = 0,1,2,\ldots)$$

$$s = -1/\tau.$$

These poles are plotted in Figure 28.

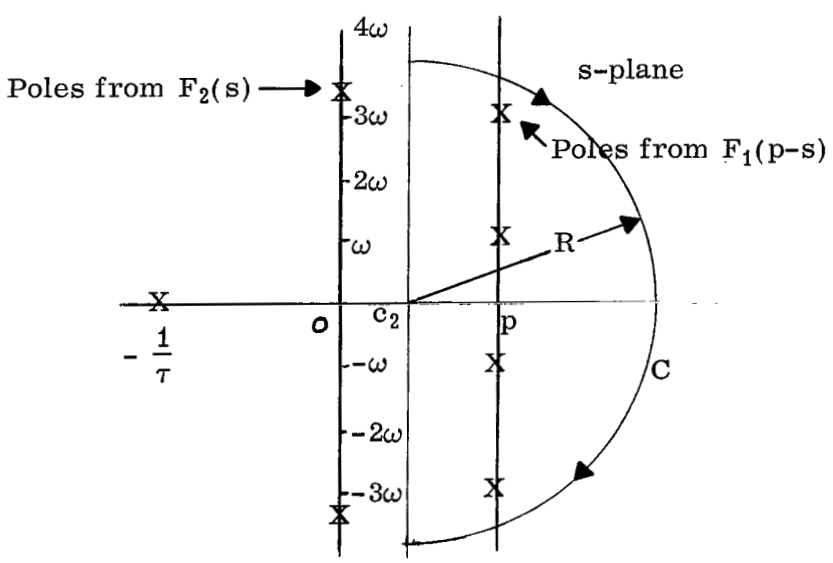

FIGURE 28. INFINITE POLES FROM $F_1(p-s)$ AND $F_2(s)$

To evaluate the line integral, Equation (62), the contour enclosing the poles of $F_1(p-s)$ is suitable. The contour selected is shown in Figure 28, which consists of a semicircle C of radius R with center at c_2 and the vertical line c_2 units to the right of the origin. It can be shown that the semicircle C contributes nothing to the line integral as $R \to \infty$. Therefore, it suffices to consider the sum of the residues of $F_1(p-s)\ F_2(s)$ at the poles $s = p \pm j(2n + 1)\omega$. This sum is

$$-\frac{4}{\pi} \coth \frac{T}{4}(p - j\omega_c)\Bigg|_{\sum_{n=0}^{\infty}} \frac{(\tau p + 1)\ (2n + 1)\omega + (2n + 1)\ \omega\tau\ (p - j\omega_c)}{[(\tau p + 1)^2 + (2n + 1)^2\omega^2\tau^2][(p - j\omega_c)^2 + (2n + 1)^2\omega^2]\ (2n + 1)} \tag{63}$$

where the identity

$$\tanh [p \pm j(2n + 1)\ \omega - j\omega_c] \frac{T}{4} = \coth (p - j\omega_c) \frac{T}{4}$$

has been used. The decomposition into partial fractions of this expression (Ref. 8) is

$$\coth (p - j\omega_c) \frac{T}{4} = \frac{1}{(p - j\omega_c) \frac{T}{4}} + 2 (p - j\omega_c) \frac{T}{4} \sum_{k=1}^{\infty} \frac{1}{\left[(p - j\omega_c) \frac{T}{4}\right]^2 + k^2\pi^2}$$

Substitute this expression into Equation (63), factor $\dfrac{1}{(p - j\omega_c)}$, and let $p = j\omega_c$ to obtain

$$-FRF_1 = -\frac{8}{\pi^2} \sum_{n=0}^{\infty} \frac{(1 + j\tau\omega_c)}{(2n + 1)^2\ [(1 + j\tau\omega_c)^2 + (2n + 1)^2\omega^2\tau^2]} \tag{64}$$

where

$$FRF_1 = \frac{L\{P(t)\, y_1(t)\}}{L\{e^{j\omega_c t}\}}\Bigg|_{p = j\omega_c}.$$

Since the contour in Figure 28 is clockwise, the expression on the right-hand side of Equation (64) is equal to the negative of FRF_1 as indicated. By a similar treatment, it can be shown that

$$FRF_2 = FRF_1$$

where

$$FRF_2 = \left.\frac{L\{Q(t)y_2(t)\}}{L\{e^{j\omega_c t}\}}\right|_{p = j\omega_c}.$$

From Equation (27)

$$FRF = 2FRF_1 + (K-2). \tag{65}$$

Finally, if

$$x = 1/\omega\tau$$

$$r = \omega/\omega_c$$

then

$$FRF = (K-2) + \frac{2x}{x + jr}\left[1 - \frac{2}{\pi(x + jr)} \tanh \frac{\pi}{2}(x + jr)\right]. \tag{66}$$

This function [Equation (66)] is graphed in Figures 29 to 33 for both amplitude and phase with $x = 1/\omega\tau$ as a parameter. The distinction between K fixed and K optimal as noted on the graphs is that K optimal uses Equation (53b) for the value of K. It is interesting to note that the maximum notch depth does not usually occur at the notch frequency.

SECTION V. NONSYMMETRICAL COMMUTATING FUNCTIONS

A solution to the commutated capacitor network has been given for the ideal case of symmetrical square waves. Reference 3 shows that neither the assumptions of symmetrical square waves nor quadrature phase relationship is true in general.

This section considers some asymmetrical and nonquadrature commutating functions and solves for the output function in the same manner as Section IV-A. The analysis is restricted to the notch frequency. No attempt is made, however, to find an optimum setting.

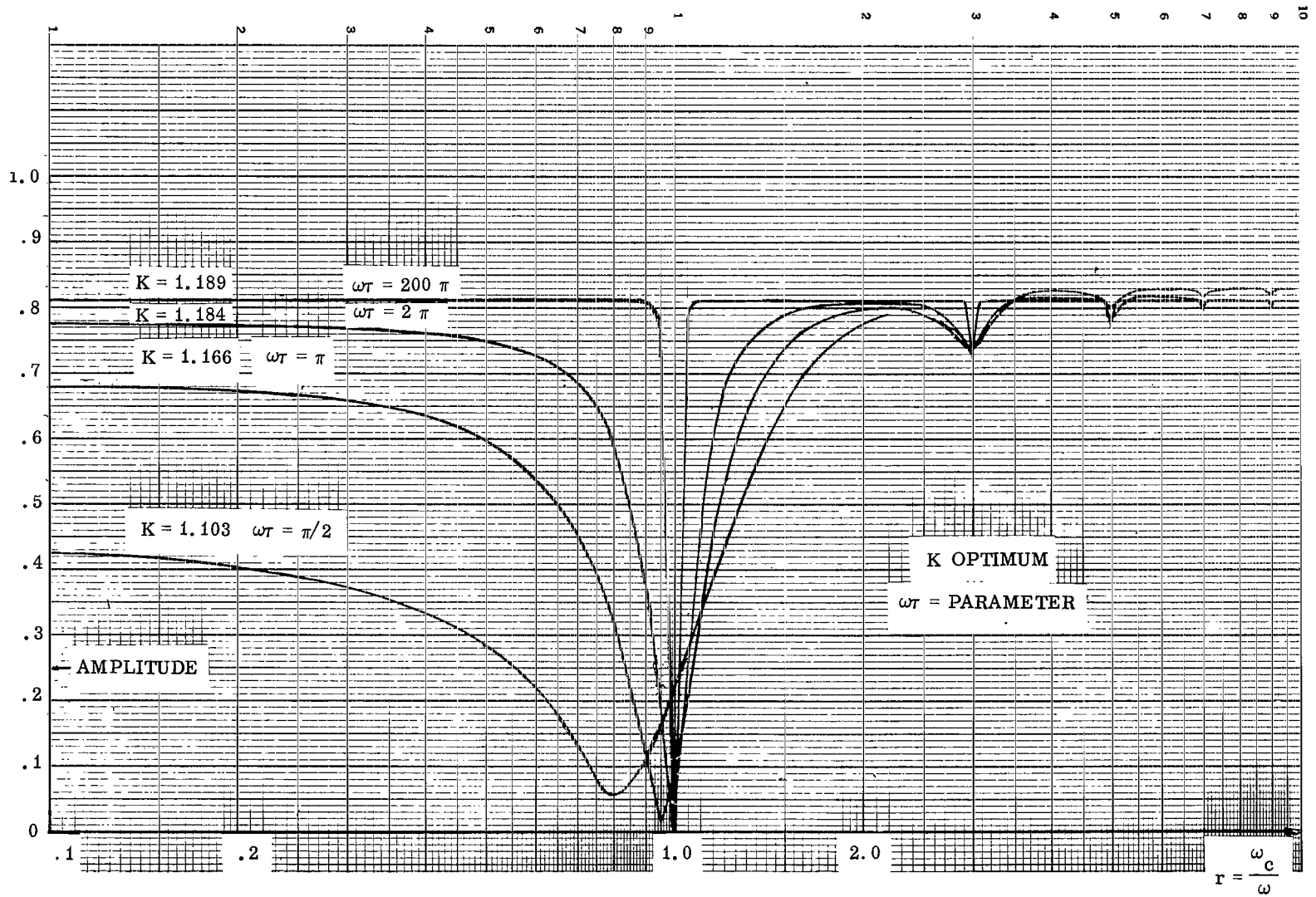

FIGURE 29. FREQUENCY RESPONSE FUNCTION - AMPLITUDE

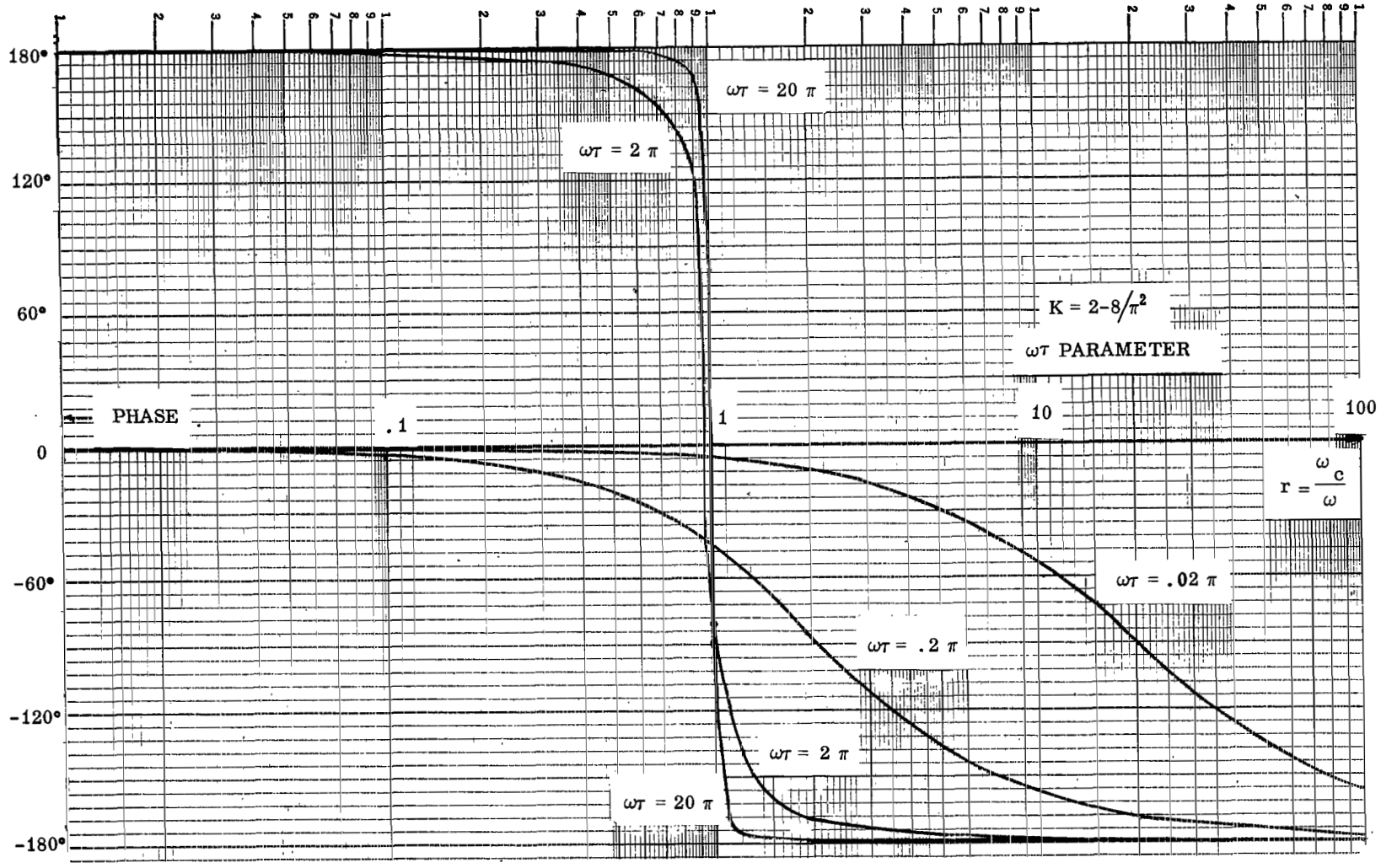

FIGURE 30. FREQUENCY RESPONSE FUNCTION - AMPLITUDE

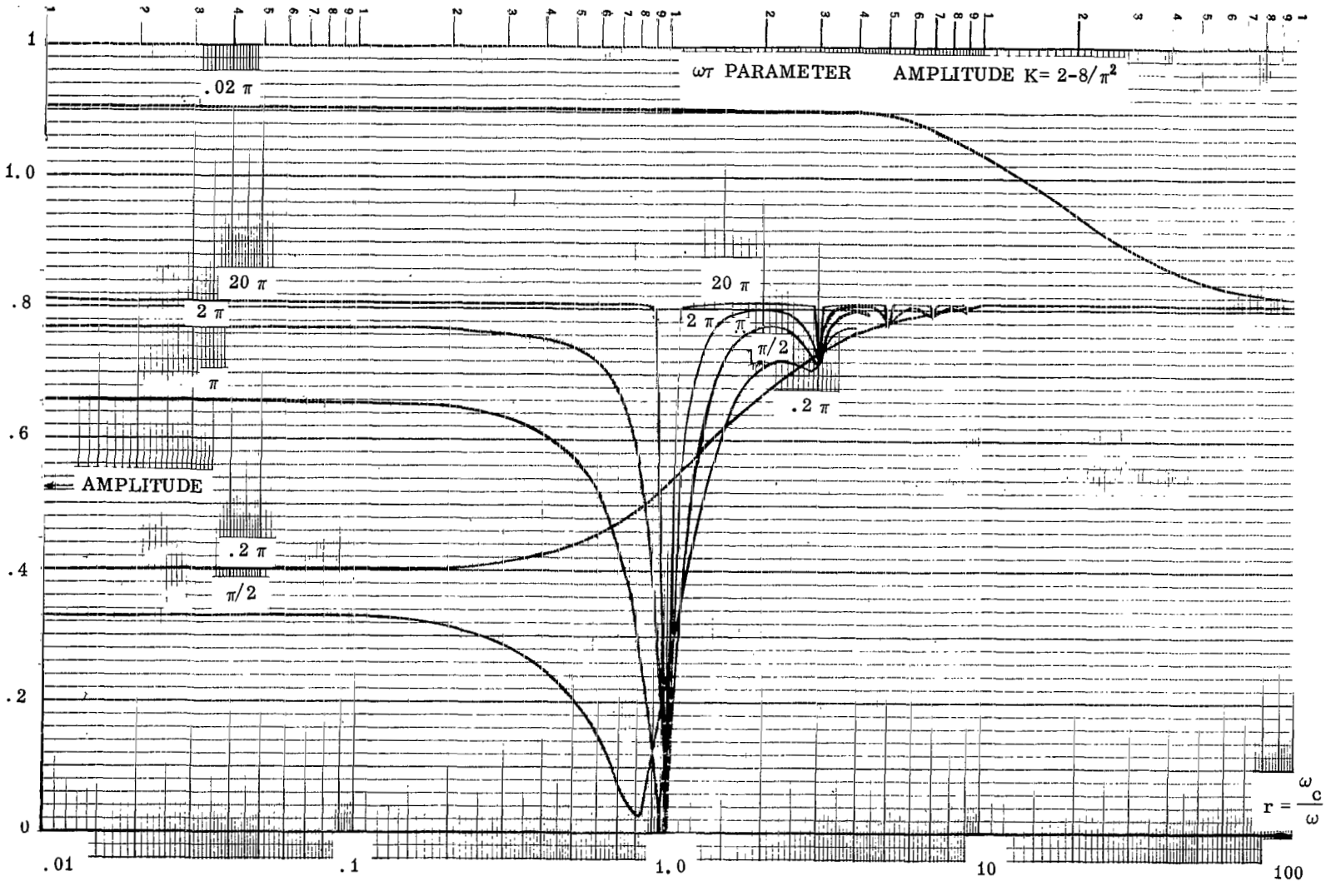

FIGURE 31. FREQUENCY RESPONSE FUNCTION - AMPLITUDE

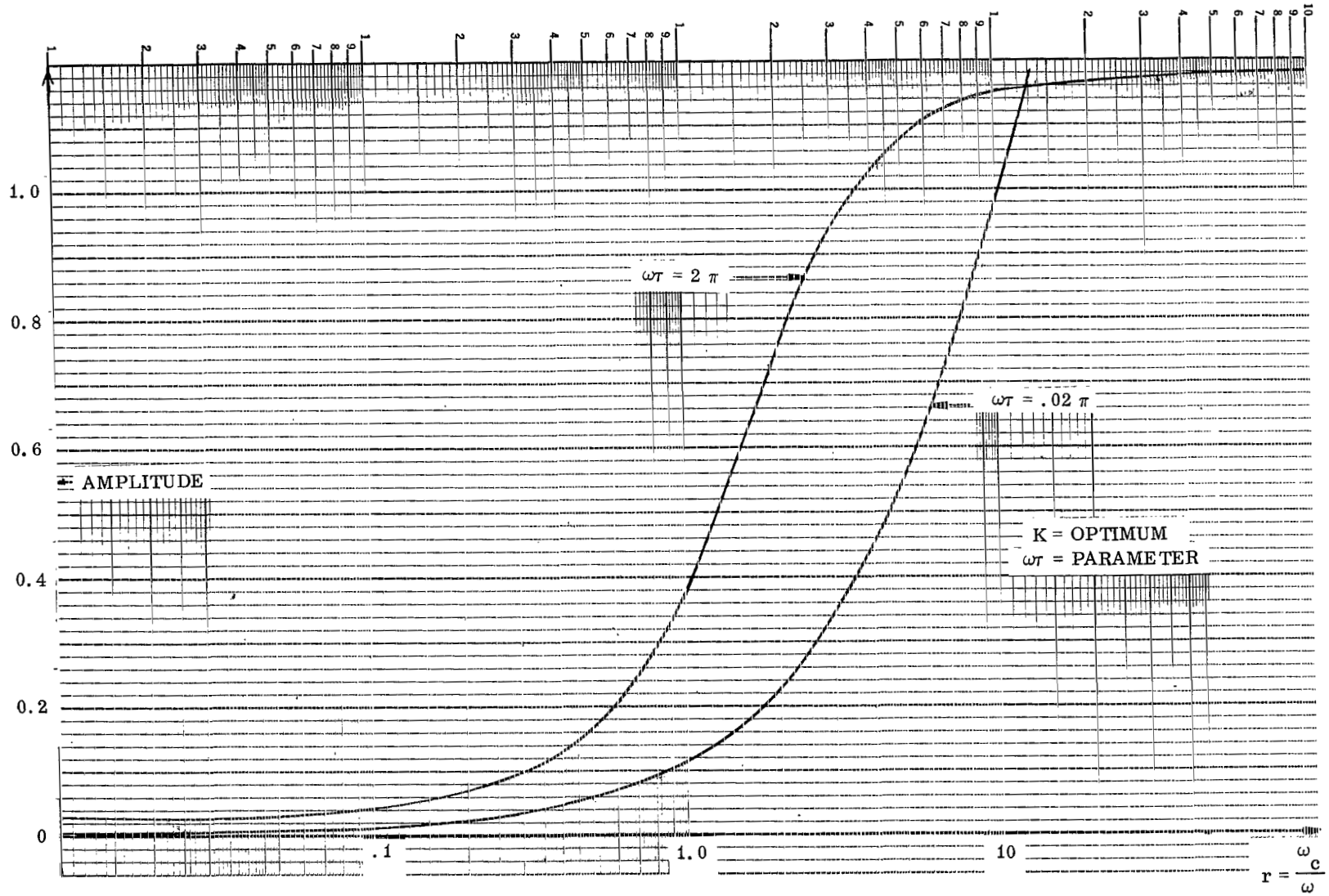

FIGURE 32. FREQUENCY RESPONSE FUNCTION - PHASE

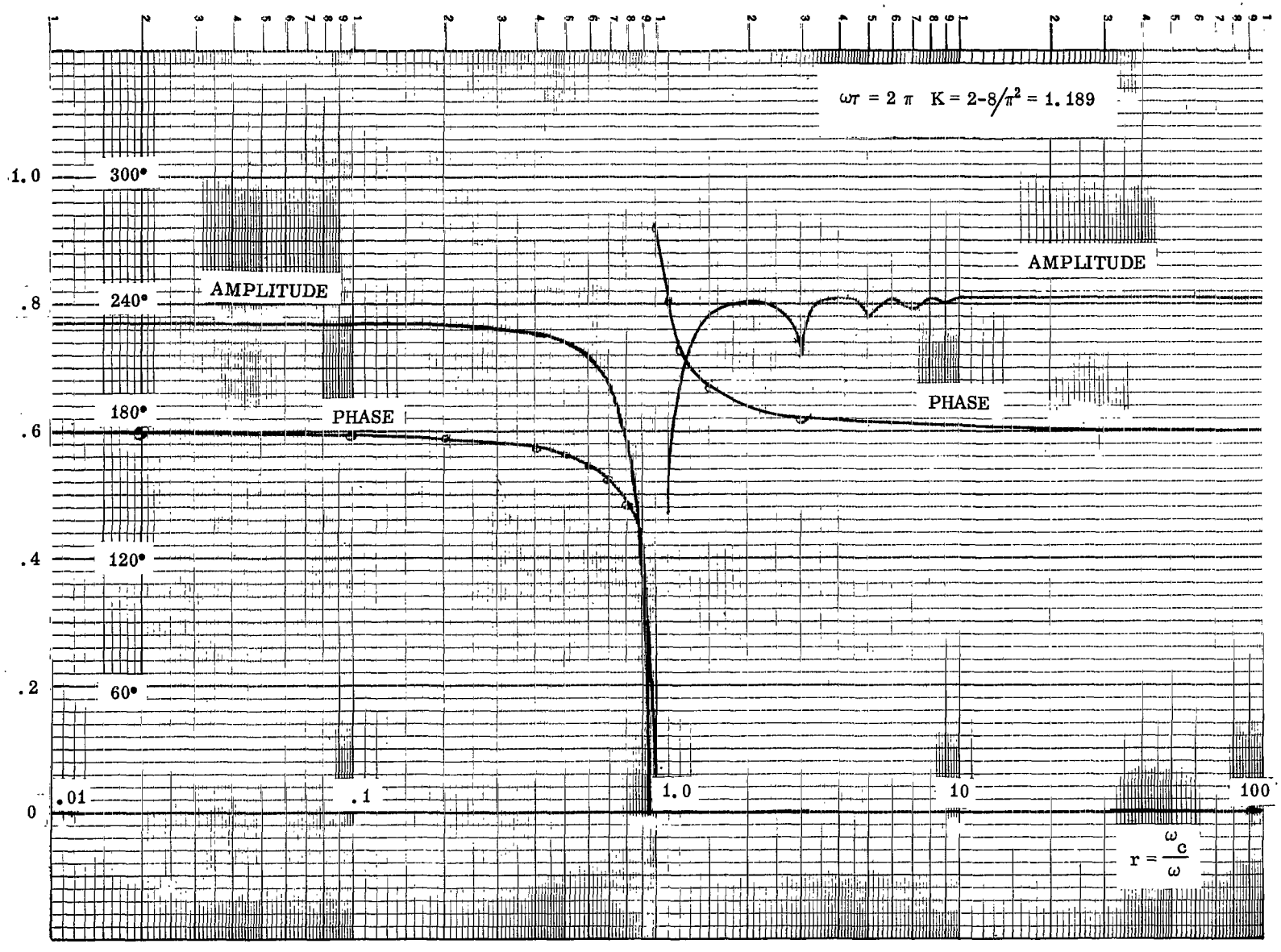

FIGURE 33. FREQUENCY RESPONSE FUNCTION

A. PHASE DIFFERENCE

Cases considered are: P(t) and Q(t) are ideal as shown in Figure 2. A Fourier analysis is performed for the case where the input frequency is the same as the notch frequency, but the input is out of phase with the notch frequency. As previously noted, the output of the notch filter (with feedforward) is independent of phase, but this is not true if the RC commutating network is considered alone.

B. PHASE LAG

Q(t) is nominal. Phase lag is equal to 3T/8 as shown in Figure 34.

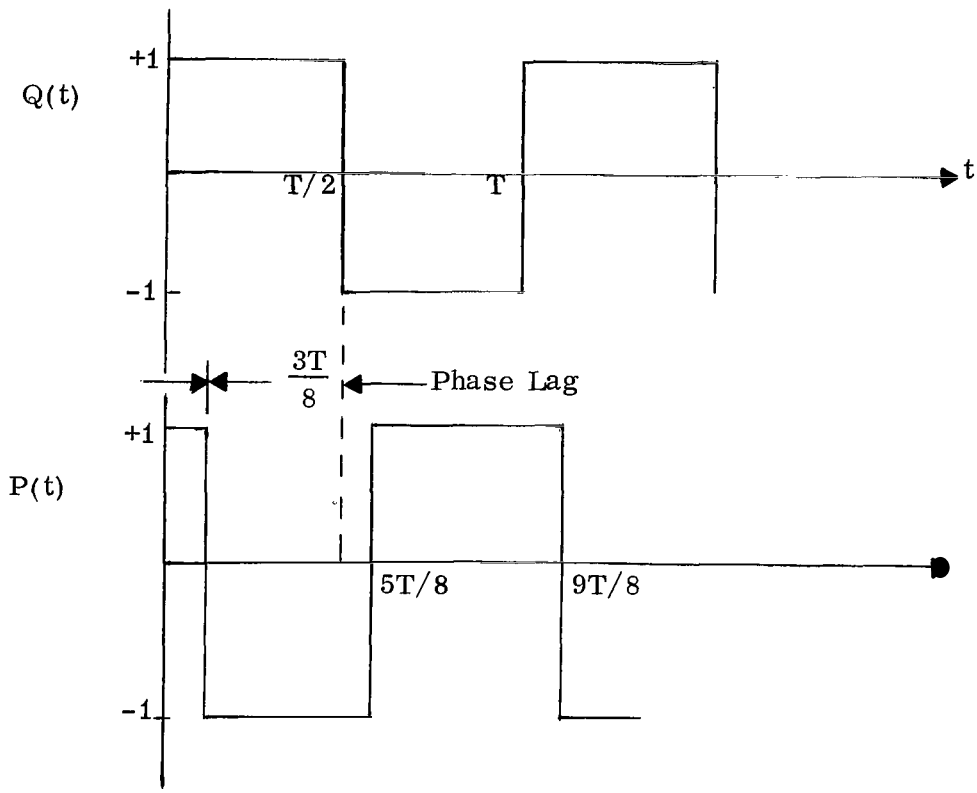

FIGURE 34. NONSYMMETRICAL COMMUTATING FUNCTIONS (PHASE LAG)

C. PHASE LAG WITH PHASE DIFFERENCE

P(t) is nominal, but shifted $\frac{T}{8}$. Q(t) is as shown in Figure 35.

Case a.

Let $e_i(t) = \sin\left(\frac{2\pi}{T}\, t + \varphi\right)$

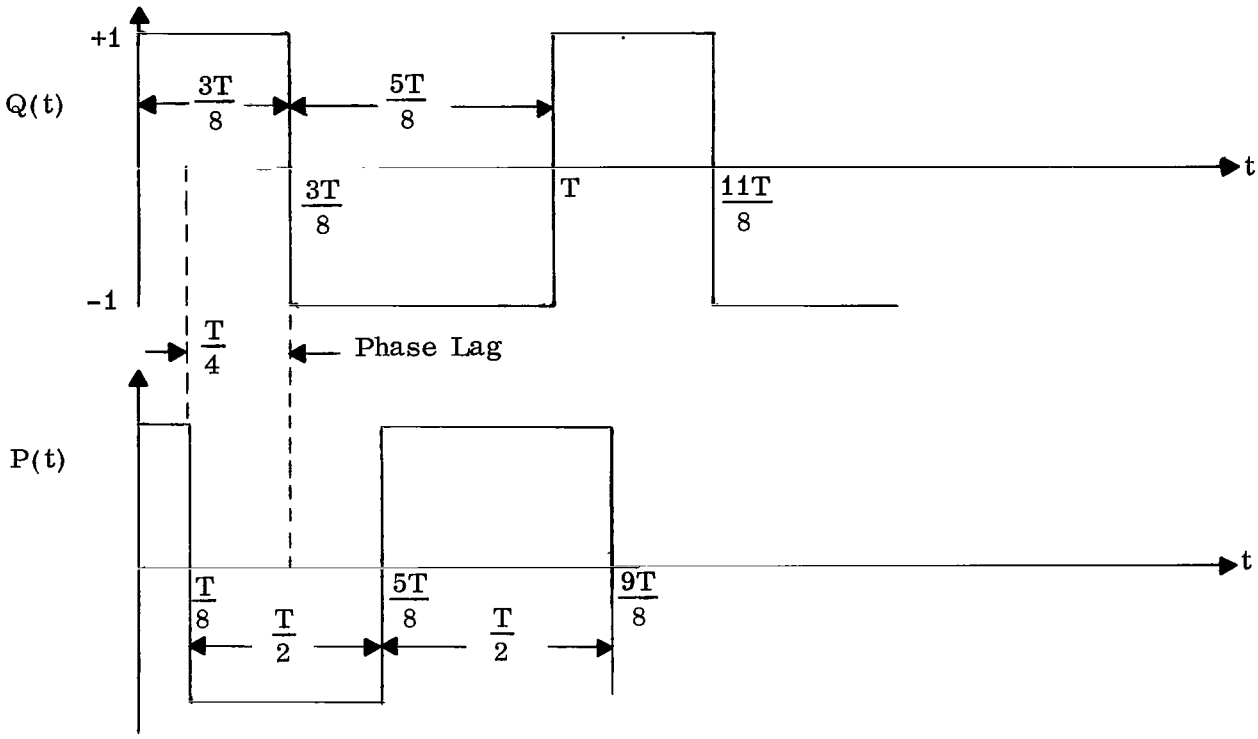

FIGURE 35. NONSYMMETRICAL COMMUTATING FUNCTIONS

The output $e_o(t)$ is given by Equation (30). If

$$x = \frac{2\lambda}{\omega} = \frac{2K'}{\omega\tau}$$

and

$$e_o(t) \sim \alpha_0 + \sum_{m=1}^{\infty} \left(\alpha_m \cos \omega_m t + \beta_m \sin \omega_m t \right)$$

then equation (30) yields

$$\alpha_0 = 0$$

$$\alpha_1 K' = \frac{x}{\pi(1+x^2)} \left\{ \begin{array}{l} \pi x \sin\varphi - \pi\cos\varphi + \dfrac{2}{(1+x^2)(1-e^{-\frac{\pi x}{2}})} \left[(x^2+2x-1) - (x^2-2x-1)\, e^{-\frac{\pi x}{2}} \right] \cos\varphi \\ \quad - \dfrac{2}{(1+x^2)(1-e^{-\frac{\pi x}{2}})} \left[(x^2-2x-1) + (x^2+2x-1)\, e^{-\frac{\pi x}{2}} \right] \sin\varphi \end{array} \right\} \quad (67a)$$

$$\beta_1 K' = \frac{x}{\pi(1+x^2)} \left\{ \begin{array}{l} \pi x \cos\varphi + \pi \sin\varphi - \dfrac{2}{(1+x^2)\left(1-e^{\frac{-\pi x}{2}}\right)} \left[(x^2-2x-1) + (x^2+2x-1)\, e^{-\frac{\pi x}{2}} \right] \cos\varphi \\ \\ - \dfrac{2}{(1+x^2)\left(1-e^{\frac{-\pi x}{2}}\right)} \left[(x^2+2x-1) - (x^2-2x-1)\, e^{-\frac{\pi x}{2}} \right] \sin\varphi \end{array} \right\} \quad (67b)$$

These functions are shown in Figures 36 through 38, with φ as a parameter.

Case b.

The output function for an input $e_i(t) = \sin \frac{2\pi}{T} t$ is

$$e_o(t) = \left\{ \begin{array}{ll} \frac{1}{\tau}\, u_1 & 0 \le t \le T/8 \\ \frac{1}{\tau}\, v_2 & T/8 \le t \le T/2 \\ -\frac{1}{\tau}\, u_3 & T/2 \le t \le 5T/8 \\ -\frac{1}{\tau}\, v_4 & 5T/8 \le t \le T \end{array} \right\} \quad (68)$$

where

$$u_1 = \frac{2}{\omega^2+4\lambda^2} \left[2\lambda \sin\omega t - \omega \cos\omega t + \frac{\frac{2-\sqrt{2}}{2}\omega + \sqrt{2}\,\lambda}{1 - e^{-\lambda T/4}}\, e^{-2\lambda t} \right] \quad 0 \le t \le T/8$$

$$v_2 = \frac{2}{\omega^2+4\lambda^2} \left[2\lambda \sin\omega t - \omega \cos\omega t + \frac{\frac{2+\sqrt{2}}{2}\omega - \sqrt{2}\,\lambda}{1 - e^{-\lambda T/4}}\, e^{-2\lambda(t-T/8)} \right] \quad \frac{T}{8} \le t \le \frac{T}{2}$$

$$-u_3 = -u_1\,(t-T/2) \qquad \frac{T}{2} \le t \le \frac{5T}{8}$$

$$-v_4 = -v_2\,(t-T/2) \qquad \frac{5T}{8} \le t \le T$$

and $\lambda = \frac{K'}{\tau}$.

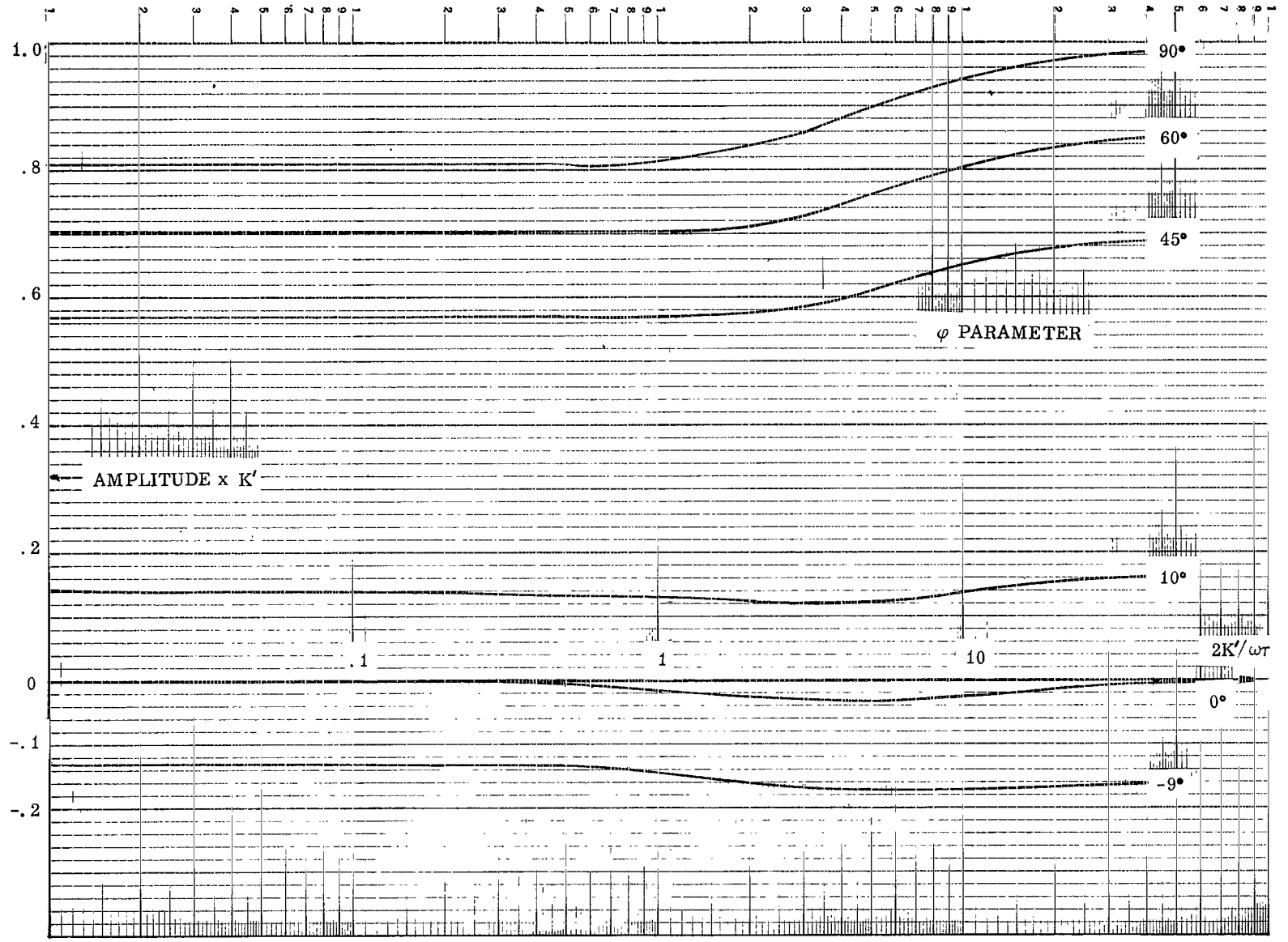

FIGURE 36. QUADRATURE COMPONENT AMPLITUDE VS $2K'/\omega\tau$ (COUPLED - $\alpha_1 K'$)

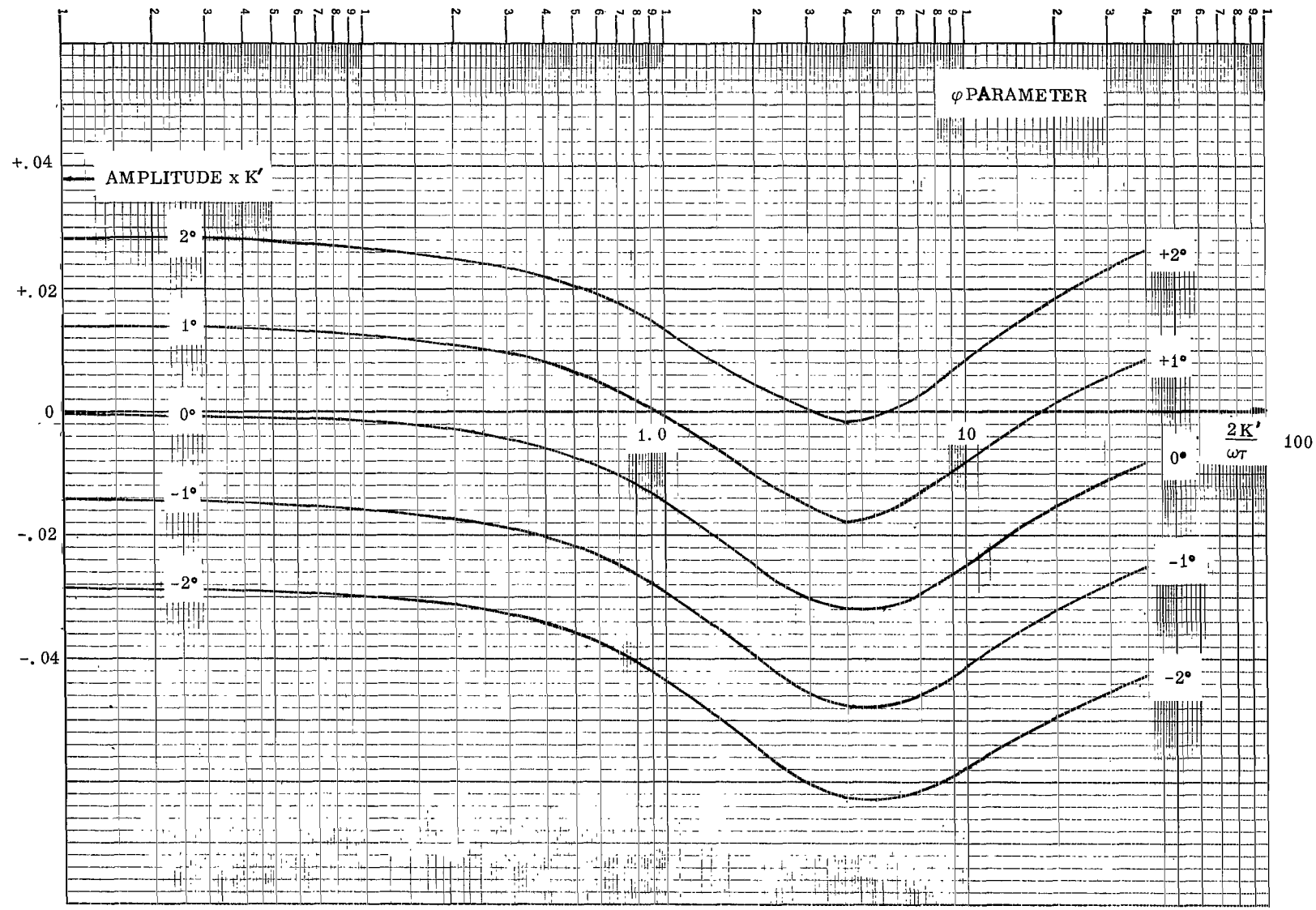

FIGURE 37. QUADRATURE COMPONENT AMPLITUDE VS 2K'/$\omega\tau$ (COUPLED - α, K', ENLARGEMENT OF FIGURE 36)

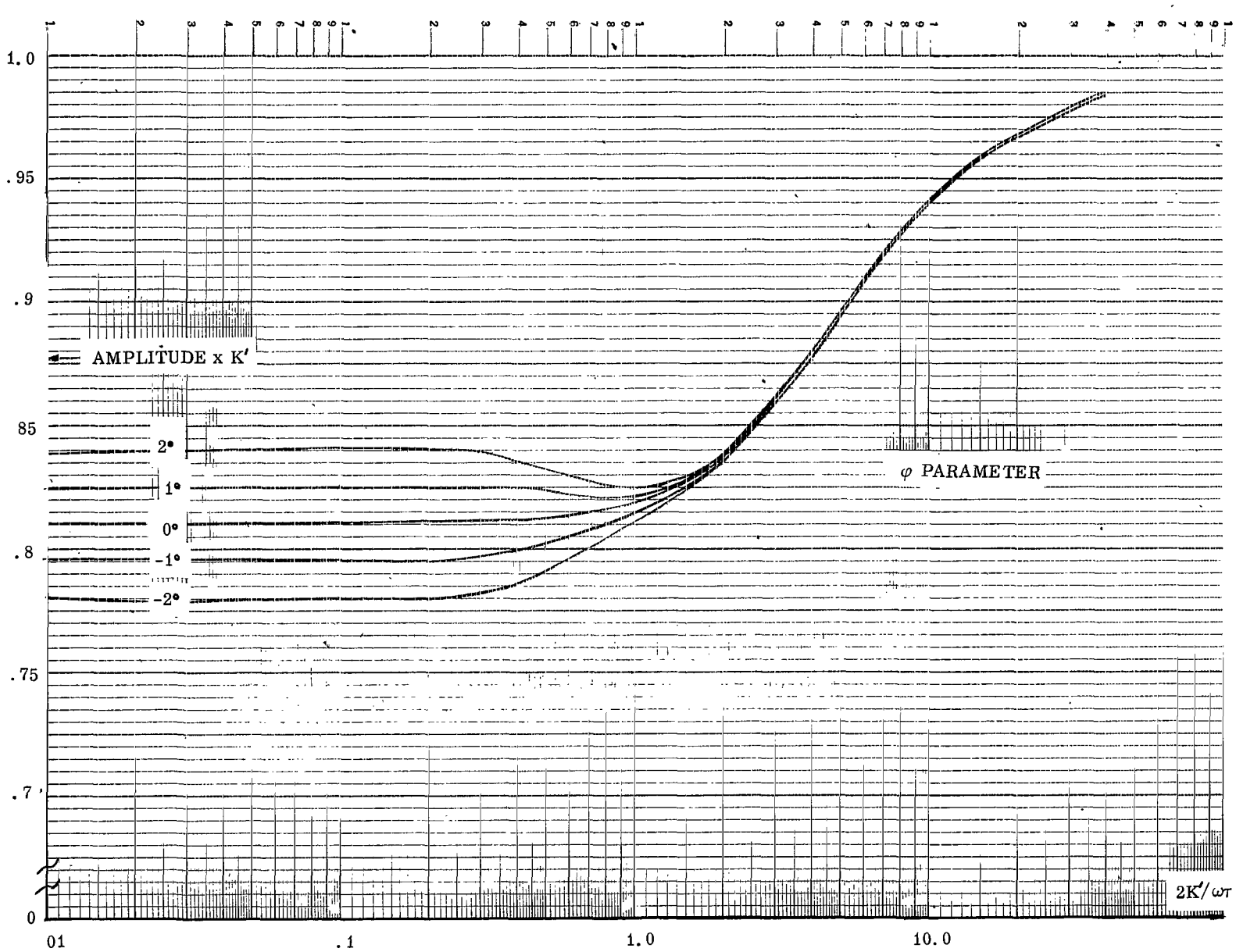

FIGURE 38. QUADRATURE COMPONENT AMPLITUDE VS $2K'/\omega\tau$ (COUPLED $\beta_1 K'$)

This function is shown below for the parametric values of

$\lambda = K'/\tau = .675/1 = .675 \qquad T = f = 1$

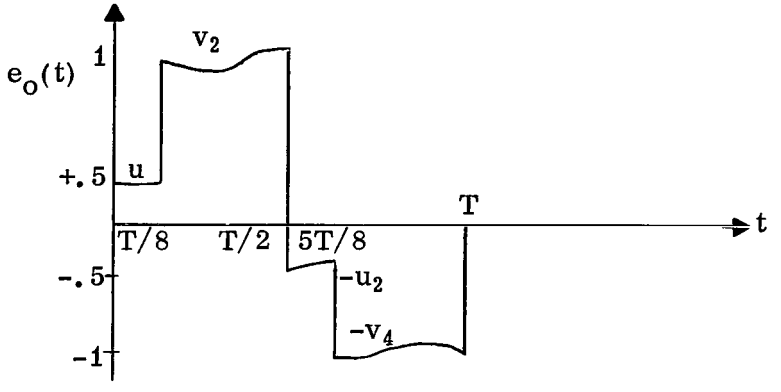

FIGURE 39. RC COMMUTATED NETWORK OUTPUT CONSIDERING A NONSYMMETRICAL COMMUTATING FUNCTION

Figure 39 shows $e_o(t)$ to be asymmetric about $t = \frac{T}{2}$ as expected. The difference in amplitude of v_2 and u_1 has appeared in most of the equipment runs (Fig. 12).

A Fourier analysis of Equation (68) yields

$$\alpha_0 = 0$$

$$\alpha K' = \frac{x}{\pi(1+x^2)} \left\{ -\pi + \frac{(2-\sqrt{2}) + \sqrt{2}\,x}{(1+x^2)(1-e^{-\pi x/4})} \left[x + (1-x)\frac{\sqrt{2}}{2} e^{-\pi x/4} \right] + \frac{(2+\sqrt{2}) - \sqrt{2}\,x}{(1+x^2)(1-e^{-3\pi x/4})} \left[x e^{-3\pi x/4} + \frac{\sqrt{2}}{2}(x-1) \right] \right\} \tag{69a}$$

$$\beta K' = \frac{x}{\pi(1+x^2)} \left\{ \pi x + \frac{(2-\sqrt{2}) + \sqrt{2}\,x}{(1+x^2)(1-e^{-\pi x/4})} \left[1 - (x+1)\frac{\sqrt{2}}{2} e^{-\pi x/4} \right] + \frac{(2+\sqrt{2}) - \sqrt{2}\,x}{(1+x^2)(1-e^{-3\pi x/4})} \left[\frac{\sqrt{2}}{2}(1+x) + e^{-3\pi x/4} \right] \right\}. \tag{69b}$$

Equations (69a) and (69b) are shown in Figure 40. A large cosine component ($\approx -.16$) can be noticed.

Case c.

$$e_i = \sin\left(\frac{2\pi}{T}\, t + \varphi\right).$$

The output $e_o(t)$ is

$$e_o(t) = \begin{cases} \dfrac{u_1}{\tau} & 0 \le t \le T/8 \\ \dfrac{v_2}{\tau} & \dfrac{T}{8} \le t \le 3T/8 \\ -\dfrac{u_3}{\tau} & \dfrac{3T}{8} \le t \le 5T/8 \\ -\dfrac{v_4}{\tau} & \dfrac{5T}{8} \le t \le T \end{cases} \qquad (70)$$

where

$$u_1 = \frac{2}{\omega^2+4\lambda^2}\left[2\lambda \sin(\omega t + \varphi) - \omega \cos(\omega t + \varphi) + \frac{(c_2 - c_1) + (c_2 + c_3)}{1 - e^{-3\lambda T/4}}\, e^{-2\lambda t}\right]$$

$$0 \le t \le \frac{T}{8}$$

$$v_2 = \frac{2}{\omega^2+4\lambda^2}\left[2\lambda \sin(\omega t + \varphi) - \omega \cos(\omega t + \varphi) + \right.$$

$$\left. + \frac{-(c_1 + c_2) + (c_3 - c_2)\, e^{-3\lambda T/4}}{1 - e^{-5\lambda T/4}}\, e^{-2\lambda t + \lambda T/4}\right]$$

$$\frac{T}{8} \le t \le \frac{3T}{8}.$$

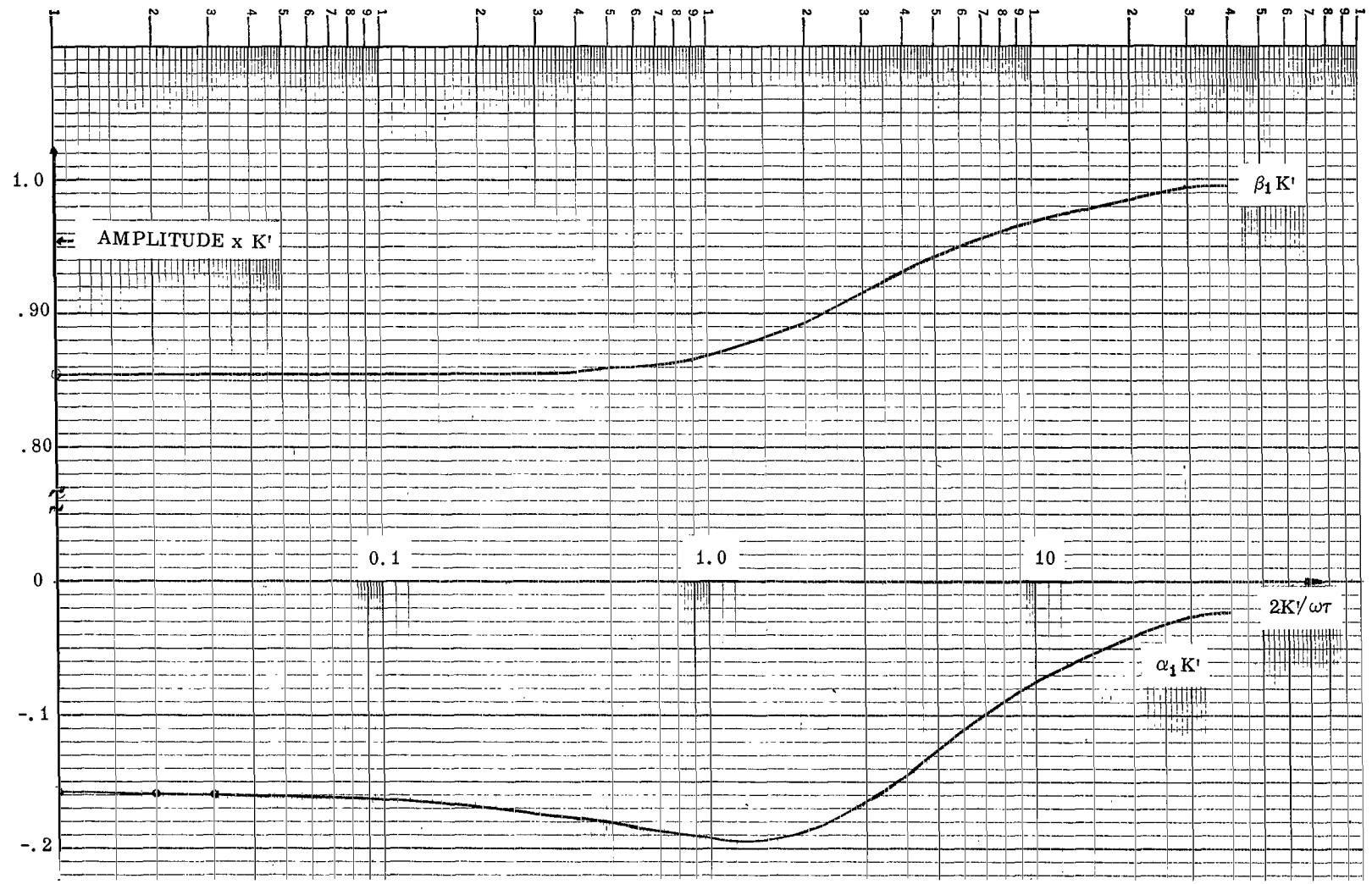

FIGURE 40. QUADRATURE COMPONENT AMPLITUDES FOR NONSYMMETRICAL COMMUTATING FUNCTIONS (COUPLED)

$$-u_3 = \frac{2}{\omega^2+4\lambda^2}\left[2\lambda \sin(\omega t+\varphi) - \omega\cos(\omega t+\varphi) - \right.$$

$$\left. - \frac{(c_2+c_3) + (c_2-c_1)e^{-\lambda T/4}}{1-e^{-3\lambda T/4}} e^{-2\lambda t+3\lambda T/4}\right]$$

$$\frac{3T}{8} \le t \le \frac{5T}{8}$$

$$-v_4 = \frac{2}{\omega^2+4\lambda^2}\left[2\lambda \sin(\omega t+\varphi) - \omega\cos(\omega t+\varphi) - \right.$$

$$\left. - \frac{(c_3-c_2) - (c_1+c_2)e^{-\lambda T/2}}{1-e^{-5\lambda T/4}} e^{-2\lambda t+5\lambda T/4}\right]$$

$$\frac{5T}{8} \le t \le T$$

and

$$c_1 = 2\lambda \sin\varphi - \omega\cos\varphi$$

$$c_2 = 2\lambda \sin\left(\varphi+\frac{\pi}{4}\right) - \omega\cos\left(\varphi+\frac{\pi}{4}\right)$$

$$c_3 = 2\lambda \sin\left(\varphi+\frac{3\pi}{4}\right) - \omega\cos\left(\varphi+\frac{3\pi}{4}\right)$$

$$\lambda = K'/\tau.$$

A Fourier analysis of Equation (70) yields

$$\alpha_0 K' = \frac{x}{2\pi(1+x^2)}\left\{\frac{\bar{A} + 2\bar{B}e^{-\pi x/4} - 2\bar{C}e^{-\pi x/2} + \bar{A}e^{-3\pi x/4}}{1-e^{-3\pi x/4}} + \right.$$

$$\left. + \frac{\bar{A} - 2\bar{D}e^{-\pi x/2} - 2\bar{E}e^{-3\pi x/4}}{1-e^{-5\pi x/4}} + \frac{\bar{A}e^{-5\pi x/4}}{1-e^{-5\pi x/4}}\right\} \quad (71a)$$

$$\alpha_1 K' = \frac{x}{\pi(1+x^2)^2} \left\{ \begin{array}{l} (\pi x \sin\varphi - \pi\cos\varphi)(1+x^2) \\ + \dfrac{A + Be^{-\pi x/2}}{1 - e^{-3\pi x/4}} \left[x + \dfrac{\sqrt{2}}{2}(1-x)e^{-\pi x/4} \right] \\ + \dfrac{B + Ae^{-\pi x/4}}{1 - e^{-3\pi x/4}} \left[\dfrac{\sqrt{2}}{2}(1+x) + \dfrac{\sqrt{2}}{2}(1-x)e^{-\pi x/2} \right] \\ + \dfrac{-C + De^{-3\pi x/4}}{1 - e^{-5\pi x/4}} \left[\dfrac{\sqrt{2}}{2}(x-1) + \dfrac{\sqrt{2}}{2}(1+x)e^{-\pi x/2} \right] \\ + \dfrac{D - Ce^{-\pi x/2}}{1 - e^{-5\pi x/4}} \left[\dfrac{\sqrt{2}}{2}(x-1) + xe^{-3\pi x/4} \right] \end{array} \right\} \quad (71b)$$

$$\beta_1 K' = \frac{x}{\pi(1+x^2)^2} \left\{ \begin{array}{l} (\pi x \cos\varphi + \pi \sin\varphi)(1+x^2) \\ + \dfrac{A + Be^{-\pi x/2}}{1 - e^{-3\pi x/4}} \left[1 - \dfrac{\sqrt{2}}{2}(1+x)e^{-\pi x/4} \right] \\ + \dfrac{B + Ae^{-\pi x/4}}{1 - e^{-3\pi x/4}} \left[\dfrac{\sqrt{2}}{2}(1-x) - \dfrac{\sqrt{2}}{2}(1+x)e^{-\pi x/2} \right] \\ + \dfrac{-C + De^{-3\pi x/4}}{1 - e^{-5\pi x/4}} \left[\dfrac{\sqrt{2}}{2}(1+x) + \dfrac{\sqrt{2}}{2}(1-x)e^{-\pi x/2} \right] \\ + \dfrac{D - Ce^{-\pi x/2}}{1 - e^{-5\pi x/4}} \left[e^{-3\pi x/4} + \dfrac{\sqrt{2}}{2}(1+x) \right] \end{array} \right\} \quad (71c)$$

where

$$\bar{A} = \left[\left(\frac{\sqrt{2}}{2} - 1\right) - \frac{\sqrt{2}}{2}\frac{1}{x}\right] \sin\varphi + \left[\frac{1}{x}\left(1 - \frac{\sqrt{2}}{2}\right) - \frac{\sqrt{2}}{2}\right] \cos\varphi$$

$$\bar{B} = \left[\left(-\frac{\sqrt{2}}{2} + 1\right) - \frac{\sqrt{2}}{2}\frac{1}{x}\right] \sin\varphi + \left[\frac{1}{x}\left(\frac{\sqrt{2}}{2} - 1\right) - \frac{\sqrt{2}}{2}\right] \cos\varphi$$

$$\bar{C} = -\sqrt{2}\left(\frac{1}{x}\sin\varphi + \cos\varphi\right)$$

$$\bar{D} = -\left[\left(1 + \frac{\sqrt{2}}{2}\right) + \frac{\sqrt{2}}{2}x\right] \sin\varphi + \left[\frac{1}{x}\left(\frac{\sqrt{2}}{2} + 1\right) - \frac{\sqrt{2}}{2}\right] \cos\varphi$$

$$\bar{E} = \sqrt{2}\left(\sin\varphi - \frac{1}{x}\cos\varphi\right)$$

$$A = \left[x\left(\frac{\sqrt{2}}{2} - 1\right) + \frac{\sqrt{2}}{2}\right] \sin\varphi + \left[\frac{\sqrt{2}}{2}x + \left(1 - \frac{\sqrt{2}}{2}\right)\right] \cos\varphi$$

$$B = \sqrt{2}\,(\sin\varphi + x\cos\varphi)$$

$$C = \left[x\left(\frac{\sqrt{2}}{2} + 1\right) + \frac{\sqrt{2}}{2}\right] \sin\varphi + \left[\frac{\sqrt{2}}{2}x - \left(1 + \frac{\sqrt{2}}{2}\right)\right] \cos\varphi$$

$$D = \sqrt{2}\,(-x\sin\varphi + \cos\varphi).$$

Equations (71a), (71b), and (71c) are shown in Figures 41 to 44, with φ as a parameter. Figure 41 depicts the dc component which has not appeared in any of the previous analyses. Figure 42 gives the amplitude of the cosine component. Figure 43 is an enlargement of Figure 42 for $\varphi = 9°$ and $\varphi = 10°$.

Cases b and c are considered to be extreme deviations from the normal symmetrical square waves. As mentioned earlier, no attempt is made to find an optimum setting for the commutating network.

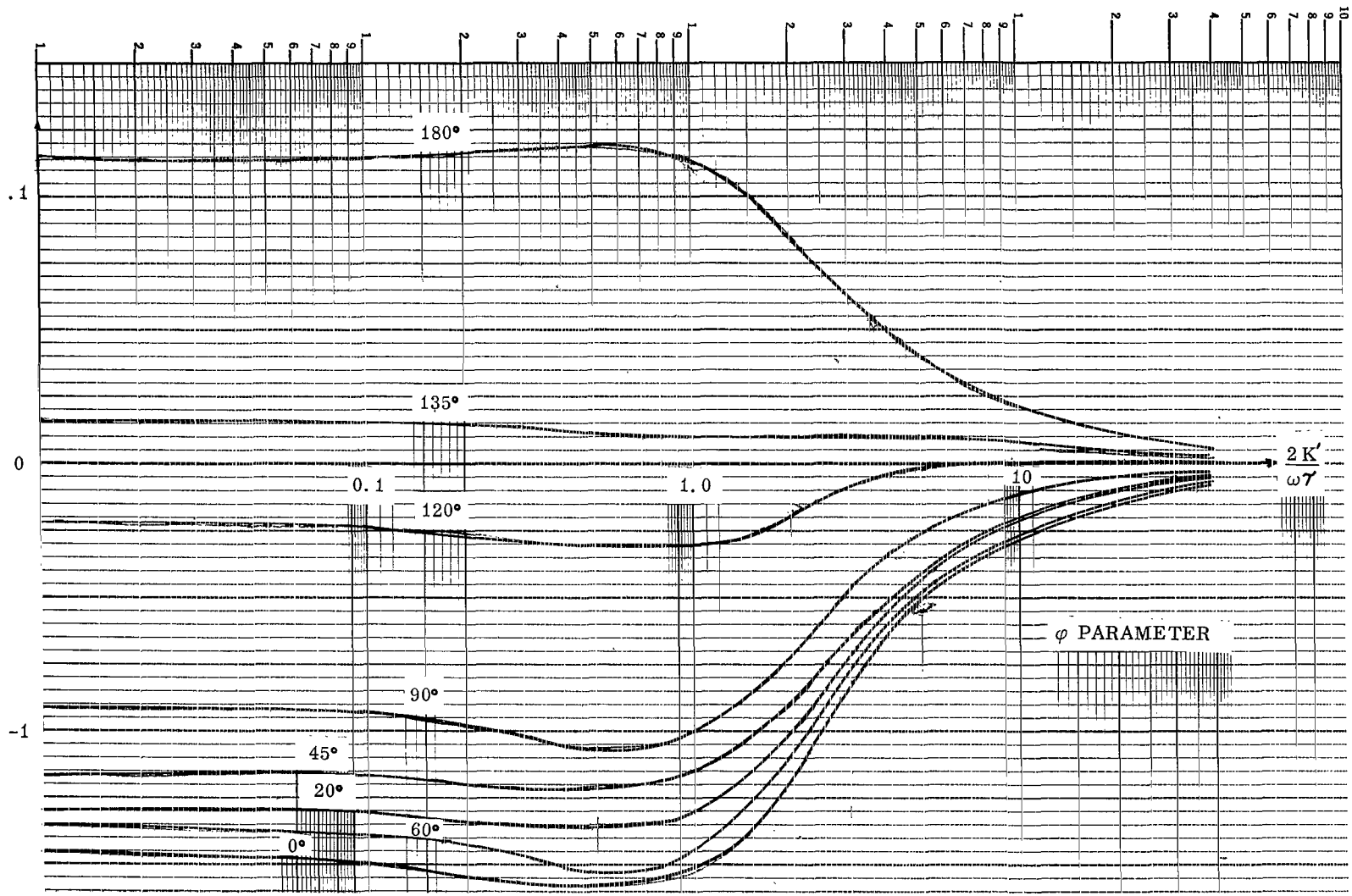

FIGURE 41. DC AMPLITUDE FOR NONSYMMETRICAL COMMUTATING FUNCTION (COUPLED)

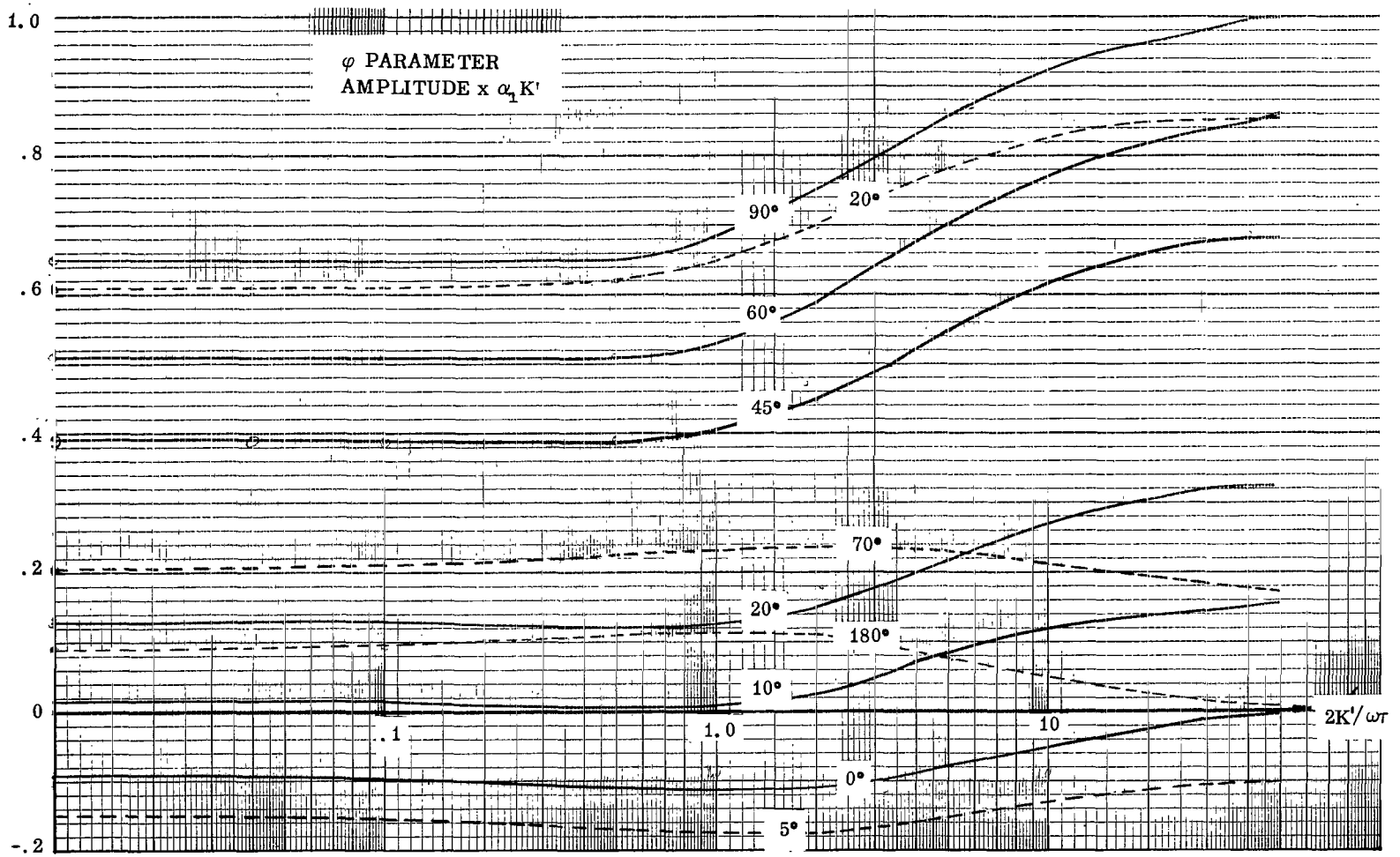

FIGURE 42. QUADRATURE COMPONENT AMPLITUDES FOR NONSYMMETRICAL COMMUTATING FUNCTIONS (COUPLED)

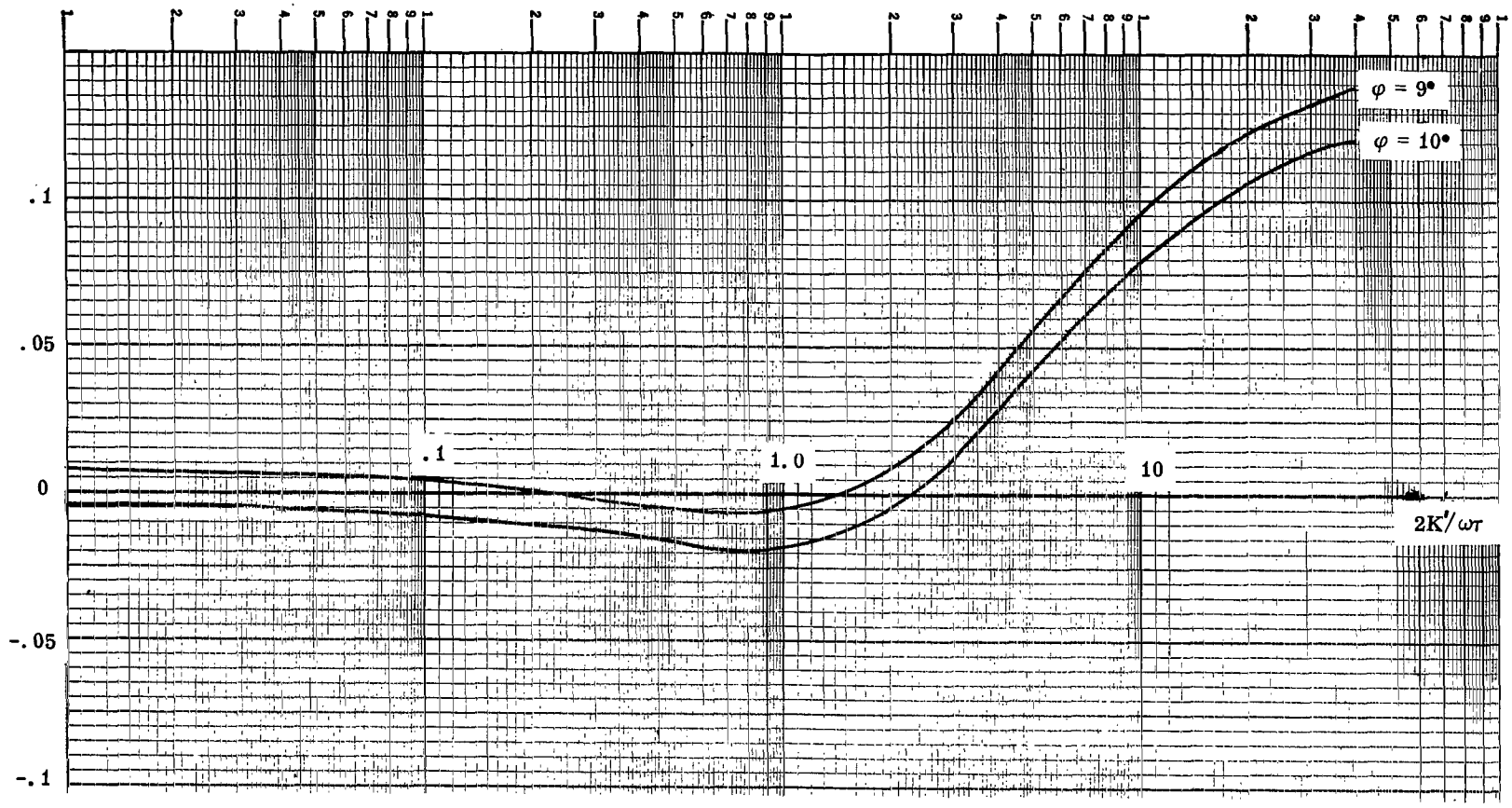

FIGURE 43. QUADRATURE COMPONENT AMPLITUDES FOR NONSYMMETRICAL COMMUTATING FUNCTIONS (COUPLED - ENLARGEMENT OF FIGURE 42)

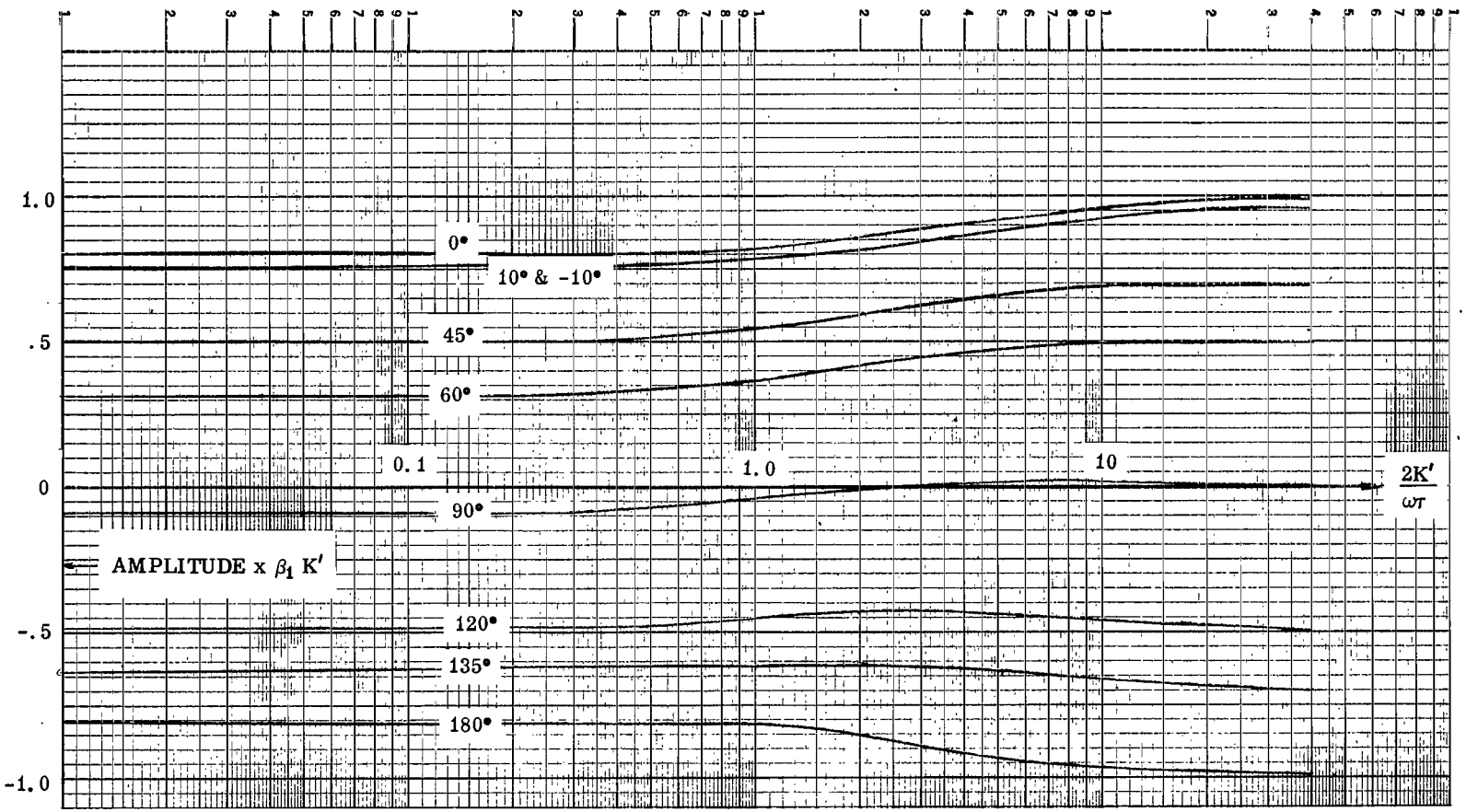

FIGURE 44. QUADRATURE COMPONENT AMPLITUDES FOR NONSYMMETRICAL COMMUTATING FUNCTIONS (COUPLED)

CONCLUSIONS

Solutions have been obtained for the equations describing an adaptive tracking notch filter. For the uncoupled case, a frequency response function is obtained in closed form, thus making it possible to analytically include the notch in a closed loop system. The coupled case does not admit to such an analysis; however, an explicit solution is still obtained for inputs considered important. Practical nonsymmetrical commutating functions are investigated and the complexity of the solutions is noted.

Equipment time traces agree with the theoretical analysis.

APPENDIX

The purpose of this appendix is to derive Equations (57) through (59). Equations (55) and (56) are common transforms and can be found in many books on transform calculus (e.g., Ref. 7). To derive Equation (57), the translation theorem

$$L\{F(t-a)\ \ 1(t-a)\} = e^{-ap} f(p) \qquad \text{(A-1)}$$

is needed. In Equation (A-1), $1(t-a)$ is the unit step function defined as

$$1(t-a) = 0 \qquad t < a$$

$$= 1 \qquad t \geq a$$

Referring to Figure A-1, the function P has first been inverted and the result translated T/4 units to the right.

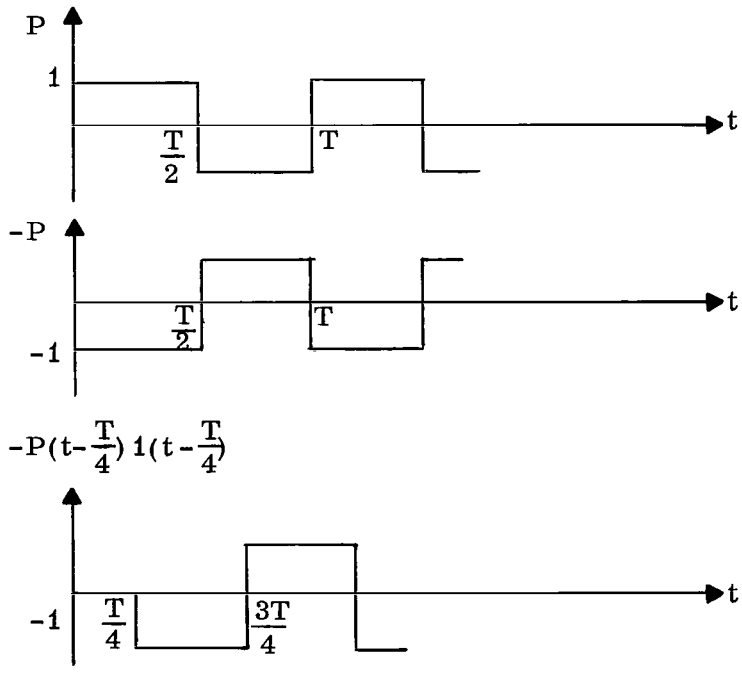

FIGURE A-1. INVERSION AND TRANSLATION OF P(t)

The corresponding Laplace transforms are

$$L\{P\} = \frac{1}{p}\tanh p\frac{T}{4}$$

$$L\{-P\} = -\frac{1}{p}\tanh p\frac{T}{4} \qquad (56)$$

$$L\{-P(t-\frac{T}{4})\,1(t-\frac{T}{4})\} = -e^{-\frac{T}{4}p}\,\frac{1}{p}\tanh\frac{pT}{4}$$

where the last equation uses the previously mentioned translation theorem. The function Q can be constructed by adding Figure A-2 to the last figure of Figure A-1.

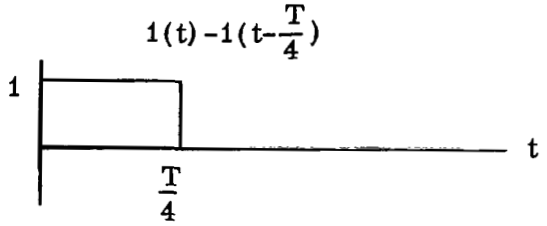

FIGURE A-2. PULSE FUNCTION

Now the Laplace transform of Figure A-2 is

$$L\left\{1(t) - 1\ (t-\frac{T}{4})\right\} = L\{1(t)\} - L\left\{1(t-\frac{T}{4})\right\}$$

$$= \frac{1}{p} - \frac{e^{-\frac{pT}{4}}}{p}.$$

Therefore,

$$L\{Q\} = L\left\{1(t)-1(t-\frac{T}{4})\right\} + L\left\{-P(t-\frac{T}{4})\ 1(t-\frac{T}{4})\right\}$$

$$= \frac{1}{p} - \frac{e^{-p\frac{T}{4}}}{p} - \frac{e^{-p\frac{T}{4}}}{p}\tanh p\frac{T}{4} \qquad (57)$$

$$= \frac{1}{p}\left[1 - \operatorname{sech} p\frac{T}{4}\right].$$

The second translation theorem (Fig. A-2)

$$L\left\{ e^{-at} F(t) \right\} = f(p+a)$$

is needed to show Equations (58) and (59). Thus

$$L\left\{ e^{+j\omega_c p} \right\} = \frac{\tanh (p-j\omega_c) \frac{T}{4}}{(p-j\omega_c)} \tag{58}$$

and

$$L\left\{ e^{j\omega_c t} Q \right\} = \frac{1}{p-j\omega_c} \left[1 - \operatorname{sech} (p - j\omega_c) \frac{T}{4} \right] . \tag{59}$$

REFERENCES

1. LePage, W. R., Cahn, C. R., and Brown, J. S., "Analysis of a Comb Filter Using Synchronously Commutated Capacitors," AIEE Trans., Part 1, 72, 1953, p. 63.

2. Franks, L. E., and Sandberg, I. W., "An Alternative Approach to the Realization of Network Transfer Functions: The N-Path Filter," The Bell System Technical Journal, Sept. 1960.

3. Borelli, M. T., and Hosenthien, H. H., "An Adaptive Tracking-Notch Filter for Suppression of Structural Bending Signals of Large Space Vehicles," Astrionics Research and Development Report No. 1, NASA TM X-53,000, Oct. 1963.

4. Hosenthien, Hans H., "Reflected Non-Linear Modulators in Alternating Current Electrical Analog Computers," Patent No. 2,961,610, Nov. 22, 1960.

5. Gardner, S. M., and Barnes, J. L., Transients in Linear Systems, John Wiley and Sons, Inc., 1957.

6. Stoker, J. J., "Non-Linear Vibrations," Interscience Publishers, Inc., 1957.

7. Scott, E. J., Transform Calculus with an Introduction to Complex Variables, Harper and Brothers, Publishers, New York, 1955.

8. Ryshik, I. M., and Gradstein, I. S., "Tables," Veb Deutscher Verlag Der Wissenschaften, Berlin, 1957.

NASA-Langley, 1965 M202

"The aeronautical and space activities of the United States shall be conducted so as to contribute . . . to the expansion of human knowledge of phenomena in the atmosphere and space. The Administration shall provide for the widest practicable and appropriate dissemination of information concerning its activities and the results thereof."

—NATIONAL AERONAUTICS AND SPACE ACT OF 1958

NASA SCIENTIFIC AND TECHNICAL PUBLICATIONS

TECHNICAL REPORTS: Scientific and technical information considered important, complete, and a lasting contribution to existing knowledge.

TECHNICAL NOTES: Information less broad in scope but nevertheless of importance as a contribution to existing knowledge.

TECHNICAL MEMORANDUMS: Information receiving limited distribution because of preliminary data, security classification, or other reasons.

CONTRACTOR REPORTS: Technical information generated in connection with a NASA contract or grant and released under NASA auspices.

TECHNICAL TRANSLATIONS: Information published in a foreign language considered to merit NASA distribution in English.

TECHNICAL REPRINTS: Information derived from NASA activities and initially published in the form of journal articles.

SPECIAL PUBLICATIONS: Information derived from or of value to NASA activities but not necessarily reporting the results of individual NASA-programmed scientific efforts. Publications include conference proceedings, monographs, data compilations, handbooks, sourcebooks, and special bibliographies.

Details on the availability of these publications may be obtained from:

SCIENTIFIC AND TECHNICAL INFORMATION DIVISION

NATIONAL AERONAUTICS AND SPACE ADMINISTRATION

Washington, D.C. 20546